The role of defense signaling pathways
in the interaction of
Arabidopsis thaliana and *Verticillium longisporum*

Dissertation

for the award of the degree

Division of Mathematics and Natural Sciences

"Doctor rerum naturalium"
of the Georg-August-Universität Göttingen

submitted by

Anjali Ralhan

from New Delhi, India

Göttingen, 2012

To my beloved family

Contents

1 INTRODUCTION

Plants are a rich source of nutrients for many micro-organisms. Although lacking an adaptive immune system comparable to animals, plants are able to defend themselves against most pathogens. Strategies adopted by plants to combat pathogen attack are either dependent on constitutive barriers or on the activation of multi-component defense responses. Constitutive defenses include preformed barriers such as cell walls, waxy epidermal cuticles as well as chemical substances with antimicrobial effects (phytoanticipins). In addition to preformed barriers, plants have the ability to detect pathogens and respond with inducible defenses including the production of toxic chemicals, enzymes, and deliberate cell death. If pathogens are able to overcome these defense barriers, often devastating effects are caused. In nature, various types of plant microbe interactions have been described. In necrotrophic interactions pathogens kills infected plants cells (e.g. *Botrytis cinerea;* Colmenares et al., 2002). In biotrophic interactions resources from living host cells are exploited (e.g. *Cladosporium fulvum;* Joosten and de Wit, 1999) and in symbiotic interactions both partners benefit each other (e.g. *Laccaria bicolor*; Lammers et al., 2004). Many pathogens first colonize their host plant as biotrophs and then switch to a necrotrophic phase in the later stages of infection by killing the host plant (e.g. *Verticillium spec.;* Klosterman et al., 2009). Such pathogens are called hemi-biotrophs.

1.1 Induced plant defense responses

Plants activate inducible defense responses after detecting pathogen or danger associated molecular patterns (PAMPs/DAMPs). A well studied PAMP is flagellin (Zipfel & Felix, 2005) which is recognized by the specific membrane bound pathogen recognition receptor (PRR) FLS2: FLAGELLIN INSENSITIVE2 (Gómez- Gómez & Boller, 2002, Jones & Dangl, 2006). Flg22 is a synthetic 22-amino-acid peptide from a conserved flagellin domain which is sufficient to induce many cellular responses (Felix et al., 1999). A genetic screen using flg22 defined the Arabidopsis leucine-rich repeat (LRR)-receptor kinase FLS2, which binds flg22 (Chinchilla et al., 2006) resulting in PAMP-triggered immunity (PTI) that can halt further pathogen colonization. Successful pathogens deploy effectors that contribute to pathogen virulence. For example, AvrPto and AvrPtoB are unrelated type III effectors that may contribute to virulence by inhibiting early steps in PTI (He et al., 2006). Effectors can interfere with PTI resulting in effector-triggered susceptibility (ETS). Effectors that enable pathogens to overcome PTI are specifically recognized by NB-LRR proteins, resulting in effector-triggered immunity (ETI). ETI often

culminates in a form of programmed cell death called the hypersensitive response (HR; Greenberg & Yao, 2004).

Infection of plants with diverse pathogens results in changes in the levels of phytohormones. On the basis of the interactions that have been studied, a general rule of hormonal action has been proposed in which resistance responses to biotrophs require salicylic acid (SA), whereas responses to necrotrophs require jasmonic acid (JA) and ethylene (ET) (Feys & Parker, 2000). Roles for ET, SA, and JA have also been proposed in regulation of susceptible responses (Bent et al., 1992; Greenberg et al., 2000; Lund et al.,1998; Pilloff et al., 2002). The gaseous hormone ET is a critical component of responses to mechanical damage, herbivory (De Vos et al., 2005), and pathogen attack in addition to normal developmental processes such as fruit ripening and senescence (Abeles et al., 1992). Because of the involvement of many hormones in responses to multiple stresses, there must be mechanisms in place to integrate these signals in an orderly manner. Thus, complex networks of hormonal interactions, both agonistic (O'Donnell et al., 1996) and antagonistic (Pieterse & van Loon, 1999) must be rapidly integrated into a single response appropriate for an external stimulus. Like many other complex biological processes, plant defense responses upon pathogen infection involve transcriptional regulation of a large number of plant host genes (Rushton & Somssich, 1998). These differentially regulated plant genes encode regulatory factors that are involved in the activation, suppression, and modulation of various signaling pathways in plant cells upon pathogen infection. Thus, transcriptional regulation of plant host genes is an integral part of plant defense responses with a critical role in induced plant disease resistance (Chen, 2002).

Plants, when exposed to variety of pathogens, induce defense responses comprising reinforcement of the cell walls, production of phytoalexins and the synthesis of defense-related proteins. The cell wall is reinforced by callose deposition, stronger lignifications and embedding of phenylpropanoids in the cell wall (Dixon et al., 1994, Lamb & Dixon 1997, Nuernberger & Lipka, 2005). In Arabidopsis, camalexin is known as the characteristic phytoalexin possessing antimicrobial activity. It has been shown that Camalexin disrupts bacterial membranes suggesting its toxic effect on *Pseudomonas* (Rogers et al., 1996). Synthesis of camalexin is induced by a variety of pathogens but it does not lead to resistance against all of them (Glawischnig, 2007). Another class of defense related proteins that are strongly induced when host plant cells are challenged by pathogen stress is Chitinases. They possess significant antifungal activities against many plant pathogenic fungi. Chitinases hydrolyzes the chitin

polymers (Van Aalten et al., 2000) which are the main structural components of fungal cell wall resulting in a weakened cell wall and rendering fungal cells osmotically sensitive (Jach et al., 1995).

Next to the local resistance, plants can evolve a systemic resistance which requires a signal that is transferred through the plant. This phenomenon is known as systemic acquired resistance (SAR) and a known possible inducer of SAR is the phytohormone SA (Durrant & Dong, 2004). SAR is based on the changes in gene expression and leads to systemic synthesis of phytoalexin and pathogenesis-related proteins (PR proteins) as well as to an increased responsiveness of the tissue to further pathogen attack.

1.2 Phytohormones in plant defense responses

Plant hormones are a structurally unrelated collection of small molecules derived from various essential metabolic pathways. These molecules act as important regulators of growth and mediate responses to both biotic and abiotic stresses.

1.2.1 Salicylic acid: biosynthesis and signaling in plants

Upon infection of plants with biotrophic pathogens, the biosysnthesis of the phytohormone SA is induced. Increased SA levels lead to transcriptional reprogramming involving the induction of up to 2000 genes. The defense gene *PR-1* has been used as a marker gene for the whole defense response (Durrant & Dong, 2004, Glazebrook, 2005). Two pathways of SA biosynthesis have been shown to be active in plants. Plants can synthesize SA from cinnamate produced by the activity of phenylalanine ammonia lyase (PAL) (Chen et al., 2009, Lee et al., 1995; Mausch-Mani and Slusarenko, 1996). Silencing of *PAL* genes in tobacco or chemical inhibition of PAL activity in Arabidopsis, cucumber and potato reduces pathogen-induced SA accumulation (Meuly et al., 1995, Coquoz et al., 1998, Mausch-Mani and Slusarenko, 1996). Genetic studies, on the other hand, indicate that the bulk of pathogen-induced SA is produced from isochorismate (Wildermuth et al., 2001a). Arabidopsis contains two *ICS (isochorismate synthase)* genes encoding *SID2*, and *ICS2.* Figure 1 depicts the pathway of SA biosynthesis (Wildermuth et al., 2001a, Chen et al., 2009) on the left and SA signaling (Pieterse et al., 2009) on the right.
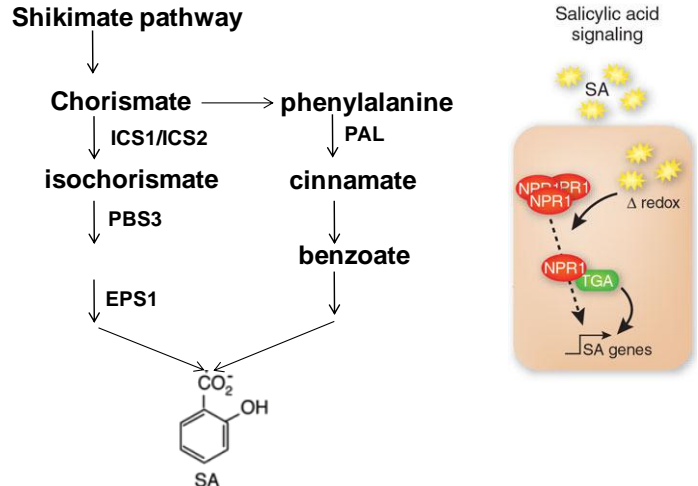
Figure 1 Simplified scheme of SA biosynthesis and signaling in plants

Isotope feeding experiments suggest that plants synthesize SA from cinnamate produced by PAL (El-Basyouni et al., 1964). Genetic studies have indicated that the bulk of SA is produced from isochorismate (Wildermuth et al., 2001a). The recently identified *PBS3* and *EPS1* are important for pathogen-induced SA production and may encode enzymes catalyzing reactions in the synthesis of a precursor or regulatory molecule for SA biosynthesis. SA accumulation changes the cellular redox potential, resulting in the reduction of the NPR1 oligomer to its active monomeric form which is then translocated into the nucleus where it functions as a transcriptional co-activator of TGA transcription factors. (Pieterse et al., 2009)

In the absence of SA, NPR1 (NONEXPRESSOR of PR GENES1) is localized in the cytoplasm, where it forms multimers. When SA levels increase, a redox change takes place in the cell (Mou et al., 2003) and the NPR1 oligomers dissociate into monomers due to reduction of disulfide bonds holding the monomers together. The monomers then enter the nucleus, where they function as transcriptional co-activators of bZIP transcription factors of the TGA family.

1.2.2 Jasmonic acid: biosynthesis and signaling in plants

The oxylipin JA and its metabolites, collectively known as jasmonates, are known to be plant signaling molecules mediating biotic and abiotic stress responses apart from playing important roles in the aspects of plant growth and development (Wasternack, 2007). In higher plants, JA is synthesized via the octadecanoid pathway (Figure 2). JA can be conjugated to form JA-IIe (active form) or converted to the volatile methyl-JA. Increased JA synthesis in response to pathogen attack, like *B. cinerea,* leads to an induction of defense genes such as *PDF1.2* (P*lant Defensin 1.2*). Concomitant activation of JA and ET response pathways is required for the induction of *PDF1.2 (*Penninckx et al., 1998*).* In contrast, ET is not required for the expression of *VSP1* (*Vegetative storage protein1*; Glazebrook, 2005), which is induced after wounding. Most JA responses are mediated through the F-box protein COI1 (CORONATINE INSENSITIVE 1).
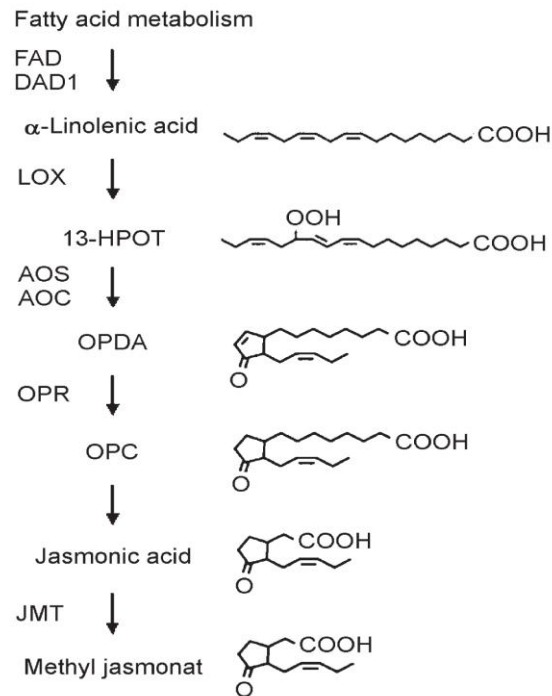
Figure 2 Simplified scheme of jasmonate biosynthetic pathway in *Arabidopsis*

Enzymes involved in biosynthesis of Jasmonate: fatty acid desaturase 3, 7 and 8 (FAD); phospholipase A1 (DAD1); lipoxygenase (LOX); allene oxide synthase (AOS); allene oxide cyclase (AOC); OPDA reductase (OPR); jasmonic acid carboxyl methyl-transferase (JMT) (Turner et al., 2002).

The jasmonate response requires SCF^{COI1} – dependent degradation of repressors much like SCF^{TIR1} targets the AUX-IAAs. JAZ proteins are degraded in a proteasome-dependent manner upon jasmonate perception by the F-box protein COI1. Based on genetic evidence that JAZ proteins negatively act on the JA pathway and the finding that JAZ proteins interact with the JA-induced transcription factor MYC2, it was proposed that JAZ proteins interfere in a JA-modulated manner with MYC2 activity (Chini et al., 2007, Fernández-Calvo et al., 2011, Song et al., 2011). Degradation of JAZ leads to the activation of JA-inducible defense genes like *VSP2* and *PDF1.2*. Pauwels and co-workers showed that the JAZ proteins recruits co-repressor TOPLESS (TPL) and TPL-related proteins (TPRs) through an adaptor protein designated Novel INteractor of JAZ (NINJA) and that both the NINJA and TPL proteins function as negative regulators of jasmonate responses.
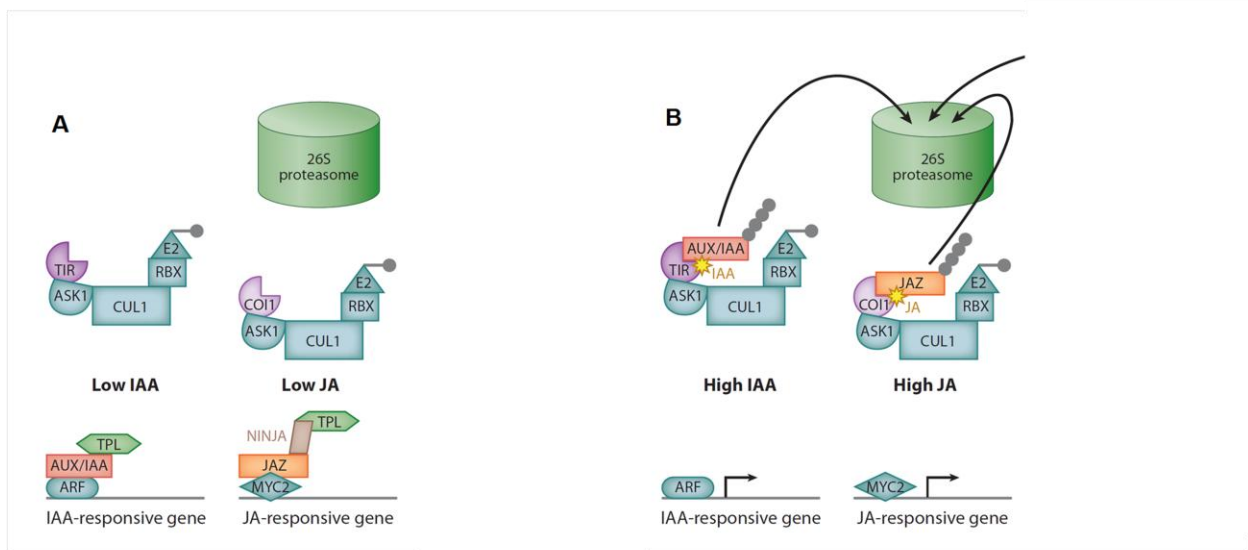
Figure 3 Signaling cascades including similarities between Auxin (IAA) and JA downstream signaling pathways (Robert-Seilaniantz et al., 2011).

(A) Inactive state of IAA and JA pathways. The negative regulators (AUX-IAA and JAZ) bind to the positive regulators (ARF and MYC2) and inactivate these transcription factors. The repression is mediated through the co-repressor TOPLESS (TPL). TPL is able to bind directly to AUX-IAA whereas it requires NINJA to bind to JAZ proteins.
(B) Active state of IAA, and JA pathways. Upon perception of the active hormones, AUX-IAA and JAZ are glued to the IAA and JA receptors- TIR1 and COI1, resp. and the degradation of the negative regulators by the 26S proteasome is triggered.

1.2.3 Ethylene: biosynthesis and signaling in plants

The plant hormone ethylene is involved in many aspects of the plant life cycle, including seed germination, root hair development, root nodulation, flower senescence, abscission, and fruit ripening (Johnson & Ecker, 1998). The biosynthetic pathway of ET was unraveled to a large extent by Yang and co-workers in 1970-1980s (Kende, 1993). The ACC Synthase (ACS) and ACC Oxidase (ACO) are the key enzymes in ET synthesis. It is synthesized from methionine which is converted to S-adenosyl-methionine (AdoMet) by the enzyme S-AdoMet synthase (ADS). AdoMet is converted by the enzyme ACS to 5' –methylthioadenosine (MTA), which is converted back to methionine via the Yang cycle and to 1-aminocyclopropane-1-carboxylic acid (ACC), the precursor of ET. ACC is finally oxidized by ACC oxidase (ACO) to form ET. The rate limiting step in ET biosynthesis is the conversion of AdoMet to ACC by ACS. Various signals modulate ET levels by regulating ACS protein levels. This is accomplished by the action of E3

enzyme of the BTB type (broad-complex, Tramtrack and bric-a-brac). Three BTB proteins, called ETHYLENE OVERPRODUCER1 (ETO1), ETO1-like1 (EOL1) and EOL2, are responsible for promoting degradation of ACS proteins via the ubiquitin-26S-proteasome pathway (Wang et al., 2004). They also reported that ETO1 interact directly with both ACS5 and CUL3 using an *in vitro* pull-down assay, and, in the case of ACS5, also a yeast two-hybrid assay. Together, these studies suggest that ETO1 acts as a substrate-specific adaptor protein for ACS5, and possibly for other ACS isoforms, to target it for degradation by the 26S proteasome. Moreover, in Arabidopsis, previous studies provide explicit indications that protein phophorylation regulates the turnover of the ACS proteins (Chae & Kieber, 2005, Liu & Zhang, 2004). Findings from Liu (2004) suggests that MPK6-mediated phosphorylation inhibits the degradation of AtACS2 and AtACS6 proteins and that both enzymes are stabilized in response to pathogens and other stresses through direct phosphorylation by MPK6 (Chae & Kieber, 2005).

ET is perceived by a two-component protein kinase receptor. The *Arabidopsis* genome encodes five ET receptors: ETR1, ERS1, ETR2, ERS2 and EIN4. These are localized in the endoplasmic reticulum (ER) and negatively regulate ET signaling. The physical interaction between the receptors and CTR1 in the absence of ET keeps the downstream signaling components, EIN2 and EIN3, inactive (Stepanova and Alonso, 2009). ET binding causes inactivation of the receptor-CTR1 complex and the accumulation of EIN3 and EIN3-like transcription factors in the nucleus (Guo and Ecker 2003). EIN2 activates EIN3 via an unknown mechanism. In the absence of ET, SCF$^{ETP1/2}$ (EIN2 targeting protein1, ETP1 and ETP2) promotes degradation of EIN2 thereby attenuating the ET response (Qiao et al., 2009). ET decreases the *ETP* expression hence permitting the accumulation of EIN2. Similarly, another pair of F-box proteins called EIN3-BINDING F-BOX1 (EBF1) and EBF2 promotes degradation of EIN3 at low levels of ET (Figure 4A). As the levels increase EIN3 degradation is reduced and ET regulated transcription is activated (Figure 4B). EIN3 is a short lived transcription factor stabilized by ET and accumulates in nuclei after an increase in ET levels (Gagne et al., 2004, Guo & Ecker, 2003). The expression of many defense target genes, such as *ORA59* and *ERF1*, are regulated by EIN3. There are 5 homologs in Arabidopsis (EIN3 like 1-5), with EIL1 most closely related to EIN3 (Chao et al., 1997). EIL1 is capable of complementing the *ein3* mutation resulting in constitutive activation of ET response. EIN3 can bind directly to the promoter of EBF2, suggesting negative feedback regulation desensitizing ET signaling (Konishi & Yanagisawa, 2008).
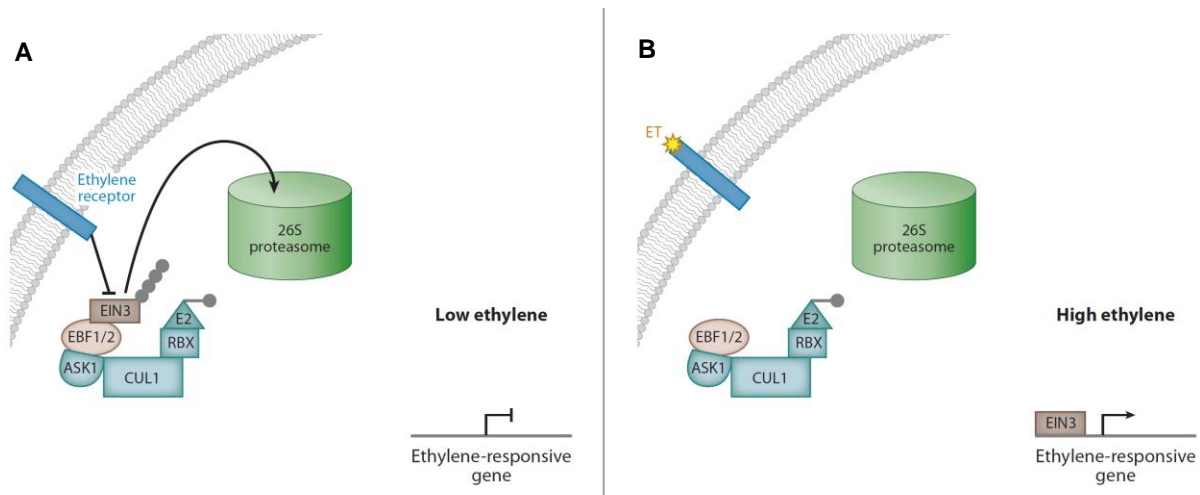
Figure 4 Scheme of ET signaling in *Arabidopsis* (Robert-Seilaniantz et al., 2011)

(A) Inactive state of ET signaling. The ET receptors negatively regulate the ET pathway. EIN3 is a transcription factor positively regulating the signaling. In the absence of ET, EIN3 is ubiquitinated and targeted to proteasome degradation by the F-box proteins EBF1 and EBF2.

(B) Active state of ET signaling. Upon ET perception, the ET receptor cannot repress the signaling pathway. EIN3 is not ubiquitinated and therefore ET signaling pathway is induced leading to the expression of ET-responsive genes.

Overexpression of *ERF1* enhances resistance against *B. cinerea* and increases susceptibility to the hemibiotroph *Pst* (Berrocal-Lobo et al., 2002, Blanco et al., 2005). *ein2* seedlings are known to be impaired in all FLS2-mediated responses (Boutrot et al., 2010). Chen *et al*., 2009 has shown that *ein3-1/eil1-1* and *ein2* mutants exhibit enhanced resistant to *Pst* inspite of suppressed FLS2 signaling.

1.2.4 Abscisic acid: biosynthesis and signaling

ABA is an isoprenoid that controls seed germination and further developmental processes and induces plant responses to stresses such as salt, cold, drought etc. Figure 5 depicts a simplified scheme of ABA biosynthetic pathway adapted from (Nambara & Marion-Poll, 2005). Many genetic studies of the mutants have suggested that the ring transformations occur first to produce ABA aldehyde and then the oxidation of aldehyde leads to the final step of ABA synthesis.

Zeaxanthin

ZEP | VDE

Antheraxanthin

ZEP | VDE

Violaxanthin

NSY?

Neoxanthin

Isomerase?

9'-cis-Neoxanthin   9'-cis-Violaxanthin

Xanthoxin

ABA2

Abscisic aldehyde

AAO3 ← MoCo

Abscisic acid
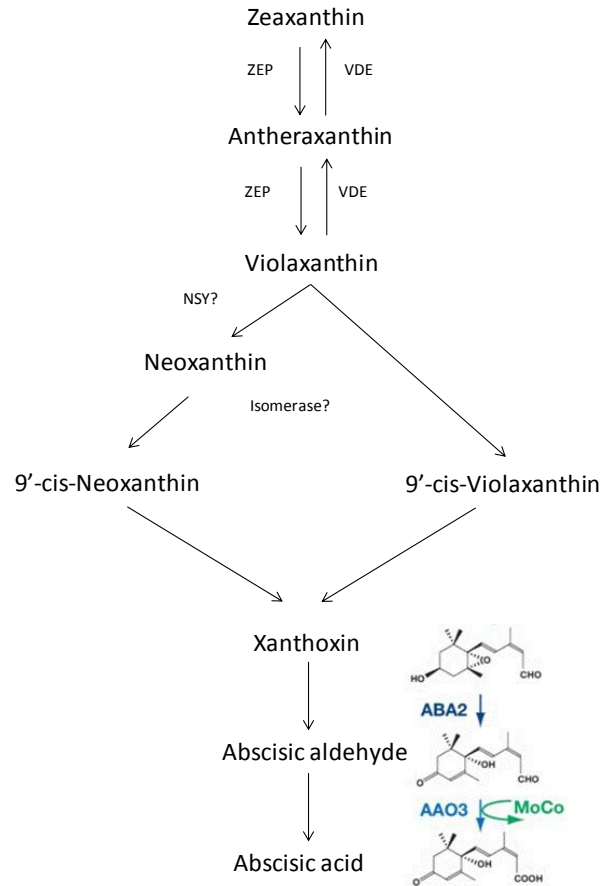
Figure 5 Simplified scheme of ABA biosynthesis

Violanxanthin is synthesized by zeaxanthin epoxidase (ZEP). A reverse reaction occurs in chloroplast in high light conditions catalysed by violaxanthin de-epoxidase (VDE). Cleavage of *cis*-xanthophylls is catalysed by a family of 9-cis-epoxycarotenoid dioxygenases (NCED). Xanthoxin is then converted by a short-chain alcohol dehydrogenase (ABA2) into abscisic aldehyde, which is oxidized to ABA by AAO3 (abscisic aldehyde oxidase).

ABA signaling is known to be regulated by at least two different pathways (Figure 6). One pathway involves the family of PYRABACTIN RESISTANCE (PYR)/REGULATORY COMPONENT OF ABA RECEPTOR (RCAR) receptor proteins (Cutler et al., 2010 ,Hubbard et al., 2010, Nishimura et al., 2010). ABA binds to PYLs (PYRABACTIN RESISTANCE LIKE) and causes a conformational change generating a new protein-protein interaction enabling ABA-bound PYLs to bind PP2Cs (Protein/threonine Phosphatase 2Cs) and inhibit their active sites. The negative regulation on PP2Cs' targets (SnRK2s) is alleviated leading to the activation of ABA signaling (Figure 6 A). Another possible way of ABA signaling is via proteasomal degradation. KEG (KEEP ON GOING) is a RING-fingure ubiquitin E3 ligase which degrades the transcriptional activator ABI5 in the absence of ABA (Figure 6 B). ABI5 accumulation is induced

by ABA through transcriptional activation and enhanced protein stability. Notably, AFP (ABI 5 binding protein) is a novel negative regulator promoting ABI5 proteasomal degradation (Liu & Stone, 2010, Lopez-Molina et al., 2003, Stone et al., 2006).
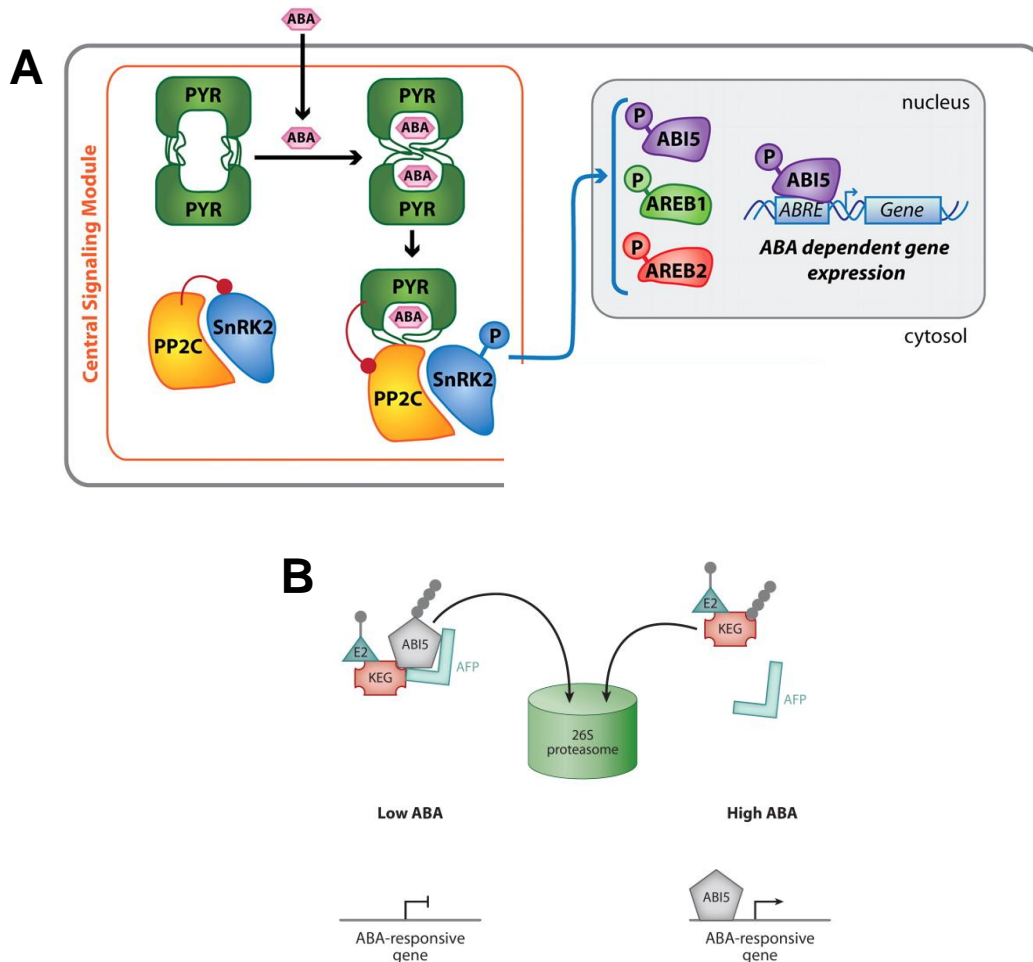
Figure 6 ABA signaling pathway

(A)   In the absence of ABA, PP2Cs inhibit protein kinase (SnRK2) activity through removal of activating phosphates. ABA is bound by intracellular PYR/PYL dimers, which dissociate to form ABA receptor–PP2C complexes. Complex formation therefore inhibits the activity of the PP2C in an ABA-dependent manner, allowing activation of SnRK2s.

(B)   Proteasome-mediated ABA signaling. At low ABA levels, the transcription factor ABI5 is targeted for ubiquitine mediated degradation, possibly through interaction with the negative regulator AFP and the RING-finger ubiquitin E3 ligase KEG. At high ABA levels, KEG is ubiquitinated and targeted for degradation, releasing ABI5. AFP is predicted to be unable to bind to ABI5 when ABA levels are high. The mechanism by which ABA concentration abolishes AFP binding to ABI5 is still unknown (Robert-Seilaniantz et al., 2011).

Negative or positive impact of ABA on the outcome of plant-microbe interaction depends on the pathogen lifestyle. ABA negatively regulates defense against the soil-borne fungus *F. oxysporum*, by antagonising JA-ET signaling pathway (Anderson et al., 2004). Also,

pretreatment of potato plants with ABA increased susceptibility to *Phytophthora infestans* and *Cladosporium cucumerinum* (Henfling et al., 1980). In mutants deficient in ABA biosynthesis, the resistance to the biotrophic pathogens, *Hyaloperonospora parasitica* and *Blumeria graminis* is enhanced (Jensen et al., 2008, Mohr & Cahill, 2003).

1.2.5 Cytokinin: biosynthesis and signaling

Cytokinins (CKs) are derived from N_6-substituted adenine and regulate root and shoot growth and leaf longevity. In addition, CK has an important role in the formation of nitrogen-fixing nodules and other plant microbe interactions (Frugier et al., 2008, Murray et al., 2007). The first step in CK biosynthesis is the production of N6-(2-isopentenyl) adenine (iP) riboside 5' –tri-, 5' – di- or 5' –monophosphate by the enzyme adenosine phosphate-isopentenyl-transferase (IPT). Active CKs are produced by a phosphoribohydrolase enzyme that converts the nucleotide to the free base (Kurakawa et al., 2007). The regulation of CK levels is complex and involves changes in both synthesis and metabolism. Role of other hormones, auxin and ABA, have been described recently in the regulation of CK biosynthesis.
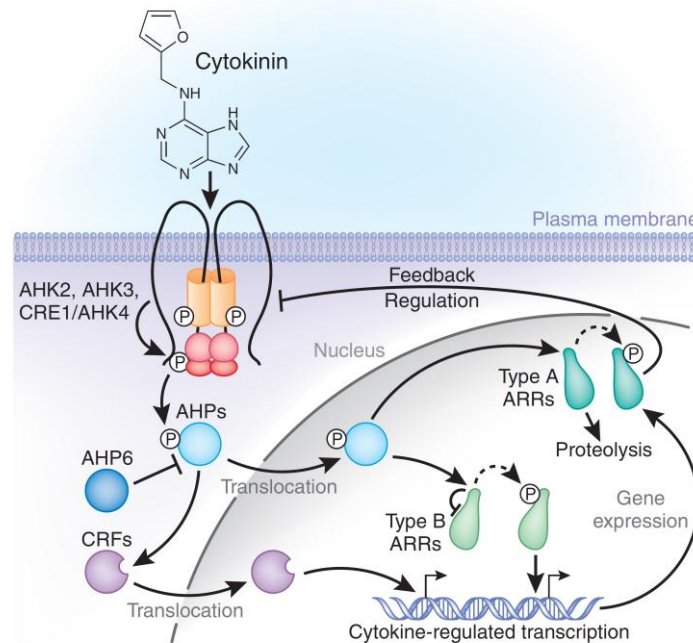
Figure 7 Cytokinin signaling pathway (Santner et al., 2009)

Cytokinin is perceived by the AHK plasma membrane receptors. Cytokinin signal is further amplified by phophorelay events starting from AHKs, which lead to the activation and subsequent nuclear translocation of AHP proteins. AHP proteins transfer the phosphoryl group to type A or type B ARR proteins. The former act as repressors of cytokinin signaling, whereas the latter act as positive transcriptional regulator of cytokinin-induced genes, including those

encoding type A ARRs. CRF proteins are also activated by cytokinin, and after translocation to the nucleus they act as activators of cytokinin-regulated genes.

Regulation of gene expression modulated by CK perception is poorly understood. Upon perception, autophosphorylation of the receptors takes place and then the phosphorylation is transferred via a phospho-relay to Arabidopsis histidine phosphotransfer proteins (AHPs). Phosphorylated AHPs are then relocated to the nucleus where their phosphate group is transferred to the response regulators (ARR) (To et al., 2007). Two types of ARRs are known: Type A and Type B. Type As are negative regulators of CK signaling pathway and are induced by CK, indicating negative feedback of CK on its own signaling. Type Bs are positive regulators and upon phosphorylation Type B ARRs bind to the DNA and activate gene expression (Muller & Sheen, 2007, Perilli et al., 2010).

Using mutant and transgenic Arabidopsis lines it has been previously demonstrated that high CK levels correlate with the increased resistance to *Pseudomonas syringae pv. tomato DC3000* (*Pst)*, increased SA biosynthesis and *PR1* expression. By contrast, plants with low CK levels are more susceptible to *Pst* (Choi et al., 2010). Suppression of high CK accumulation by overexpression of CKX1 (CYTOKININ OXIDASE/DEHYDROGENASE 1) can affect both CK and *PR1* expression. Direct interaction between TGA3 and ARR2 has been reported suggesting that TGA3 recruits ARR2 to defense gene promoters when SA signaling is activated.

Production of phytohormones and their mimics by plant pathogens has been well documented. Many microbes involved in pathogenic interactions can produce various phytohormones (Costacurta & Vanderleyden, 1995). To date, production of cytokinin (CK) (Murphy et al., 1997), abscisic acid (ABA); (Siewers et al., 2006), auxin (Spaepen et al., 2007), jasmonic acid (JA) (Mittal & Davis, 1995), and ethylene (ET) (Weingart et al., 2001) have been reported in different bacterial and fungal species. For example, ET and indolic compounds related to auxin are known to be produced by *Ralstonia solanacearum* (Valls et al., 2006). Marumo et al., (1982) demonstrated that the necrotrophic fungus *Botrytis cinerea* produces ABA and CK. Microbial pathogens have also developed the ability to manipulate the defense-related regulatory network of plants by producing phytohormones or their functional mimics. For example, many strains of *P. syringae* produce coronatine (COR), a mimic of the bioactive JA-isoleucine (Fonseca et al., 2009). COR is described as a multifunctional suppressor of plant immunity by activating or modulating the JA signaling to suppress SA signaling (Laury-Berry et al., 2006). In addition to producing hormones themselves pathogens induce hormone production by their host. O'Donnell

et al (2003), Schmelz et al (2003) showed that type III effectors (TTEs) delivered by *P. syringae* pv. *tomato* (*Pst*) DC3000 are able to induce auxin and ABA production which acts antagonistically on the plant defense pathways (Adie et al., 2007, de Torres-Zabala et al., 2007, Mohr et al., 2007). Further support for effector-driven increase in ABA as virulence mechanism is derived from the enhanced resistance to bacterial and fungal pathogens in ABA biosynthetic mutants (Asselbergh et al., 2007, de Torres-Zabala et al., 2007) and enhanced susceptibility in NCED5 (*9 cis-epoxycarotenoid dioxygenase 5*) overexpressors (Fan et al., 2009).

1.3 Verticillium species

Verticillium species belong to the phylum Ascomycota. The genus includes six plant pathogenic species (Barbara & Clewes, 2003) of which *V. dahliae* and *V. albo-atrum* attack a high number of host species. *Verticillium* spp are soil-borne phytopathogenic fungi causing vascular diseases in various plant species in the moderate and subtropic regions (Pegg & Brady, 2002). Many important crop plants like sunflower, cotton, potato, tomato, olive trees and woody plants are infected by *V. dahliae*. Disease symptoms of these plants vary from species to species and include growth retardation, wilt (e.g. in case of *V. dahlia*), chlorosis, necrosis and discoloration of the vascular tissue (Beckman, 1987). The host range of *V. longisporum* is mainly restricted to cruciferous hosts (Zeise & Von Tiedemann, 2002).

1.3.1 Verticillium longisporum

V. longisporum was described as a variant to *V. dahliae* by (Stark, 1961). Karapapa et al (1997) proposed *V. longisporum* as a new species, based on molecular and morphological differences. It was suggested to be a heterozygous diploid of *V. dahliae* and *V. albo-atrum*. In further studies it was shown that the spores of *V. longisporum* are twice as long as *V. dahliae* and the morphology of the microsclerotia also differs (Zeise & Tiedemann, 2001). The DNA content in *V. longisporum* is usually twice as high as that found in other non-longispored *Verticillium* isolates (Steventon et al., 2002). A recent phylogenetic study based on seven nuclear loci showed that *V. longisporum* may have evolved in different ways (Inderbitzin et al., 2011). They have suggested that it originated three times in independent hybridization events with all hybrids sharing *V. dahliae* and a common parent of a so far unknown taxon. *V. longisporum* infects predominantly crucifers and belongs to the most important diseases of *Brassicaceae*, in particular oil seed rape (Zeise & Von Tiedemann, 2002, Zhou et al., 2006) which are not infected by *V. dahliae*. The yield depression can be expected between 10-15% based on soil and climatic conditions (Dunker et al., 2008). *V. longisporum* does not cause wilting in the

infected plants rather the symptoms includes chlorosis and necrosis of the lateral branches and leaves, brown coloration of the stems and premature ripening. The symptoms of infection are visible at late stages of the disease and can be easily confused with the symptoms of senescence or infection by other fungi (Dunker et al., 2008).

1.3.2 Disease cycle

The infection cycle of *V. dahliae* and *V. longisporum* is quite comparable (Johansson et al., 2006). As already described, these pathogens possess a hemibiotrophic life cycle (Figure 8). It starts with microsclerotia which are abundant in contaminated soils and which can survive for more than a decade (Wilhelm, 1955). The microsclerotia are dark melanized thick-walled hyphae. The germination of microsclerotia is stimulated by root exudates (Mol et al., 1995) secreted from the root tip and the root hair. After germination *V. longisporum* hyphae get in contact with the root hairs and form a hyphal network (Eynck et al., 2007). The hyphae enter the roots through the junction of epidermal cells or through direct penetration of the cells. They grow inter- and intracellular to the central cylinder where they have to pass the endodermis (Eynck et al., 2007). It is proposed that the infection takes place in young parts of the roots where no endodermis is developed yet or at sites of damage of this barrier (Bishop & Cooper, 1983, Pegg & Brady, 2002). After entering the xylem, the fungus stays most of its life cycle in this mal-nutritional environment. It spreads through the plant by generating conidia which are transported upwards with the vascular stream in the plant (Beckman, 1987). These spores can be trapped at the end of vessel cells where they germinate and invade the neighboring vessels (Beckman, 1987). In contrast to *V. dahliae*, *V. longisporum* is restricted to individual vessels, which may be the cause of the absence of wilting symptoms in these infections (Eynck et al., 2007). At the later stages of the infection cycle, the pathogen starts colonizing the non-vascular tissue (necrotrophic or saprophytic phase) and forms microsclerotia on the senescing and dead tissue.
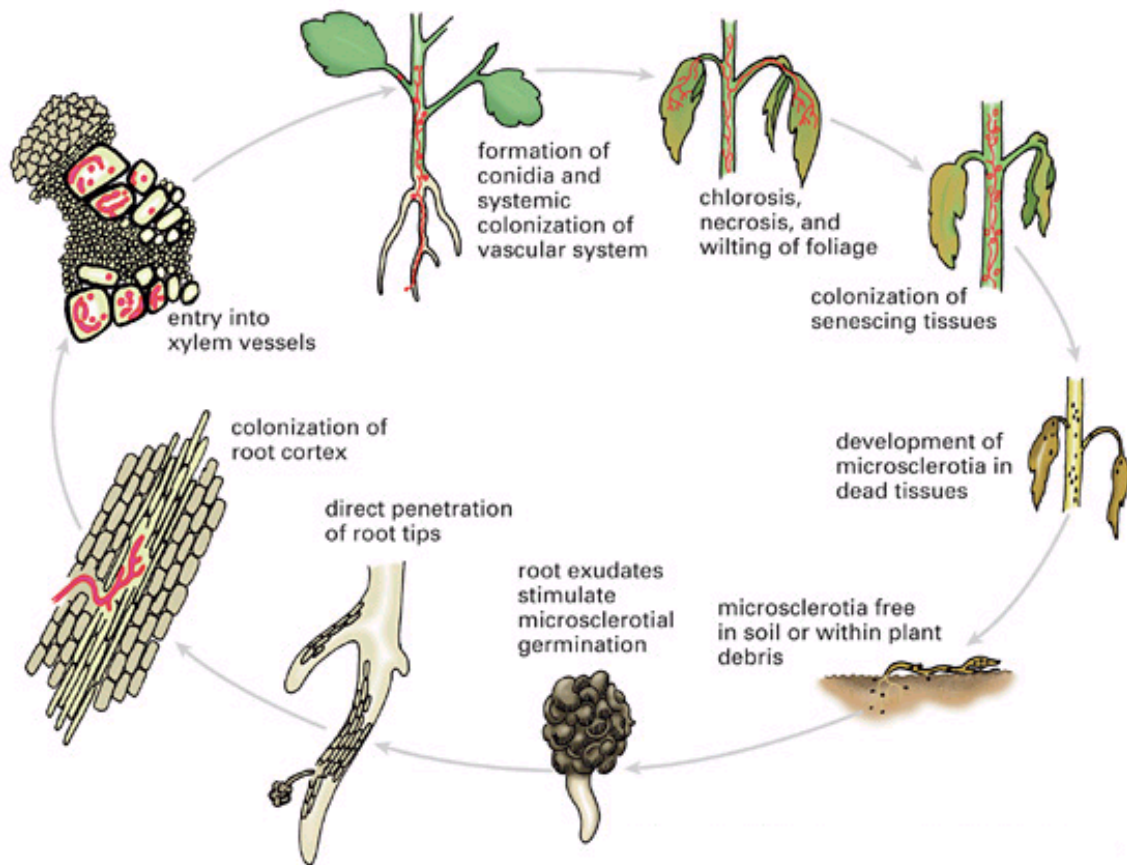
Figure 8 Disease cycle of Verticillium species (Berlanger & Powelson, 2000)

1.3.3 Disease control

Verticillium-induced diseases are difficult to control. Because of the very high viability of microsclerotia and broad host range of *Verticillium* species, the fungus can persist in the soil for many years. At early stages of the infection, the pathogen grows and propagates inside the vascular tissue of the plants which make any chemical control impossible without killing the plant. The microsclerotia in the soil are resistant against many chemicals (Berlanger & Powelson, 2000, Pegg & Brady, 2002). There are different efforts in the resynthesis of resistant plants by interspecific hybridization of *Brassica rapa* and *Brassica oleracea.* In *B. oleracea* different lines are known to be resistant against *V. longisporum*, which are therefore promising candidates for hybridization (Rygulla et al., 2007). Several specific loci have been identified that are involved in resistance against *Verticillium* wilt. For example, *Ve* locus provides resistance in tomato ((Schaible et al., 1951)). *Ve1* and *Ve2* genes encode leucine –rich repeat (LRR) proteins that belong to the class of receptor-like proteins (RLP; (Kruijt et al., 2005)). A separate locus

(VET1: *V. dahlia* tolerance) controlling *V. dahlia*-induced disease in Arabidopsis has been found (Veronese et al., 2003).

1.4 Plant defense against *Verticillium* infection

The knowledge about genetic bases of defense against *V. longisporum* is insufficient. (Ratzinger et al., 2009) have shown that SA and its glucoside (SAG) are enriched in infected xylem sap of root and hypocotyls of *B. napus* after *V. longisporum* infection. Induction of different proteins in the apoplast of infected *B napus* has been demonstrated (Floerl et al., 2008). Some of these protein were identified as endochitinase, peroxidase, PR4-proteins and α-1,3-glucanase. Additionally, it could be shown that the xylem sap from infected plants leads to reduction in fungal growth which supports the idea that plants secreted some defense proteins in response to fungal infection. Several studies using Arabidopsis mutants were done using an *in vitro* infection system where Arabidopsis seedlings were grown axenically and inoculated on MS medium supplemented with sugar while the response of soil-grown *Arabidopsis* plants to *V. longisporum* infection still remains elusive. One study reported that *Arabidopsis* mutants impaired in SA pathway (*eds1-1*, *nahG*, *npr1-3*, *pad4-1* and *sid2-1)* did not show enhanced susceptibility towards *V. dahliae*. In contrast *npr1-1* mutant showed enhanced *V. dahliae* susceptibility and decreased responses after ACC and MeJA pretreatment. Expression of the SA-dependent *PR1*, *PR2* and ET-dependent *PR4* was enhanced after 7 dpi. It has been reported by (Veronese et al., 2003) that impairment in the SA or JA dependent signaling did not cause hypersensitivity to *V. longisporum* infection, whereas ET insensitivity led to reduced chlorosis and ABA deficiency led to reduced anthocyanin accumulation. Floerl et al., 2012 suggested that *V. longisporum* enhances its virulence by down regulation and delay of induction of plant defense genes for e.g transcript levels of germin-like protein GLP3 and lectin-like, chitin inducible protein (CILLP) were reduced at early time points in the apoplast of infected plants.

Arabidopsis and *Brassica* are very closely related based on average coding domain sequence similarity of 86% (Parkin et al., 2005). *Arabidopsis* is a model system with short generation time and multiple mutants generated in defined pathways. Various publications showed that it is a suitable host to study the *V. longisporum* pathosystem (Floerl, 2010; Haffner et al., 2010; Johansson et al., 2006). In *Arabidopsis, Verticillium* infection leads to stunting of the aerial parts, comparable to the stunting of the stem of *B. napus* plants in the greenhouse. At later stages, chlorosis and necrosis of the leaves occur. It was already investigated that these symptoms are not related to water clogging or nutrient depletion (Floerl, 2010). In this thesis *Arabidopsis* was

used as a model organism to elucidate several different processes and defense responses against *V. longisporum*.

2 MATERIAL AND METHODS

2.1 Materials

2.1.1 Organisms

Strain	Reference
Agrobacterium tumefaciens GV3101	(Deak et al., 1986)
Botrytis cinerea BMM	Brigitte Mauch-Mani, University of Neuchatel, Switzerland
eGFP-*Vertcillium longisporum* 43	(Deak et al., 1986, Eynck et al., 2007)
Escherichia coli DH5α	(Hanahan, 1983)
Pseudomonas syringae pv maculicola ES4326	(Whalen et al., 1991)
Verticillium longisporum 43	(Zeise & Von Tiedemann, 2002)

2.1.2 Genotypes

Genotype	Description	Reference
aba2-1	ABA-deficient 2 mutant	N156*
acx1/5	JA-biosynthesis mutant	(Schilmiller et al., 2007)
coi1-1	Knock out line lacking COI1, impaired in most JA dependent responses	(Feys et al., 1994, Xie et al., 1998)
coi1-1/nahG	*Col-gl* background	Dr. Mark Zander
coi1-1/sid2-2	*Col-gl* background	This thesis
coi1-t	T-DNA insertion within COI1 gene	(Mosblech et al., 2011)
Col-gl	Wild type	
Columbia, Col-0	Wild type	N1092*
dde2-2	mutation in the ALLENE OXIDE SYNTHASE	(Park et al., 2002)
tir-nbs-lrr class	T-DNA insertion mutant (AT1G57630)	N441305 (This thesis)
ein2-1	ethylene insensitive	(Guzmán & Ecker, 1990)
ein3-1/eil1-2		(Binder et al., 2007)
erf53/erf54		This thesis
etr1-1		Prof. Corne' Pieterse (Bleecker *et al.*, 1988)
fad3,7,8	JA-deficient mutant	(McConn & Browse, 1996)
jar1-1	mutant deficient in JA-Ile biosynthesis	(Staswick et al., 1992)
nahG	Col-0 carrying *NahG* transgene	(Lawton, 1995)
npr1-1		(Cao et al., 1994)
P_{PER21}:*luciferase*	PER21 gene promoter cloned upstream of FIREFLY LUCIFERASE reporter gene (Col-0)	Hella Tappe, 2008
sid2-2	SA biosnthesis mutant	(Nawrath & Métraux, 1999) (Wildermuth et al., 2001a)
sid2-2-gl	*Col-gl* background	This thesis

2.1.3 Enzymes and size markers

Enzymes and size markers	Suppliers
DNAse I	MBI Fermentas
GeneRUler 1kb DNA ladder	MBI Fermentas
BP clonase-Mix	Invitrogen, karlsruhe, Germany
LR clonase-Mix	Invitrogen, karlsruhe, Germany
Biotaq DNA polymerase	Bioline
HiDi Mix	ABI PRISM
iProof High-Fidelity DNA Polymerase	BioRad
Reverse transcriptase H-	MBI Fermentas
Restriction endonucleases	MBI Fermentas, New England Biolabs
RNase A (DNAse free)	Qiagen
Advantage 2 polymerase Mix	Clonetech

2.1.4 Kits

Kits	Suppliers
BigDye Trminator Cycle Sequencing Ready Reaction Kit v.3.1	Perkin-Elmer Corporation
DNeasy Kit	Quiagen (Hilden, Germany)
Nucleo Spin Extract II	Macherey-Nagel
Nucleo Spin Plasmid	Macherey-Nagel

2.1.5 Buffers and solutions

Buffers/Solutions	Components and Concentration
Buffer I for alkaline lysis	50 mM Tris-HCl, pH 8.0, 10 mM EDTA, 100 µg/µl RNase A
Buffer II for alkaline lysis	0.2 M NaOH, 1 % (w/v) SDS
Buffer III for alkaline lysis	29.4 g potassium acetate, 5 ml formic acid, water up to 100 ml
DNA Extraction Buffer	200 mM tris HCl pH 7,5; 250 mM NaCl; 25 mM EDTA pH 8,0;

	0,5 % SDS
HSB	1.2 M NaCl, 0.8 M tri-sodium-citrate
MEN (10x)	200 mM MOPS, 50 mM NaOAc, 10 mM EDTA, pH 7.0 with 1 M NaOH
RNA loading buffer (3x)	100 µl bromphenolblue/xylenecyanol, 80 µl 0.5 M EDTA, pH 8.0, 3333µl 10x MEN, 1200 µl glycerol (100 %), 4286 µl formamide, 1001 µl fomaldehyde, add 6 µl EtBr per ml loading buffer direct before using
TAE (20 x)	0.8 M Tris, 2.3 % (v / v) acetic acid, 20 mM EDTA
TE	10 mM Tris, 1 mM EDTA, pH 7.5
Trizol buffer	380 ml/l phenol with 0.1M citric buffer, pH 4.3 saturated; 0.8 M guanidinium thiocyanat, 0.4 M ammonium thiocyanat, 33.4 ml Na-Acetate, 3 M, pH 5.2, 5% glycerol

2.1.6 Media

Media	Components and Concentrations/ Suppliers
CPD	Czapek Dox (SIGMA, Steinheim, Germany)
LB	10 g/l tryptone, 5 g/l yeast extract, 10 g/l NaCl, pH 7.0 (NaOH)
MS	4.4 g/l MS medium, pH 5.7 with KOH, 6.8 g/Llselect agar
PDB	Potato Dextrose Broth (SIGMA, Steinheim, Germany)

	20 g/l tryptone,
dYT	10 g/l yeast extract,
	10 g/l NaCl
	10 g/l tryptone,
LB	5 g/l yeast extract,
	10 g/l NaCl

2.1.7 Additives

Additives	Working Concentration	Stock Solution, Solvent
Cefotaxim	500 mg /l	250 mg/ml, H_2O
Kanamycin	50 mg/l	50 mg/ml, H_2O
Gentamycin	25 mg/l	25 mg/ml, H_2O
Rifampicin	50 mg/l	10 mg/ml, H_2O
MeJA	50 µM	0,5 M, EtOH

2.1.8 Plasmids

Plasmids	Description	Reference/Source
pB2GW7	gateway™ vector for plant transformation, contains the CaMV 35S promoter and a BASTA resistance gene as selection marker, *spnr*	(Karimi et al., 2002)
pB2GW7-HA	gateway™ vector for plant transformation, contains the CaMV 35S promoter, a 3× HA-tag (N-terminal), and a BASTA resistance gene as selection marker, *spn*	C. Thurow, personal communication
pB2GW7-HA-*AtERF54*	pB2GW7-HA derivative containing the *AtERF54* coding sequence	This thesis
pDONOR201	gateway™ entry vector for cloning of PCR fragments, *km*	Invitrogen
pDONOR201-AtERF54		This thesis
pSK-T	Cloning and sequenicing vector; pBluescriptII SK (Stratagene, Cedar Cree, Texas) was restricted with EcoRV and treated with terminal transferase in presence of ddTTP; lacZα, *ampr*	Guido Kriete, unpublished
pSK-T_actin8	pSK-T vector with actin8 insert (genomic DNA); ampr	Katja Rindermann, unpublished

2.1.9 Oligonucleotides

Oligonucleotides for RT-PCR

Primer	Sequence 5'→3'
act8fwd	GGT TTT CCC CAG TGT TGT TG
act8rev	CTC CAT GTC ATC CCA GTT GC
AT1G33960 (AIG1)	QT00873117*
AT1G57630 (TIR-NBS-LRR class)	QT00882448*
AT1G60190 (Armadillo)	QT00883547*
AT1G74590 (GSTU10)	QT00893396*
AT2G20880 (AtERF53)	QT00753662*
AT3G01420 (AtALPHA-DOX)	QT00772737*
AT3G13790 (AtFRUCHT1)	QT00769055*
AT4G05100 (AtMYB74)	QT00799015*
AT4G28140 (AtERF54)	QT00816893*
AT4G29740 (CKX4)	QT00818034*
AT4G33550 (LTP)	QT00820764*
AT5G59780 (MYB59)	QT01134791*
Olg70	CAG CGA AAC GCG ATA TGT AG
Olg71	GGC TTG TAG GGG GTT TAG A
PDF1.2 RT fwd	CTTGTTCTCTTTGCTGCTTTC
PDF1.2 RT rev	CATGTTTGGCTCCTTCAAG
PER21	QT00718277*
PR1 fwd	CTG ACT TTC TCC AAA CAA CTT G
PR1 rev	GCG AGA AGG CTA ACT ACA ACT AC
UBQ5fwd	GAC GCT TCA TCT CGT CC
UBQ5rev	GTA AAC GTA GGT GAG TCC A
VSP2 fwd RT	CAAACTAAACAATAAACCATACCATAA
VSP2 rev RT	GCCAAGAGCAAGAGAAGTGA

*= catalog number of Qiagen for QuantiTect®

Oligonucleotides for genotyping

Primer	Description	Sequence 5'→3'
08409 mod	Gabi-Kat lines	CCATATTGACCATCATACTCATTGC
*drp-tir-class*_LP	GK_431C01	TGTCTCTCACGTTCAGGCTATGC
*drp-tir-class*_RP	GK_431C01	GCTTGTGCGTTTCATTGCTATTTC
*erf53*_LP	SM_3_16589	TGACGACAAATCGCTAACCTTCG
*erf53*_RP	SM_3_16589	TTGAGCCTAGCGGTCTCTCCCCTC
*erf54*_LP	SAIL_73_C12	TCTTGCATGATAGGCAGAGGTCATTATAAC

erf54_RP	SAIL_73_C12	TCCACGTCCCCAAGATCTATGAAG
LB3	SAIL lines	TAGCATCTGAATTTCAATACCAATCTCGATACAC
LBb1	SALK lines	GCG TGG ACC GCT TGC TGC AAC T
Spm32	JIC SM lines	TACGAATAAGAGCGTCCATTTTAGAGTGA

Oligonucleotide for sequencing

Primer	Sequence 5'→3'
pDonor201 (Seq-L1)	TCGCGTTAACGCTAGCATGGATCTC
pDonor201 (Seq-L2)	GTAACATCAGAGATTTTGAGACAC
pB2GW7(-HA) fwd	CACAATCCCACTATCCTTCGCA
pB2GW7(-HA) rev	CATGAGCGAAACCCTATAAGAACC

Oligonucleotide for cloning

Primer	Sequence 5'→3'
At4g28140upGW	GGGGACAAGTTTGTACAAAAAAGCAGGCTTCATGGACTTTGACGAGGAGCTAAATC
At4g28140lowGW	GGGGACCACTTTGTACAAGAAAGCTGGGTCTCAAAAGAAAGGCCTCATAGGACAAG

2.1.10 Consumables

Material	Supplier
Fluted filter	Macherey-Nagel (Düren, Germany)
Aqua-Deco Bodengrund (silica grit)	Vitakraft, Nr. 12262 (Bremen, Germany)
Ton-Granulat für Zimmerpflanzen (clay granulate)	Masterfoods GmbH (Verden/Aller, Germany)

2.1.11 Software

Software	Supplier
Arabidopsis eFP Browser	http://bar.utoronto.ca/efp/cgi-bin/efpWeb.cgi
Bildanalyseprogramm 1.0.4.6	Datinf GmbH (Tübingen, Germany)
Bio-Rad iQ5	BioRad (Munich, Germany)
Chromas 1.55	Technelysium Pty Ltd (Shannon Co. Clare, Ireland)
Clone v7	Scientific and Educational Software (Groningen, Netherlands)
Graphpad Prism 5	http://www.graphpad.com/welcome.htm
LAS AF lite	Leica Microsystems CMS GmbH
NCBI	http://www.ncbi.nlm.nih.gov/
Oligo 4.0	MedProbe (Olso, Norway)
Tair	http://www.arabidopsis.org/

2.2 Methods

2.2.1 *V. longisporum* growth and cultivation

V. longisporum was cultivated in PDB medium supplemented with 0.5 mg l^{-1} cefotaxim. 120ml of PDB was inoculated with glycerol stock solution in a special indented conical flask. The fungal culture was grown for 2-3 weeks on a rotary shaker at 85 rpm and 23ºC in the dark. Sporulation was induced by transferring the mycelium to CPD medium for 2-4 days. The spores were harvested by filtering through Nucleo Bond Folded filters. The flow through was centrifuged at 4000 x g for 10 min at RT. After discarding the supernatant spores were re-suspended in sterile tap water and subsequently washed 2 times. Spore concentration was determined by using Thoma cell counting chamber and diluted to 1 x 10^6 spores ml^{-1} for further infection studies.

2.2.2 Plant growth and cultivation

Arabidopsis seeds were grown either on soil or under sterile conditions on Murashige and Skoog (MS) medium.

For soil grown plants, sterilized seeds were sown on autoclaved soil and stratified for 2 days in the dark at 4 °C. The plants were grown under long day (16 h light/8 h dark) condition in climate chambers at 22 °C, 60 % humidity and light intensity of 120-150 µmol m-2 s-1.

For growth on sterile medium, seeds from all genotypes were surface sterilized and sown on agar plates containing MS medium. 50 µM MeJA was added to the plates in order to segregate homozygous *coi1* population. Plates were stratified for two days in case of *coi1-t and coi1-1* or three days in case of wild-type and other mutants at 4°C in the dark. Plates were incubated subsequently under controlled conditions (22 °C, ~ 140 µmol m^{-2} sec^{-1} PAR; 8-h-light/16-h-dark photoperiod). After two weeks, plants were transferred to boxes containing a 1:1 mixture of silica grit (Vitakraft, Nr 12262, Bremen, Germany) and soil (Archut, Fruhstorfer Erde, T25, Str1 fein) over a layer of seramis (Masterfoods GmbH, Verden/Aller, Germany) and were grown in a short day chamber. Initial watering of the boxes was done with 0.1% of the fertilizer Wuxal (Manna, Düsseldorf, Germany) using a 50 ml needle syringe.

2.2.3 Plant treatments

2.2.3.1 *V. longisporum* infection

For infection of Arabidopsis plants in a soil system, root dip infection method was used. Seeds were sown directly on silica grit:soil mixture (1:1) over a layer of seramis or first on MS plates supplemented with MeJA (Section 3.2.2) and then transferred on silica grit and soil mixture as in case of *coi1* seed population. After stratification at 4 °C for 2 days, plants were grown for three-four weeks under short day conditions in climate chambers. The boxes were covered with transparent hoods to maintain initial humidity. After 7 days the hood was removed and plants were watered at regular intervals with tap water. For the infection, plants were uprooted and the roots were gently rinsed with tap water to remove the residual amount of soil substrate. Roots were then incubated in conidial suspension (10^6 spores ml^{-1}) for 45 min. For mock treatment, roots were incubated in autoclaved tap water and plants were re-planted into the pots containing soil. Plants were then grown under high humidity conditions covered with a plastic hood for 2 days under short day conditions.

For the investigation of lignin accumulation in root tissue, Arabidopsis plants were grown and infected on MS plates. Surface sterilized seeds were sown on angular 0.5 MS-plates and were stratified for 24 h at 4°C. They were grown for two weeks under long day conditions (16 h light-dark, 22 ° C / 8 h, and 18 ° C). Seedlings were then transferred to angular 1% agarose plates to facilitate the fungal entry into the roots in a nutrient deficient environment. After three days, *V. longisporum* infection was done by spraying the roots with fungal spore suspension (10^5 spores ml^{-1}) and mock infection was done by spraying autoclaved tap water. The ¾ of the plates were wrapped with aluminium foil. After 3, 4, 6 and 7 dpi roots were removed from the agar surface for lignin staining and microscopy.

2.2.3.2 Sampling

In general, for infection experiments, plants were either mock-infected or infected with *V. longisporum*. After 15 dpi, petiole and lamina from ~16 plants were harvested separately and the material was stored at -80 °C for further measurements. Due to the amount of material needed for the analysis, petiole and lamina from 4 plants were pooled respectively to make 3-4 pools per treatment per genotype.

For fungal quantification in *V. longiporum*-infected Arabidopsis roots infected in a soil system, roots were harvested at 10 and 16 dpi. First they were washed under running tap water to get

rid of the adhering soil substrate. After washing, individual roots were kept in a glass petri dish containing tap water and were sonicated (TranssonicTP690, ELMA®) for 3 minutes. Sonication procedure helps in removing the hyphal fragments adhering to or protruding from the root cortex and thus minimizing the risk of quantifying fungal biomas that is merely attached at the outer surface of the root.

2.2.4 Leaf area measurement

To measure the projected leaf area of the whole rosette for mock and infected Arabidopsis plants photographs from single plants were taken using a digital camera and the leaf area was quantified using custom-made software (Bildanalyseprogramm, Datinf GmbH Tübingen, Germany).

2.2.5 Molecular biology methods

2.2.5.1 DNA isolation

2.2.5.1.1 Genomic DNA isolation from Arabidopsis leaves for genotyping (Quick and Dirty)
For genotyping, frozen leaf material was pulverized in a 1.5 ml reaction tube using a pestle. DNA extraction buffer containing EDTA was added to inactivate the DNAses. After centrifugation (RT, 14000 rpm) for 5 min isopropanol was added to the supernatant for precipitation. Additional centrifugation (RT, 14000 rpm) was performed for 5 min and the smeared DNA pellet was washed subsequently with 70% EtOH. After centrifugation (5 min, RT, 14000 rpm) and drying (10 min, 37 °C) DNA was extracted in 100 µl Milli-Q water.

2.2.5.1.2 Genomic DNA isolation from Arabiodpsis petioles for fungal DNA quantification
DNA extraction from infected petioles was done by using the DNeasy Plant Mini Kit (Qiagen, Hilden, Germany) following manufacturer's instructions including the optional recommendations. The DNA was eluted two times with 30 µl of EB provided.

2.2.5.1.3 Alkaline lysis
Plasmid DNA was isolated from *E. coli* using a modified alkaline lysis method (Le Gouill et al., 1994). First, 1.5 ml of overnight culture of *E. coli* (stationary phase) was collected by centrifugation at 13000 rpm for 1 min. The supernatant was removed and the cells were resuspended in 100 µl buffer I (50 mM Tris-HCl pH 8.0, 10 mM EDTA, 100 µg/µl RNase A). 200 µl buffer II (0.2 M NaOH, 1 % (w/v) SDS) was added to the cell suspension and incubated for 5 min on ice. The suspension was neutralized by adding 150 µl buffer III (29.4 g potassium

acetate, 5 mL formic acid and water to 100 ml) and inverted 6–8 times. The suspension was centrifuged for 10 min at 13000 rpm at RT, and the aqueous solution (~400 µl) was transferred into a new microcentrifuge tube containing 1 ml 96 % (v/v) ethanol. The DNA was precipitated from the solution by incubating for 20 min at –20°C. Plasmid DNA was collected by centrifugation with 13000 rpm for 10 min at 4°C. The pellet was washed with 70 % (v/v) EtOH and dried for 10 min at 37°C. The DNA was extracted in 20 µl EB buffer (10 mM Tris-HCl pH 8.5).

2.2.5.1.4   Isolation of high-quality plasmid DNA

For sequencing and gateway® cloning, high-purity plasmid DNA was isolated using the Nucleospin Mini Kit (Macherey-Nagel) following the manufacturer's instructions including recommended optional steps. 5-ml overnight culture was used to isolate plasmids and the isolated DNA was eluted with 50 µl (high-copy plasmids) or 30 µl (low-copy plasmids) EB buffer or water (ultra-pure).

2.2.5.2 RNA isolation

The TRIZOL extraction method was used in this study to isolate RNA from plant material. ~100 mg of plant material was pulverized in liquid nitrogen and 1.3 ml trizol buffer (380 ml/l phenol saturated with 0.1 M citrate buffer pH 4.3, 0.8 M guanidiniumthiocyanate, 0.4 M ammoniumthiocyanate, 33.4 ml 3 M Na-acetate pH 5.2, 5 % glycerol) was added. The tubes were vortexed continuously for 15 min. After adding 260 µl chloroform the tubes were vortexed for another 15 minutes. Centrifugation step with 14000 rpm at 4 °C for 45 min was performed. 900 µl of supernatant was taken in a separate microcentrifuge tube. 325 µl precipitation buffer (HSPB, 1.2 M NaCl, 0.8 M Na-citrate) and 325 µl 2-propanol were added to each sample. The tubes were inverted several times and were incubated for 10 min at RT. After the centrifugation step with 14000 rpm at 4 °C for 45 min, pellets were washed with 70% EtOH. After complete removal of EtOH, pellets were dried at 37 °C for 5 min. The pellet containing RNA was dissolved in 40-60 µl of autoclaved MilliQ water.

2.2.5.3 cDNA synthesis

cDNA synthesis was performed with 1 µg of DNA-free RNA. In order to prevent genomic DNA contamination, 1 µl of 10x DNAase I reaction buffer (Fermentas, St. Leon- Roth, Germany) along with 1 µl DNase I (RNase free) were added to the RNA samples. RNAase free water was

added to make up the volume uptil 10 µl. The mixture was incubated at 37 °C for 30 min. DNAase I was denatured by adding 1 µl 25 mM EDTA and incubated at 60 °C for 10 min.

In order to synthesize cDNA, 20 pmol of oligo-dT primer and 200 pmol of random nonamer oligonucleotides were added. The reaction mixture was heated to 70 °C for 10 min and immediately cooled down on ice. Subsequently, 20 nmol dNTPs, 4 µl RT 5x first-strand reaction buffer and 60 U reverse transcriptase H– were added and brought to a final volume of 20 µl with H_2O. The mixture was incubated at 42°C for 70 min and then heated to 70°C for 10 min.

2.2.5.4 Microarray analysis

Wild-type, *dde2-2* and *coi1-t* mutants were grown and infected as described in section 2.2.3.1. Petioles from 12 plants per treatment (mock and infected) were combined giving 6 samples per experiment and genotype. From three independent experiments 18 pools were generated. RNA was extracted as described in section 2.2.5.2 and purified using the RNeasy Plant Mini Kit (Quiagen, Valencia, CA, USA). Microarray analysis were performed with Arabidopsis ATH1 genome arrays and done by the NASC´s International Affymetrix Service. The data from the scanned arrays was normalised using the Robust Multichip Average (RMA) methodology (Bolstad et al., 2003) with the publicly available RMA Express package. For data analysis and statistics the Robin software was used (Lohse et al., 2010). Cluster analysis was performed with MarVis (Kaever et al., 2009).

2.2.5.5 Polymerase chain reaction (PCR) based genotyping

In order to identify homozygous mutant-lines, PCR with genomic DNA as a template (isolated as described in section *2.2.4.1.1*) and Advantage *Taq* DNA polymerase was performed.The wild type allele was identified with the combination of RP and LP primers. Correspondingly, the T-DNA insertion was indentified with the combination of LB and RP primers. Eventually, homozygous mutant plants were identified only by a PCR-fragment with LB and RP primers, heterozygous plants yielded a PCR fragment with both primer combinations and homozygous wild type plants yielded with LP and RP primers corresponding to the wild type allele.

The PCR reaction was carried out in a 20 µl reaction volume with the following constituents: 1 µl template DNA, 10 pmol of each primer (LP, RP and LB), and 0.2 mM dNTPs, 1 µl of 10 x Advantage buffer, 2 U polymerase and H2O filled to a total volume of 20 µl. The amplification reaction was done in a PCR thermocycler.

2.2.5.6 Quantification of *V. longisporum* DNA

Fungal biomass was quantified by determination of fungal DNA in infected plants with q-real-time PCR. DNA extraction from infected petioles was conducted as described in section 2.2.4.1.2. The iCycler System (BioRad, Hercules, CA, USA) was used for the amplification and quantification of *V. longisporum* DNA using primers OLG70 (5'-CAGCGAAACGCGATATGTAG-3') and OLG71 (5'-GGCTTGTAGGGGGTTTAGA-3') spanning internal transcribed sequences of ribosomal RNA genes (Eynck et al., 2007). The amplification mix consisted of Advantage buffer (Clontech, Mountain View, CA, USA), 200 µM of each dNTP, 0.3 µM of primer OLG70 and OLG71, 0.25 U Advantage cDNA polymerase (Clontech, Mountain View, CA, USA), 10 nM Fluorescein (BioRad, Hercules, CA, USA), 100,000 x diluted SYBR Green I solution (Cambrex Bio Science Rockland Inc., Maine**,** USA) and 25 ng of template DNA. The total reaction volume was made upto 25 µl with double distilled water. To normalize for different DNA preparations, the Arabidopsis *Actin8* gene (At1g49240) was amplified with the primers *act8fow* (5'-GGTTTTCCCCAGTGTTGTTG-3') and *act8rev* (5'-CTCCATGTCATCCCAGTTGC-3').

2.2.5.7 Quantitative real time RT-PCR

The iCycler System (Bio Rad, Hercules, CA, USA) was used for the amplification and quantification of cDNA using QuantiTect®-primers (Qiagen, Hilden, Germany). The amplification mix consisted of 1x NH4-reaction buffer (Bioline, Luckenwalde, Germany); 2 mM MgCl2; 100 µM of dNTPs; 0.4 µM of primers, 0.25 U BIOTaq DNA polymerase (Bioline Luckenwalde, Germany); 10 nM Fluorescein (BioRad, Hercules, CA, USA); 100,000 times diluted SYBR Green I solution (Cambrex, Rockland, ME, USA); 1 µl of a 1:10 diluted cDNA as template. Double distilled water was used to make up the total volume to 25 µl. Calculations were done according to the $2^{-\Box CT}$ method (Livak & Schmittgen, 2001). The Ct values of both mock- and *Verticillium*-infected samples were normalized to an endogenous housekeeping gene (*UBQ5*, (Kesarwani et al., 2007)).

2.2.5.8 Separation of DNA on agarose gel

The electrophoretic separation of DNA for analytical preparations was done in a horizontal agarose gel (10 cm x 7 cm x 0.3 cm, 16 lanes) with 1x TAE as running buffer. DNA fragments ranging between 500 bp and 14 kb were run on 1 % agarose gel and lower size DNA fragments were run on 2 % (w/v) agarose gel. DNA samples were mixed with 1/10 volume of 10 x DNA loading buffer, loaded in separate lanes and run at 120 V for 35-45 min. DNA fragments were

stained with 0.1% w/v EtBr. UV light (260 nm) was used to detect the DNA. Preparative gels were examined at larger wavelengths UV light (320 nm). Gels were visualized under a UV trans-illuminator in a gel-documentation set up. The sizes and amount of the DNA fragments were determined using a DNA standard, MassRuler™ DNA Ladder Mix (MBI Fermentas, St Leon Rot, Germany).

2.2.5.9 Isolation of DNA fragments from agarose gel

The elution of DNA fragments from agarose gel was done using the Nucleospin Extract II Gel Extraction kit (Macherey-Nagel, Düren, Germany) following the manufacturer's instructions. The eluted fragments were verified by electrophoresis as described in section 2.2.5.8.

2.2.5.10 BP clonase II recombination reaction and restriction digestion

To generate *AtERF54* over expresser plants, the *AtERF54* fragment was amplified using iProof high-fidelity DNA polymerase. For creating an appropriate entry vector for gateway cloning, BP clonase II recombination reaction was performed. The fragment was cloned into pDONR-201 Gateway-adapted vector and attL-flanked entry clone was generated. To perform BP recombination reaction equimolar amounts of pDONR201 vector and *AtERF54* fragment were taken. To stop the reaction 1 µl protienase K was added. The mixture was incubated for 10 min at 37 ⁰C. The whole reaction mixture was then transformed (section 2.2.5.12) into DH5α competent *E. coli* cells. After alkaline lysis was performed, restriction digestion of the alkaline lysate was done using HpaI (KSpA) using 3 µl of alkaline lysate, 3 U KspA in 1 µl blue buffer and total volume was made up to 10 µl. The restriction reaction was incubated overnight at 37 °C.

2.2.5.11 LR clonase II recombination reaction and restriction digestion

LR-Clonase II was used following manufacturer's instructions. Clonase reaction was performed by mixing 1 µl of the pDONR201 entry vector including *ERF54* contruct, 1 µl pB2GW7 and 1 µl pB2GW7-HA Gateway vectors in two separate cloning reactions. 2 µl of Clonase II enzyme was added and the total volume was made up to 10 µl. The mixture was incubated at room temperature over night. To stop the reaction 1 µl protienase K was added. The mixture was incubated for 10 min at 37 ⁰C. The whole reaction mixture was then transformed (section 2.2.5.12) into DH5α competent *E. coli* cells. After alkaline lysis was performed, restriction digestion of the alkaline lysate was done using Nco I and Hind III using 3 µl of alkaline lysate, 3

U enzyme in 1 µl buffer tango (1x) and total volume was made up to 10 µl. The restriction reaction was incubated overnight at 37 °C.

2.2.5.12 Transformation of competent *E. coli* cells

The transformation procedure was followed as per Hanahan (1983). In brief, 200 µl competent *E. coli* cells were thawed on ice for 20 min, ~50 ng of plasmid DNA were added to the cells and mixed gently. The mixture was incubated on ice for 30 min. After a heat shock for 90 sec at 42°C the cells were placed immediately on ice for 5 min. 800 µl of dYT medium were added to each vial and the suspension was mixed on a horizontal roller for 60 min at 37°C depending on selectable antibiotic resistance marker. Different volumes of the culture were plated on plates containing dYT medium supplemented with antibiotics. The plates were incubated overnight at 37°C.

2.2.5.13 Transformation of *Agrobacterium tumefaciens*

Gene transfer in *A. tumefaciens* was done by electroporation using Gene Pulser II. Bacterial competent cells were thawed on ice slowly before adding 0.5 µl of plasmid DNA. The mixture was transferred into an ice-cooled electroporation cuvette (2 mm electrode distance). The cuvette was subjected to electroporation at 25 µF, 2.5 kV, 400 Watt. The cells were suspended immediately in 1 ml YEB medium and incubated for 2 h at 29 °C. The culture was plated on YEB medium supplemented with antibiotics (Ref/Gen/Spec) and incubated for 2 days at 29 °C.

2.2.5.14 Transformation of *Arabidopsis thaliana*

Arabidopsis plants were transformed via *A. tumefaciens* mediated gene transfer using the floral dip method (Clough und Bent, 1998). Cells were precultured overnight v in 20 ml YEB medium supplemented with 25 µg ml-1 kanamycin and 50 µg ml-1 rifampicin. This culture was used to inoculate 400 ml YEB medium and incubated at 28 °C under constant shaking. Cells were harvested by centrifugation (2000 x g, 20 min) and the resulting pellet was dissolved in 200 ml of 5 % (w/v) saccharose solution. After dissolving the pellet, 100 µl SylWet was added and inflorescences of Arabidopsis plants were dipped into the solution. Plants were kept under high humidity over night. Positive T1 transformed lines were selected by BASTA selection.

2.2.5.15 Sequencing reaction

DNA sequencing was done using the BigDye Terminator RR Mix Cycle Sequencing Kit. The principle of DNA sequencing is based on the chain termination method (Sanger, 1977). The

PCR sequencing reaction was performed using 500–1000 ng plasmid DNA, 5 pmol primer, 2 µl ready reaction (RR) mix and H_2O up to 10 µl. The samples were subjected to 25 cycles of 10 s at 95°C, 5 s at 50°C, and 4 min at 60°C in a thermocycler. Precipitation of DNA product was done by using 9.5 µl water and 30.5 µl absolute ethanol and left for 1 h. The DNA was collected by centrifugation for 20 min at 13,000 rpm. The pellet was washed using 125 µL 70 % ethanol and then centrifuged for 10 min at 13,000 rpm. The pellet was dried at 95°C for 1 min and resuspended in 10 µl of HiDi reagent. The samples were placed on ice. The reactions were loaded onto an ABIPrism 3100 capillary electrophoresis sequencing station for analysis.

2.2.6 Microscopy of *V. longisporum* infected plant material

2.2.6.1 Confocal laser scanning microscopy (CLSM) with infected roots

GFP-tagged *V. longisporum* strain was used in this particular experiment. Wild type, *dde2-2*, and *coi1-t* plants were infected as described in section 2.2.3.1. To observe the initial colonization events of the fungus in these three genotypes, roots at different time points were analyzed. Starting from 1 dpi until 10 dpi 6-8 roots were observed everyday under CLSM (Leica, SP5).

2.2.6.2 Anatomical studies with infected petiole cross sections

Petioles (2 to 4 mm) were stored in a mixture of 37 % formaldehyde, 100% acetic acid and 70 % ethanol (FAE, 5:5:90, v/v/v). Samples were successively infiltrated with the following solutions: 70% ethanol for 24 h, 80% ethanol for 2 h, 90 % ethanol for 2 h, 100% ethanol for 2 h, 100 % ethanol for 12 h, 100 % ethanol : 100% acetone (1:1) for 2 h, 100 % acetone for 2 h (2 times), acetone : plastic (1:1) for 4 h, acetone : plastic (1:3) for 12 h, 100 % plastic for 12 h (2 times). Plastic was a mixture of styrene (Merck, Darmstadt, Germany) and butyl methacrylate (Sigma, Steinheim, Germany) (1:1) containing 2 % dibenzoylperoxide with 50 % phthalate (Peroxid Chemie GmbH, Pullach, Germany). The samples were transferred into gelatine capsules (Plano GmbH, Wetzlar, Germany), mounted with fresh plastic solution which were polymerized at 60°C for 3 days and at 37°C for 10 additional days. Transverse cross-sections (1 µm) of the embedded samples were obtained with a microtome (Autocut, Reichert-Jung, Heidelberg, Germany) using a diamond knife (Chisto Diatome, Drukker International, Cuijk, Netherlands). The sections were placed on glass slides which were covered with 0.5 % (w/v) gelatine containing 1.77 mM $KCr(SO_4)_2$ in distilled H_2O. For histochemical analyses, cross sections were stained with 0.05 % toluidine blue in 1% boric acid for 10 min at 60°C, mounted in DePex

(Serva, Heidelberg, Germany) and observed under a bright field microscope (Axioskop, Zeiss, Oberkochen, Germany). Cross sections and staining was performed by the department of Prof. Andrea Polle, University of Goettingen (Germany).

2.2.6.3 Lignin accumulation in root tissue

To stain the lignin in root tissues, the phloroglucinol-HCl stain (1.6 M Phloroglucinol stain, 76% EtOH and 7.4% HCl (37%)) is used. The cinnamaldehyde end groups of lignin appear to react with phloroglucinol-HCl to give a red-violet color (Gahan and B., 1984.). The whole root was stained for 6-7 min directly on a clean glass slide and covered with a cover slip. Roots were kept in dark during the staining procedure because of the light sensitive nature of the stain. The roots were examined under a light microscope. The lignified tissues in the root should appear red.

2.2.7   Phytohormone analyses

Determination of phytohormone concentrations was performed by the Department of Plant Biochemistry (Prof. Dr. I. Feußner), University of Göttingen (Germany), using GC-MS/MS analyses.

3 RESULTS

3.1 Disease phenotype of *Verticillium longisporum*-infected *Arabidopsis* plants

Arabidopsis plants were infected via root dip infection as described in section 2.2.3.1. In short, plants were grown on a sand-soil mixture for three to four weeks. After uprooting, the roots were washed gently with tap water and were incubated in a spore suspension for 45 min before being transplanted back into soil. Reduction in the leaf area after infection was already visible at 15 dpi. Yellowing of the leaf veins could be noticed in infected leaves at this time point of infection (Figure 9A and 9B). At 21 dpi, petioles started to become yellow (Figure 9C) and as the disease progressed, the lamina also started to become senescent. In contrast to the natural senescence, this process started from the bottom of the leaf. At 32 dpi, the growth of fungal hyphae and the development of microsclerotia on dead and senescent plant material, especially on the petioles, was visible (Figure 9D). Cross sections of uninfected and infected petioles revealed that the paired cells derived from pro-cambium had disappeared in the infected tissue. Formation of additional xylem-like cells was observed. At 15 dpi, these cells appeared at the abaxial side in the wild-type, where the phloem is normally localized. The layer of cells with dense cytosol was interspersed with cells displaying a xylem vessel-like appearance (large lumen, lignified cell walls; Figure 9E).
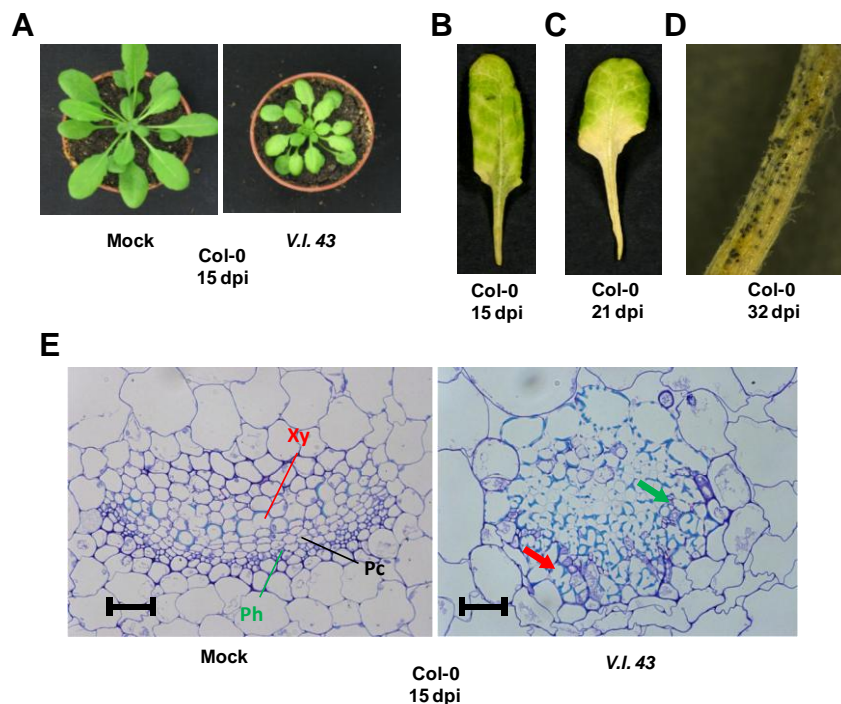
Figure 9 Disease phenotype of *V. longisporum* infected *Arabidopsis* plants

(A) Four week old Col-0 plants were inoculated with *V. longisporum*. Typical stunting of the leaf area was observed at 15 dpi.
(B) *V. longisporum*-infected leaf showing yellowing of the leaf veins at 15 dpi.
(C) Typical yellowing of the leaf at 21 dpi starting from the bottom of the leaf.
(D) Formation of microsclerotia on infected Col-0 petiole at 32 dpi.
(E) Cross section of petioles from mock and *V. longisporum* infected Col-0 plant at 15 dpi. Sections were stained with toluidine blue to detect lignifications of secondary cell walls (AG Polle). Xy: xylem vessels, Ph: Phloem, Pc: Procambium-derived paired cells. Red arrow: xylem-like cells, Green arrow: Phloem-like cells more to the center of the vascular bundle. Bar= 20 µm (Photos: AG Polle).

3.2 Role of salicylic acid in *Arabidopsis*/*Verticillium longisporum* interaction

3.2.1 *V. longisporum*-induced set of genes reveals strongest correlation with SA

In general, infection of *Arabidopsis* plants with biotrophic pathogens leads to the activation of salicylic acid (SA)-mediated defense responses. A whole genome microarray at 15 dpi reveals significant up-regulation of 1219 genes (> 2-fold. $p < 0.05$) and down regulation of 473 genes in the petioles of *V. longisporum*-infected wild type plants as compared to the control plants. The transcriptional response of *V. longisporum*-infected *Arabidopsis* wild-type plants was compared with publically available microarray database (Genvestigator; Hruz *et al*., 2008) obtained from various *Arabidopsis* mutants and wild-type plants exposed to biotic, abiotic, chemical stresses and hormone treatments. To evaluate the extent of correlation Spearman rank correlation coefficient (r_s) was calculated (Corinna Thurow; Spearman, 1904). The r_s value can range from +1.0 to -1.0 and this is used to rank the correlation list. Perfect positive and negative correlation of expression gives an r_s value of +1.0 and -1.0 respectively. When analyzing the 1693 genes either induced or repressed after infection, the strongest correlations were found with the datasets from *Pseudomonas syringae*-infected leaves ($r_s = 0.603$, $p < 0.0001$), leaves from the *cpr5* mutant ($r_s = 0.59$, $p < 0.0001$) which is characterized by enhanced SA levels (Bowling *et al*., 1997) and SA treated leaves ($r_s = 0.58$, $p < 0.0001$). This correlation between *V. longisporum* and SA-regulated genes was further supported by the negative correlation with SA signaling mutants, *npr1* and *pad4* (Supplement table 1).

To elucidate the role of SA in response to *V. longisporum,* levels of free SA and its conjugates were measured in *V. longisporum*-mock and -infected petioles at 15 dpi (measurements were done by the department of Prof. Feussner). Free SA levels did not increase after infection in the wild-type plants. On the contrary, the SA glucoside (SAG) and the SA-derived metabolite dihydroxybenzoeic acid (DHBA) levels were found to be elevated after infection (Figure 10A).

PR1 expression, known to be a marker gene for SA defense response, was also elevated after *Verticillium* infection correlating with the increased SA-derived metabolite levels (Figure 10B).

To further characterize the SA defense response, *Arabidopsis* mutants deficient in SA biosynthesis as well as signaling were inoculated. The disease symptoms were scored by measuring the projected leaf area at 15 dpi from mock as well as infected plants. The *SA induction deficient 2 (sid2-2)* mutant (Nawrath and Metraux, 1999; Wildermuth *et al.*, 2001) and transgenic plants expressing the SA-hydrolyzing bacterial enzyme NahG (Lawton *et al.*, 1995) showed wild-type-like reduction of leaf area at 15 dpi. Consistently, reduction in the leaf area of *Arabidopsis* plants impaired in NPR1 (nonexpressor of pathogenesis related genes), a key regulator of the SA-dependent defense response (Cao et al., 1997), was comparable to the wild type plants at 15 dpi (Figure 10C and 10D). To measure the fungal biomass, petioles were harvested at 15 dpi. No significant differences in the amounts of fungal DNA were detected in *sid2-2*, *nahG* and *npr1-1* as compared to the wild type (Figure 10E). To further characterize the disease phenotype, photos from single plants were taken at 21dpi (Supplement figure S1). Stunting and yellowing of the leaves were comparable in all the genotypes at later stages of the infection.

To show that the induction of *PR1* after *Verticillium* infection is indeed due to the known pathogen-induced SA biosynthesis pathway, *PR1* expression was assessed in *sid2-2*, *nahG* and *npr1-1* mutant plants after infection at 15 dpi. Induction of the *PR1* transcript was completely abolished in *sid2-2* (Dewdney et al., 2000, Wildermuth et al., 2001b) and *nahG* (Lawton et al., 1995) (Figure 10B). Also, the SAG and DHBA levels were reduced in *sid2-2* and *nahG*, when measured at 21 dpi in mock and infected petioles of the respective genotypes (Figure 10F) and correlated with the *PR1* levels (Figure 10B) indicating SAG and DHBA as possible inducers of *PR1* transcripts at least after *Verticillium* infection. In summary, our data indicate that the SA pathway is induced. However, this defense program is not effective against *V. longisporum.*
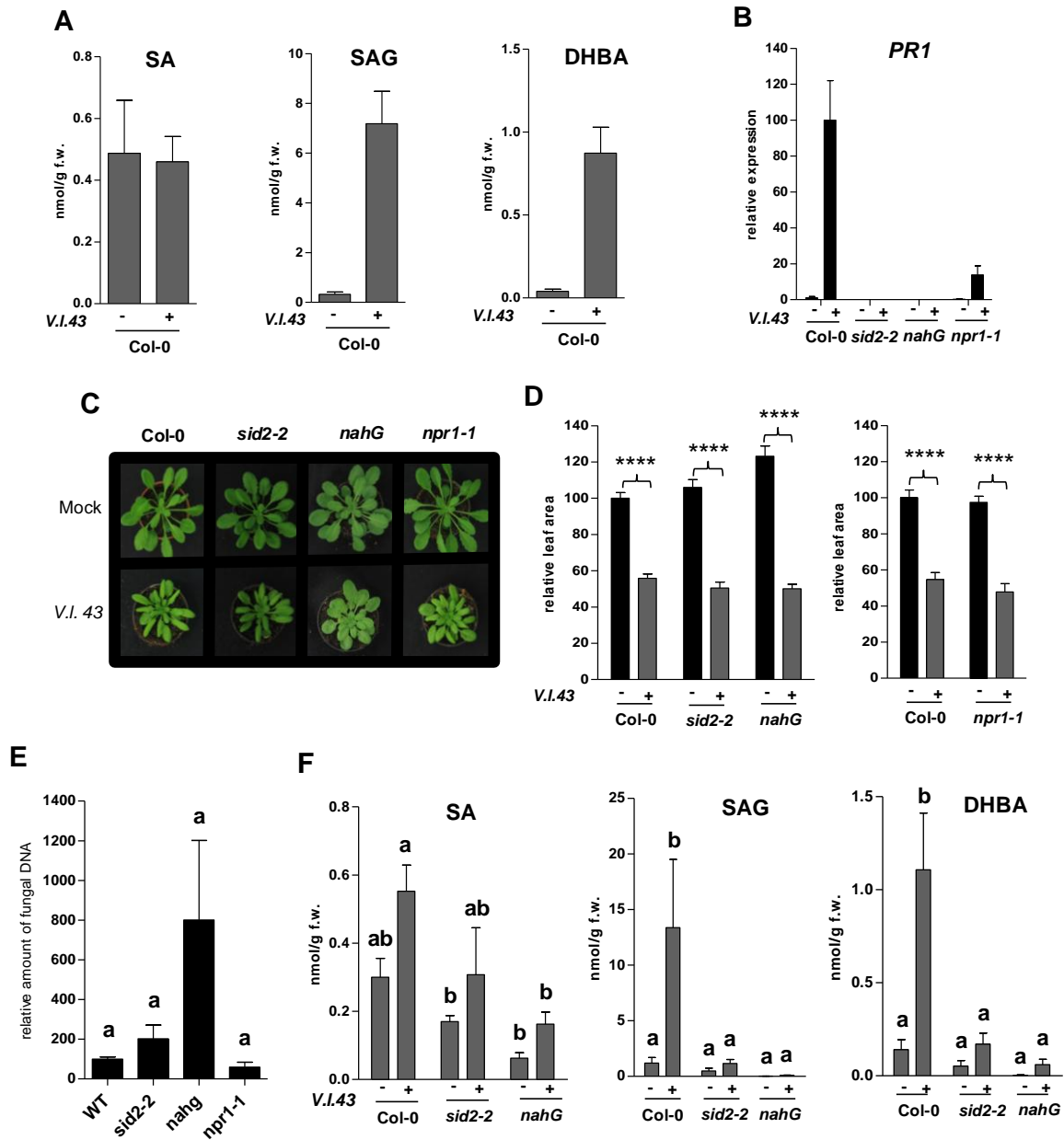
Figure 10 SA, SAG and DHBA measurements, *PR-1* gene expression, disease phenotype of SA biosynthesis and signaling mutants and fungal DNA quantification

(A) HPLC-MS/MS analysis for detection of SA, SAG and DHBA levels in petioles from Col-0 plants at 15 days after mock and *V. longisporum* infection. Data are the means (+/- SEM) of four replicates with each replicate consisting of a pool of petioles from four plants.

(B) Quantitative real time RT PCR analysis of relative *PR-1* transcript levels in petioles of Col-0, *sid2-2*, *nahG* and *npr1-1* plants at 15 days after mock and *V. longisporum* infection. Data indicate means (+/- SEM) of four biological replicates with each replicate consisting pool of petioles from four plants.

(C) Representative pictures of Col-0, *sid2-2*, *nahG* and *npr1-1* plants 15 days after mock and *V. longisporum* infection.

(D) Projected leaf area of mock and *V. longisporum* infected Col-0, *sid2-2*, *nahG* and *npr1-1* at 15 dpi. Data indicate means (+/- SEM) of 29-34 replicates from two independent experiments. Stars indicate significant differences between mock and *V. longisporum* infected samples (two-way ANOVA followed by Bonferroni multiple comparison test; P< 0.0001).

(E) Quantification of fungal biomass by real time RT PCR in 15 dpi Col-0, *sid2-2*, *nahG* and *npr1-1*. DNA was extracted from *V. longisporum* infected petioles. Data indicates means (+/- SEM) of four biological replicates with each replicate consisting of petioles from four plants. Letters on the bar denote significance test performed using one-way ANOVA followed by Tukey-Kramer multiple comparison test).

(F) HPLC-MS/MS analysis for detection of SA, SAG and DHBA levels in petioles from Col-0, *sid2-2*, *nahG* and *npr1-1* at 21 days after mock and *V. longisporum* infection. Data denote means (+/- SEM) of four replicates with each replicate consisting pool of petioles from four plants. Different letters show significant differences between the samples (one-way ANOVA followed by Tukey Kramer multiple comparison test; P< 0.0001 for (B); P< 0.05 for (F); SA and SAG; P< 0.001 for (F)

3.3 Role of jasmonic acid in *Arabidopsis/Verticillium longisporum* interaction

Infection with necrotrophic pathogens generally elicits jasmonic acid/ethylene (JA/ET)-dependent defense responses. To assess the role of JA in *A. thaliana* after *V. longisporum* infection, jasmonate levels were measured in wild-type mock and infected petioles at 15 dpi (measurements performed by AG Feussner). JA levels were increased significantly in infected wild-type plants (Figure 11A) and so were the levels of the active form JA-Ile (Figure 11B). To compare the overall activation of the JA pathway after infection with that induced after wounding, JA and JA-Ile levels were measured in the petioles two hours after wounding. The JA levels increased to a higher extent after wounding than after *V. longisporum* but JA-Ile levels were comparable in both the treatments.
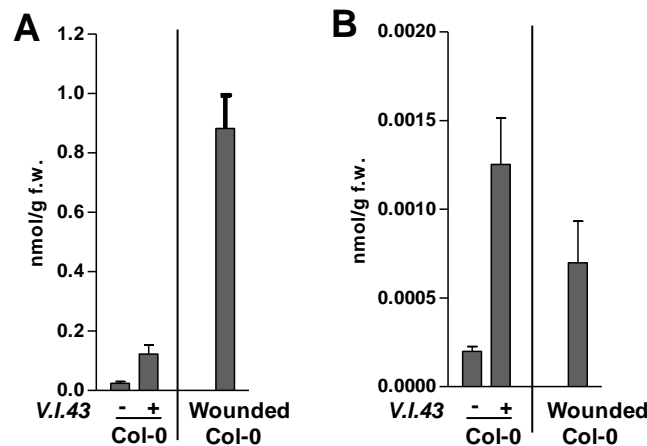
Figure 11 Activation of the JA biosynthesis pathway in *V. longisporum*-infected wild type plants

(A) HPLC-MS/MS analysis for detection of JA levels in petioles from wild-type plants at 15 days after mock and *V. longisporum* infection.

(B) HPLC-MS/MS analysis for detection of JA-Ile levels in petioles from wild-type plants at 15 days after mock and *V. longisporum* infection.

Data are the means (+/- SEM) of eight replicates from two independent experiments. Each replicate is a pool of four plants. As positive controls, petioles were wounded with forceps and harvested after 2 hours. Data are from 3 biological replicates.

3.3.1 Disease phenotype of jasmonic acid biosynthesis and signaling mutants

Further, to dissect the role of JA biosynthesis and signaling in plant defense against *V. longisporum*, mutants impaired in JA biosynthesis and early signaling were screened for altered resistance/susceptibility. The mutants used for this analysis included *dde2-2, fad3-2 fad7-1 fad8, acx1/5, jar1-1, coi1-t and coi1-1.* Among the JA biosynthesis mutants, *fad* mutants have defective levels of three fold unsaturated fatty acids that are JA precursors, with *fad3-2* being defective in the desaturation of linoleic acid (18:2) to linolenic acid (18:3) (Browse et al., 1993), and the *fad7-1 fad8* double mutant showing decreased levels of trienoic fatty acids (16:3 and 18:3) (McConn et al., 1994). Similarly, the *dde2-2* is defective in the catalysis of the first step in the conversion of 13-hydroperoxy linolenic acid (13-HPOT) to 12-oxophytodienoic acid (12-OPDA) (Stintzi and Browse, 2000; Park et al., 2002) and the *acx1/5 (Schilmiller et al., 2007)* double mutant is impaired in two of the acyl-coenzyme A oxidases (*ACX1* and *ACX5*) involved in the conversion of OPDA to JA. Another JA-Ile-deficient mutant, *jar1-1*, exhibits a defect in an enzyme converting JA to its amino acid conjugate JA-Ile. JA-Ile receptor mutant, *coi1-t*, exhibits a T-DNA insertion in the *COI1* gene (Mosblech et al., 2010). At 15 dpi, leaf area was reduced down to 50 to 60% in wild-type and the JA biosynthesis mutant *dde2-2* but not in the JA receptor mutant *coi1-t* (Figure 12A and 12B). Also, as shown in (Figure 12I), the very well characterized *coi1-1* mutant had less severe reduction in leaf area. Reduction in leaf area of the two independent JA biosynthesis mutant *fad3-2 fad7-2 fad8 and acx1/5* and JA-Ile-deficient mutant, *jar1-1* was also consistent with *dde2-2* and wild type plants (Figure 12G and H). At 22 dpi, senescence-like symptoms became apparent in infected wild-type and *dde2-2* plants. These symptoms were much less pronounced in *coi1-t*. At 35 dpi, most of the wild-type and *dde2-2* plants were dead while most of the *coi1-t* plants had remained green (Figure 12D). Appearance of microsclerotia correlated with this disease phenotype resulting in 73% wild-type, 79% *dde2-2* and 25% infected *coi1-t* plants carrying microsclerotia primarily around the petioles (Figure 12E and 12F).
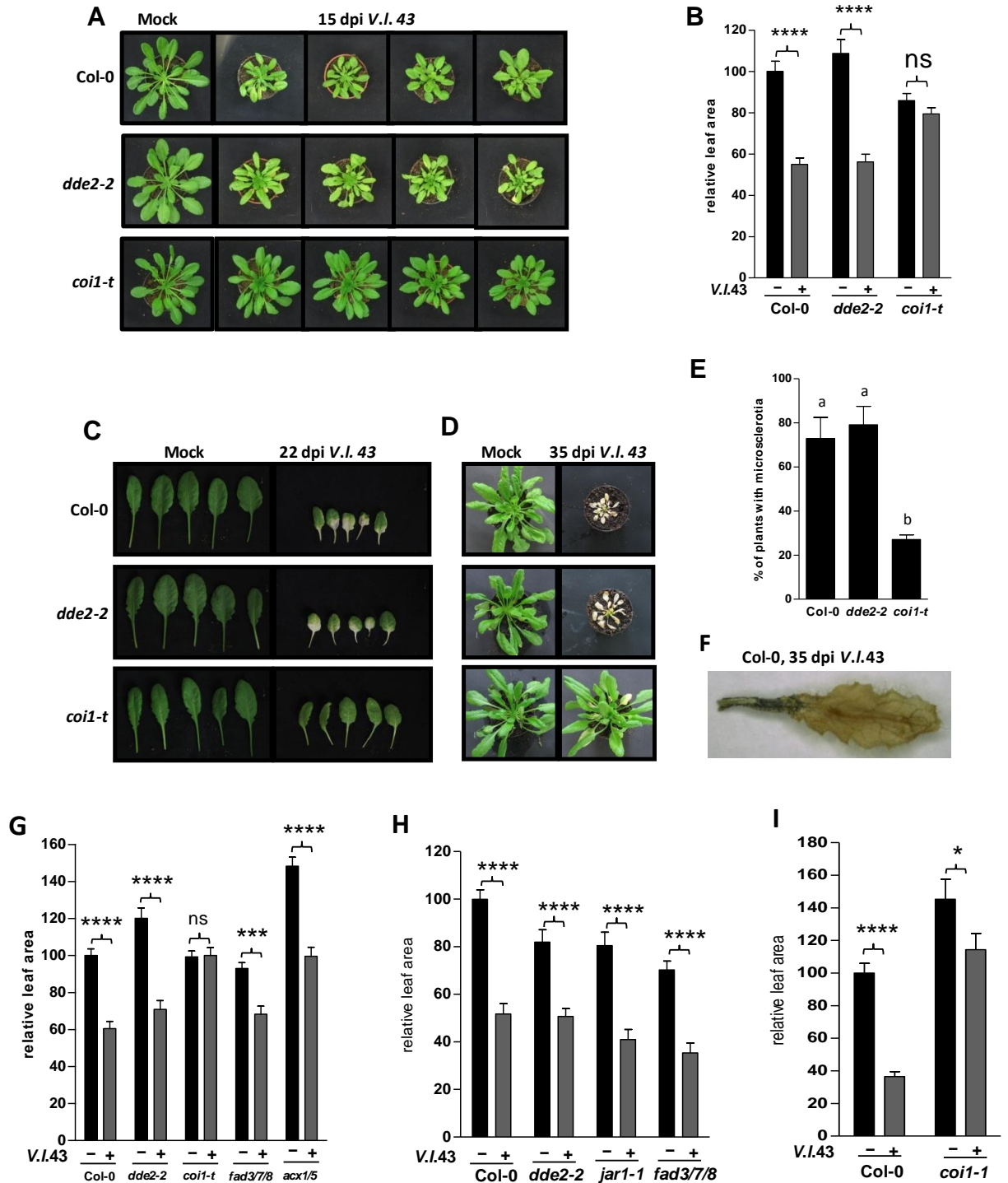
Figure 12 Disease phenotype of JA biosynthesis (*dde2-2*, *fad3/7/8*, *jar1-1* and *acx1/5*) and perception (*coi1-t* and *coi1-1*) mutants after *V. longisporum* infection

(A) Typical *V. longisporum (V.l.)* disease symptoms of wild-type (upper row), *dde2-2* (middle row) and *coi1-t* (lower row) plants at 15 dpi. One representative mock-treated plant of each genotype (left row) and 4 representative infected plants of each genotype are shown.

(B) Projected leaf area of mock-infected and *V. longisporum*-infected wild-type, *dde2-2* and *coi1-t* plants. Data indicate means (+/- SEM) of 3 independent experiments with 14 to 16 mock-infected and 14 to 16 *V. longisporum*-infected plants/experiment. Stars indicate significant differences at P < 0.0001 (two-way ANOVA followed by Bonferroni multiple comparison test; ns, not significant) between *V. longisporum* (*V.l.*)- and mock-infected samples.

(C) Single leaves of mock-infected and *V. longisporum*-infected wild-type, *dde2-2* and *coi1-t* plants at 22 dpi. Leaves from corresponding positions (mock- and *V. longisporum*-infected) are shown.

(D) Representative disease symptoms of wild-type (upper row), *dde2-2* (middle row) and *coi1-t* (lower row) plants at 35 dpi. One representative mock-treated plant and one infected plant are shown.

(E) Percentage of wild-type, *dde2-2* and *coi1-t* plants with microsclerotia after 35 dpi. Numbers are from three independent experiments with 16 mock- and 16 *V. longisporum*-infected plants per experiment. Microsclerotia were only observed on plants showing the severe phenotype as shown in (d). Different letters indicate significant differences at P < 0.01 (one-way ANOVA followed by Tukey-Kramer multiple comparison test).

(F) Photograph of a typical *V. longisporum*-infected Col-0 leaf at 35 dpi showing microsclerotia primarily around the petiole.

(G) and (H) Projected leaf area of mock-infected and *V. longisporum*-infected wild type, *dde2-2*, *coi1-t*, *fad3/7/8, jar1-1* and *acx1/5* plants. Data indicate means (+/- SEM) of 1 experiment with 16-18 mock- and V. longisporum infected plants per experiment. Stars indicate significant differences at *P<0.05 and ***P< 0.0001 (two-way ANOVA followed by Bonferroni multiple comparison test; ns, not significant) between *V. longisporum*- and mock-infected samples.

(I) Projected leaf area of mock- and *V. longisporum*-infected wild type and *coi1-1* plants at 15 dpi. Data indicate means (+/- SEM) of 1 experiment with18 mock- and *V. longisporum*-infected plants. Stars indicate significant differences at *P<0.05 and ***P<0.0001 (two-way ANOVA followed by Bonferroni multiple comparison test; ns, not significant) between *V. longisporum*- and mock-infected samples.

Alterations in vascular bundle of wild-type, *coi1-t* and *dde2-2* plants were analyzed as well. Sampling was done at three different time points as part of one time course experiment at 10, 12, and 15 dpi. At 10 dpi, the cytosol of the phloem cells became denser in infected wild-type vascular bundles. At 15 dpi, the layer of cells with dense cytosol was interspersed with cells displaying a xylem vessel-like appearance (large lumen, lignified cell walls) and the paired cells derived from pro-cambium had disappeared. Consistent with the less severe disease phenotype, these changes were less pronounced in *coi1-t*: At 10 dpi, the layer of cells with a denser cytosol was thinner as compared to the wild-type and at 15 dpi; cells with lignified cell walls were not yet formed (Figure 13A, B and C). Again, the *dde2-2* mutant showed comparable phenotype to the wild-type in this assay.
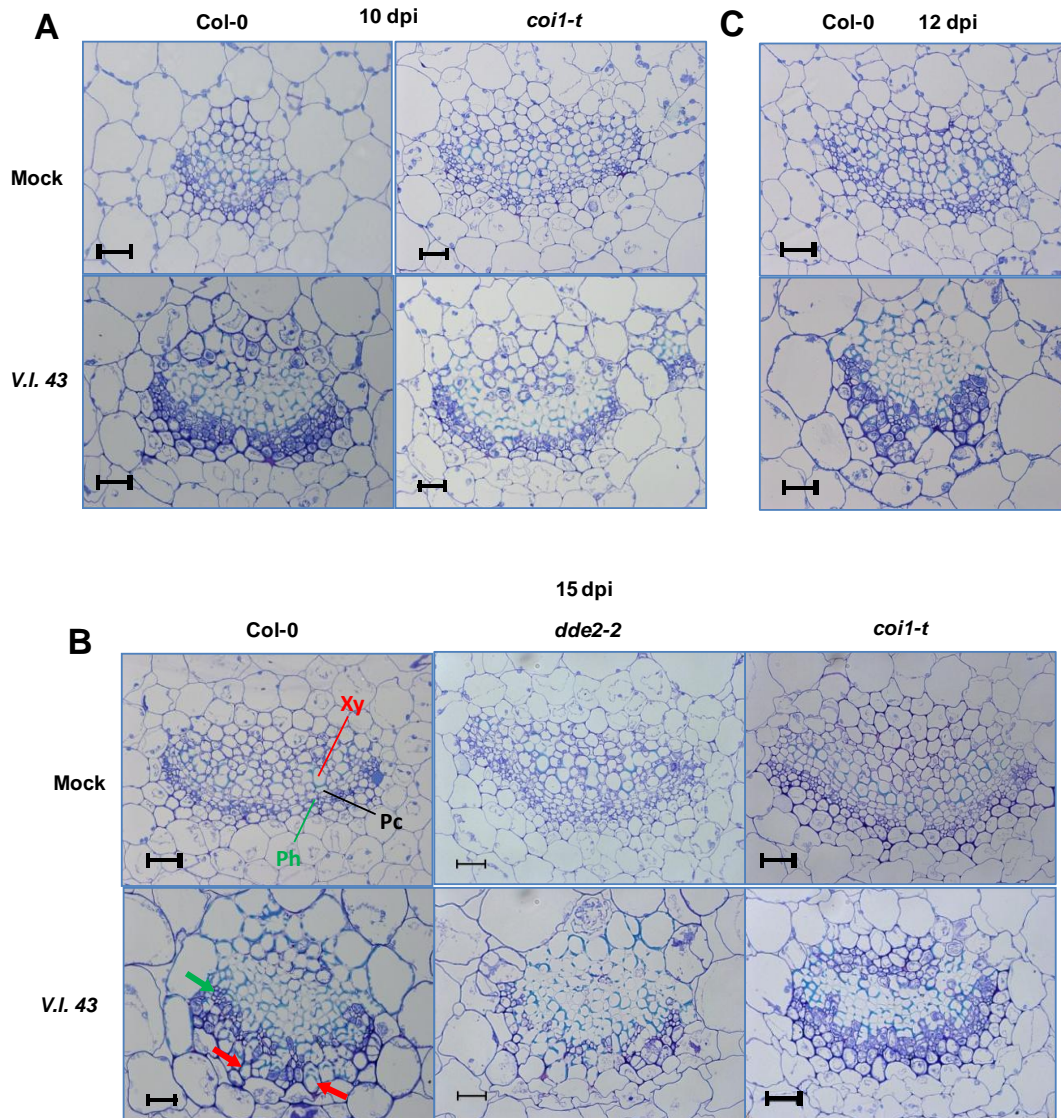
Figure 13 Structure of the vascular bundle in petioles of *V. longisporum*-infected plants

(A) Cross-sections of petioles from mock-inoculated and *V. longisporum*-infected Col-0 and *coi1-t* plants at 10 dpi. Sections were stained with toluidine blue to detect lignification of secondary cell walls.
(B) Cross-sections of petioles from *V. longsiporum*-infected Col-0 plants at 12 dpi (bar = 20 µm).
(C) Cross-sections of petioles from *V. longisporum*-infected Col-0, *dde2-2* and *coi1-t* plants at 15 dpi (bar=20 µm).Xy, xylem vessel; Ph, phloem; Pc, procambium-derived paired cells. Red arrows exemplarily denote two cells which look like xylem vessels at the abaxial side, the green arrow exemplarily marks putative phloem cells in the middle of the vascular bundle (bar = 20 µm).

3.3.2 *Verticillium longisporum* propagation in *coi1-t*

To determine whether *V. longisporum* penetration in *coi1-t* roots was hampered, roots of GFP-tagged *V. longisporum* inoculated plants were examined by confocal laser scanning microscopy.

42

As previously observed when analyzing *Brassica napus* roots with GFP-tagged *V. longisporum,* the fungus could indeed penetrate into the xylem vessels of *Arabidopsis* roots (Figure 14B). Although the results of confocal microscopy are considered qualitative and not quantitative, microscopic analysis of roots from 6-8 plants/genotype indicated equal amount of fungal colonization of the vascular system of wild type, *dde2-2* and *coi1-t* roots. To test whether a restriction of post-penetration fungal growth has a role in the *coi1-t* resistant phenotype, the fungal biomass was measured in petioles of infected wild type, *dde2-2* and *coi1-t* plants via quantitative real time RT-PCR analysis of extracted DNA, using *Arabidopsis* and *V. longisporum* specific primers. At 10 dpi, no significant differences in the amounts of fungal DNA were detected in *coi1-t* as compared to the wild-type (Figure 14A). At later time points, fungal proliferation was less efficient in *coi1-t* as compared to wild-type and *dde2-2* plants. At 15 and 19 dpi, *dde2-2* plants contained more fungal DNA than wild-type plants supporting the idea that the JA-Ile-mediated defense pathway can restrict fungal growth whereas a yet unknown COI1-dependent pathway supports fungal proliferation.
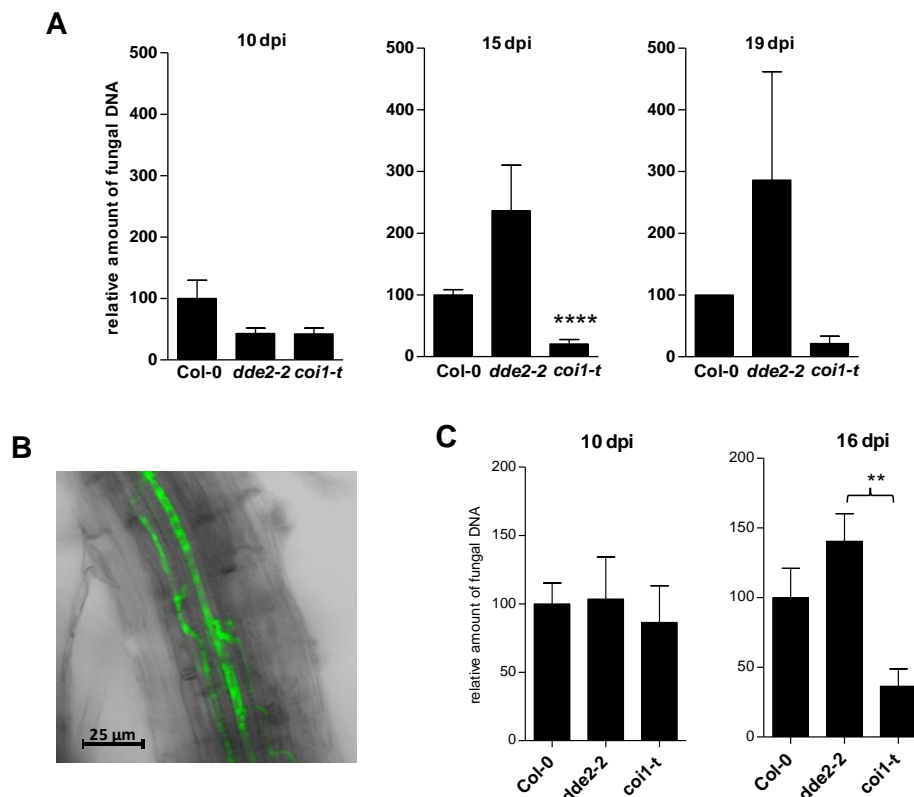
Figure 14 Fungal biomass of Verticillium longisporum infected wild type, *dde2-2* and *coi1-t* plants (petioles and roots) and root colonization of *coi1-t*

(A)   Relative quantification of fungal biomass by real time PCR on DNA isolated from petioles of *V. longisporum* infected wild type, dde2-2 and coi1-t plants at 10, 15 and 19 dpi. Amplification values for fungal internal ribosomal spacer regions were normalized to the abundance of Arabidopsis *Actin8* sequences. Relative amounts of fungal DNA

were set to 100% for the wild type. 10 and 15 dpi: Bars indicate means (+/- SEM) of 11 biological replicates from three independent experiments. Each replicate contains petioles from four plants. 19 dpi: Bars indicate means (+/- SEM) of three independent experiments, with three biological replicates. Each replicate represents a pool of four plants. Stars indicate significant differences at P < 0.0001 (unpaired t-test) between Col-0 and coi1-t.

(B)   Confocal image of a *coi1-t* root infected with a GFP-tagged *V. longisporum* strain at 7 dpi.

(C)   Relative quantification of fungal biomass by real time PCR with DNA isolated from roots of *V. longisporum* infected wild type, *dde2-2* and *coi1-t* plants at 10 and 16 dpi. Amplification values for fungal internal ribosomal spacer regions were normalized to the abundance of Arabidopsis *Actin8* sequences. Relative amounts of fungal DNA were set to 100% for the wild type. 10 and 16 dpi: Bars indicate means (+/- SEM) of 8 biological replicates from two independent experiments. Each replicate contains roots from four plants. Stars indicate significant differences (ONE-WAY ANOVA followed by Tukey-Kramer multiple comparison test) between *dde2-2* and *coi1-t*.

In addition, efforts were made in quantifying the fungal biomass in the roots of wild type, *dde2-2* and *coi1-t* plants at 10 and 16 dpi via quantitative real time RT-PCR. Since the soil system was used for the infection, harvested roots were cleaned and sonicated (section 2.2.3.2) prior to DNA extraction. 3 pools containing roots from 4 plants per genotype and treatment were made. At 10 dpi, equal amounts of fungal DNA were detected in all three genotypes including *coi1-t* roots indicating that the initial penetration of the roots by the fungus is independent of the genotype. Since this analysis does not confirm that the fungal biomass is actually from the vascular tissue, confocal studies confirmed the fact that the vascular colonisation is not hampered in all three genotypes. However, at 16 dpi, the fungal biomass was reduced significantly in *coi1-t* roots as compared to *dde2-2* roots (Figure 14C), in accordance with the reduction of fungal biomass in the petioles.

3.3.3 Expression analysis of known defense genes of the JA pathway in *dde2-2* and *coi1-t* mutants

Since disease development depends on COI1 but not on plant-derived JAs, jasmonate levels were determined (measurement done by the department of Prof. Feussner) in all three genotypes at 15 dpi in mock and infected petioles (Figure 15A). JA levels were increased significantly in infected wild type plants and were absent in *dde2-2*. In *coi1-t*, JA levels were slightly elevated in mock-infected plants and did not show a significant increase after infection. Like JA levels, levels of the active hormone JA-Ile were increased in wild-type petioles and was absent in the *dde2-2* mutant. The *coi1-t* mutant had increased JA-Ile levels already after mock infection and reacted to the fungus with a further increase. The lack of any biochemically detectable JA or JA-Ile in the infected *dde2-2* mutant suggested that *V. longisporum* cannot synthesize JA. In order to investigate whether *V. longisporum* might produce a yet unknown JA mimic to activate COI1, transcript levels of two marker genes of the JA-Ile-dependent COI1

response, namely *VSP2* and *PDF1.2,* were determined in petioles at 15 dpi,. Both genes were only induced in wild-type plants (Figure 15B) indicating that no fungal-derived JAs or JA mimics that would activate the established COI1-dependent defense genes are effective in *V. longisporum*-infected *dde2-2* plants. Consistent with the result those similar amounts of JA-Ile were found in wild-type plants after *V. longisporum* infection and wounding (Figure 11A and B), *VSP2* transcript levels were induced to comparable levels under both conditions. In contrast, the JA/ET marker gene *PDF1.2*, which is highly expressed after infection with the foliar pathogen *Botrytis cinerea*, is not efficiently induced in *V. longisporum*-colonized plant tissue. The observed increase in ABA (Figure 15A), which is known to inhibit the JA/ET pathway, might explain the low *PDF1.2* transcript levels (Anderson et al., 2004)*.*
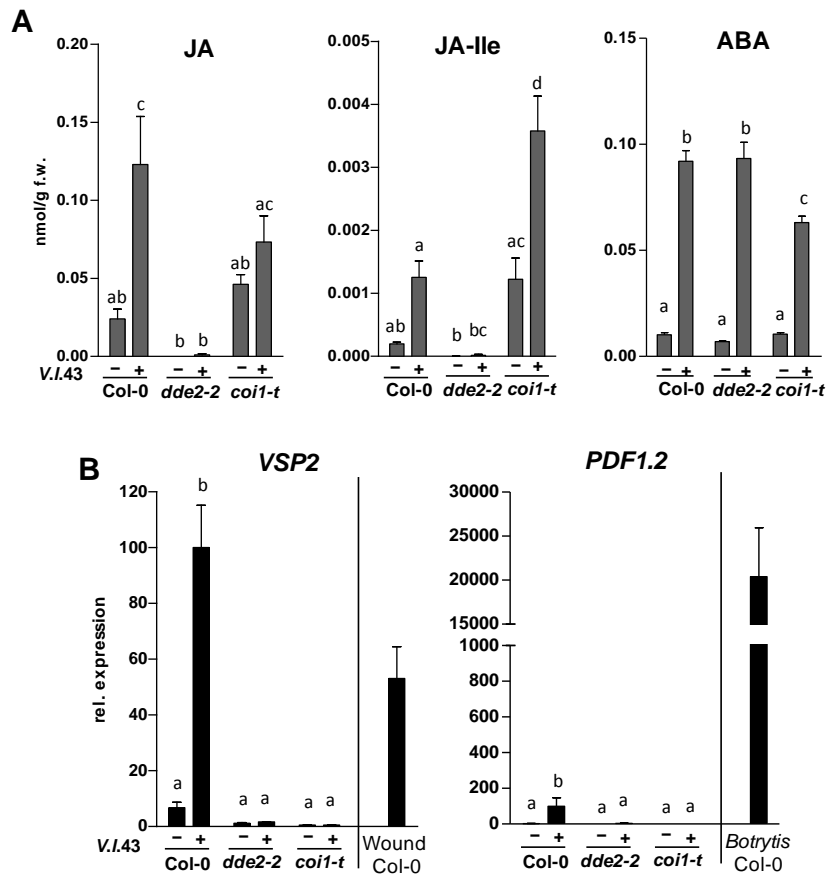
Figure 15 Activation of JA biosynthesis and signaling pathways in V. longisporum-infected wild-type, *dde2-2* **and** *coi1-t* **plants**

(A) HPLC-MS/MS analysis for detection of JA-, JA-Ile and ABA levels in petioles from wild-type *dde2-2* and *coi1-t* plants at 15 days after mock and *V. longisporum* infection. Data are the means (+/- SEM) of eight replicates from two independent experiments. Each replicate is a pool of four plants.

(B) Quantitative RT-PCR analysis of relative *VSP2* and *PDF1.2* transcript levels in petioles from wild-type *dde2-2* and *coi1-t* plants at 15 days after mock and *V. longisporum* infection. Data indicate means (+/- SEM) of three independent experiments with 16 individual plants/experiment. Wounded petioles were harvested for RNA extraction after two hours (three biological replicates), *Botrytis cinerea*-infected samples were harvested after three days (four biological replicates). Relative transcript levels of the infected wild-type were set to 100%. Different letters denote significant differences between samples (one-way ANOVA followed by Tukey-Kramer multiple comparison test; P < 0.05 for (a) and (b) *PDF1.2*; P < 0,001 for (b) *VSP2* and (c).

3.3.4 The role of salicylic acid defense pathway in the *coi1*-mediated tolerance

Increased resistance of the *coi1* mutant has been detected before in a screen for resistance against the hemibiotrophic pathogen *Pseudomonas syringae* (Kloek *et al.*, 2001). In this interaction, the bacterial JA-Ile mimic COR activates COI1 to suppress the SA pathway (Kloek et al., 2001, Laurie-Berry et al., 2006). To analyze, whether a similar scenario would explain the *coi1*-mediated tolerance towards *V. longisporum*, SA synthesis and SA signaling were analyzed in infected wild-type, *dde2-2* and *coi1-t* plants (Figure 16A). Free SA levels did not increase after infection in wild-type plants and reached similar levels in all three infected genotypes. Lower basal SA levels were detected in *dde2-2*. In contrast, the SA glucoside (SAG) and the SA-derived metabolite dihydroxybenzoeic acid (DHBA) were elevated in all three genotype after infection. Like the relative levels of SAG and DHBA, which showed the highest values in the wild-type followed by intermediate levels in the *dde2-2* mutant and even lower levels in *coi1-t*, *PR-1* expression followed the same pattern (Figure 16B). However a slight increase in the SAG and DHBA levels was observed in mock-treated *coi1-t* plants.
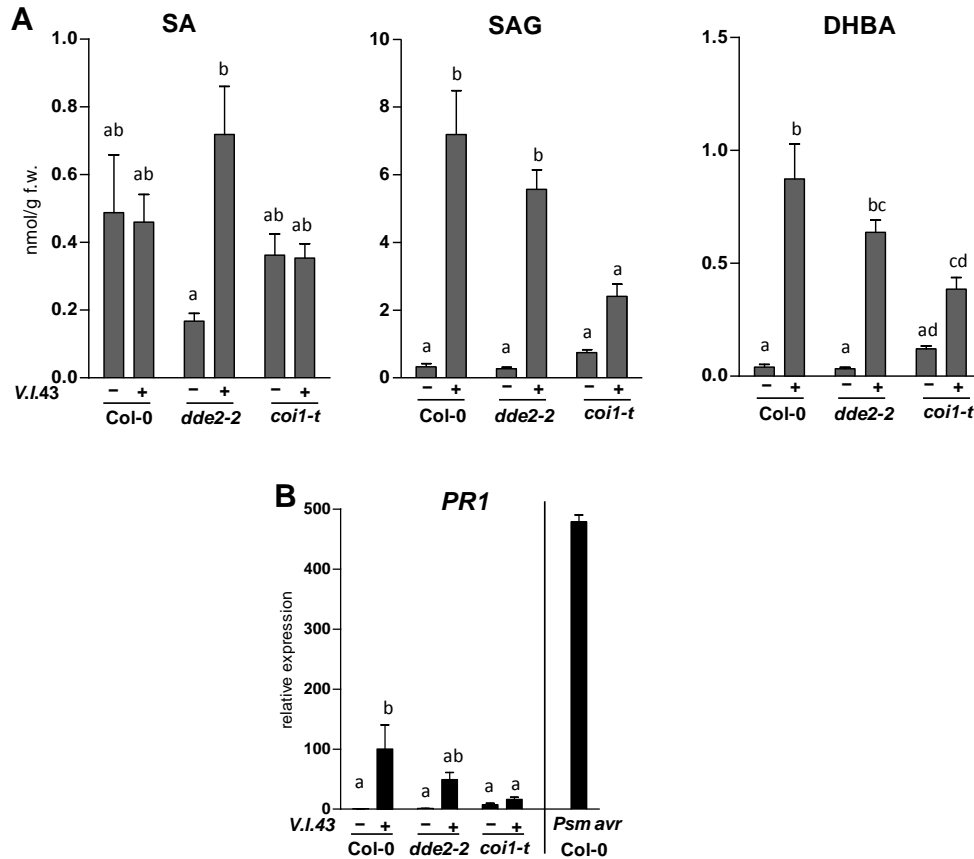
Figure 16 Activation of SA biosynthesis and signaling pathways in *V. longisporum*-infected wild-type, *dde2-2* and *coi1-t* plants

(A) HPLC-MS/MS analysis for detection of SA-, SAG and DHBA levels in petioles from wild-type, *dde2-2* and *coi1-t* plants at 15 days after mock and *V. longisporum* infection. Data are the means (+/- SEM) of eight replicates from two independent experiments. Each replicate is a pool of four plants (same material as in Fig. 4).

(B) Quantitative RT-PCR analysis of relative *PR-1* transcript levels in petioles from wild-type *dde2-2* and *coi1-t* plants at 15 days after mock and *V. longisporum* infection. Data indicate means (+/- SEM) of three independent experiments with 16 individual plants/experiment (same material as in Fig. 4). *Pseudomonas syringae* pv. *maculicola* ES4326/*avrRps4*-infected leaf samples were harvested after three days (three biological replicates). Relative transcript levels of the *V.l.*-infected wild-type were set to 100%.

Different letters denote significant differences between samples (one-way ANOVA followed by Tukey-Kramer multiple comparison test; $P < 0.01$ for (a), SA and SAG; $P < 0,05$ for (a), DHBA and (b)).

To investigate whether this slight increase in the SAG and DHBA levels confers resistance in *coi1* plants, *coi1-1/nahG* double mutant plants were checked for susceptibility. *coi1-1/nahG* plants have also been previously known to lack induced expression of *PR1* (Kloek et al., 2001). Like *coi1-t*, *coi1-1/nahG*, *nahG*, *coi1-1* and *Col-gl* were inoculated with a *V. longisporum* spore suspension. In two independent experiments, the leaf areas of mock and infected plants were measured at 15 dpi (Figure 17). *coi1-1* showed similar resistance to the fungus like *coi1-t* but *coi1-1/nahG*, in contrast, showed significant reduction in the leaf area comparable to the wild

type in one experiment (Figure 17A). In the second experiment, *coi1/nahG* showed no reduction in the leaf area after infection as compared to the wild type (Figure 17B). Since catechol, produced as a result of SA hydrolyses by NahG enzyme, might alter the susceptibility an independent crossing between *coi1-1* and *sid2-2* was initiated and analyzed. *coi1-1/sid2-2* plants also showed reduced disease symptoms like *coi1-1* plants (Figure 17C). These results indicate that the resistant/tolerant *coi1* phenotype is not due to pre-induction of the SA pathway.
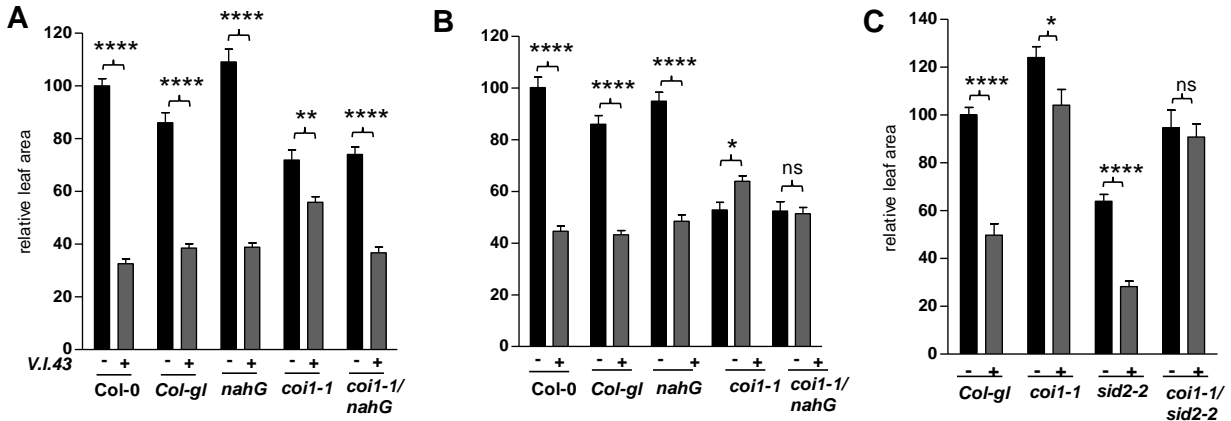
Figure 17 Disease phenotype of V. longisporum-infected wild type, *nahG*, *coi1-1* and *coi1-1/nahG* plants

(A) Projected leaf area of mock- and *V. longisporum*-infected wild-type, *nahG, coi1-1* and *coi1-1/nahG* plants first experiments.
(B) Projected leaf area of mock- and *V. longisporum*-infected wild-type, *nahG, coi1-1* and *coi1-1/nahG* plants from second experiments.
(C) Projected leaf area of mock- and *V. longisporum*-infected wild-type, *coi1-1*, *sid2-2* and *coi1-1/sid2-2* plants from a single experiment at 19 dpi.

Data indicate means (+/- SEM) of 16-18 replicates. Stars indicate significant differences at P < 0.0001 (two-way ANOVA followed by Bonferroni multiple comparison test; ns, not significant) between *V. longisporum* - and mock-infected samples.

3.3.5 Analysis of wild type, *dde2-2* and *coi1-t* roots after *V. longisporum* infection

To provide evidence that the roots of the *V. longisporum*-infected plants are still intact and have not been harmed after infection and also that the wild-type roots do not show any difference than the *coi1-t* roots after fungal penetration, photographs of mock and infected roots were taken at 10 dpi (Figure 18A). Roots of all three genotypes did not show any signs of maceration or browning after infection. Another observation revealed that the wild-type roots after infection became smoother and easier in removing the soil debris. Interestingly this effect was observed already in *coi1* mock roots and was not reinforced after infection. Infected *dde2-2* roots showed

similar effects like the wild-type.This observation suggests that the *V. longisporum*-induced cell wall damage in the root cells might trigger ectopic lignin deposition. These results prompted us to stain mock and infected roots of all the three genotypes with a lignin stain to observe any lignin deposition. Phloroglucinol-HCl stained whole roots grown and infected on 0,5 MS plates (Section 2.2.3.1) were examined under a light microscope at 3 dpi and 7 dpi. Representative pictures from two independent experiments are shown in Figure 18B. At 3 dpi moderate amounts of lignin were observed in mock treated wild-type roots. In contrast, more lignin spots observed in the roots of *dde2-2* and *coi1* plants. No obvious difference between mock and infected roots of all three genotypes was observed at this time point.

At 7 dpi, the difference between mock and infected roots became more prominent in the wild type roots. Lignin deposition in *dde2-2* plants showed a difference between mock-treated and infected roots. However, *coi1* in general showed more lignin already in the mock-treated roots especially in the xylem which did not change after infection. The lignified spots appeared mostly near the root cap in the wild type roots whereas in *coi1* and *dde2-2* roots, they got more prominent in the lateral roots including the area of the main root from where it begins (Figure 18B). This difference in the lignifications of roots of Col-0, *dde2-2* and *coi1* does not affect initial penetration by the fungus.
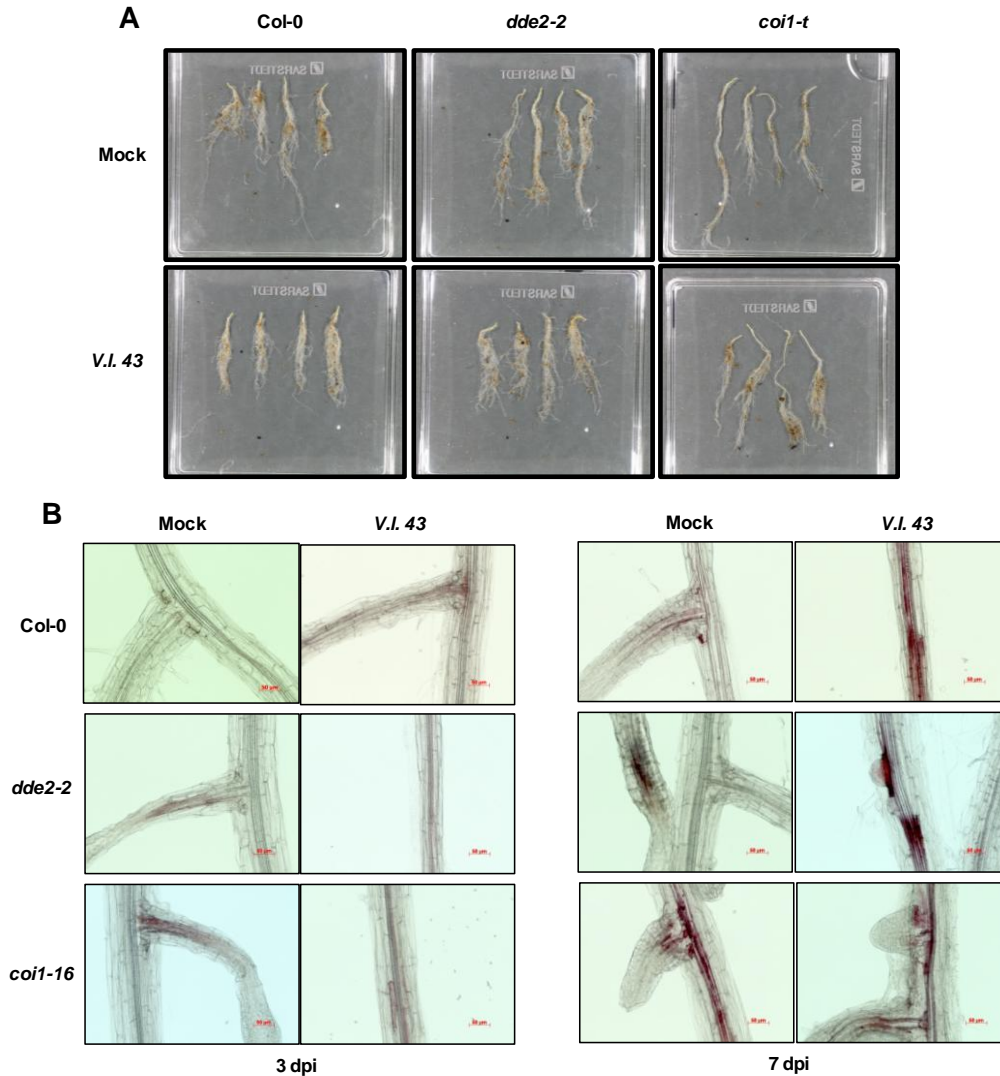
Figure 18 Root phenotype and lignin deposition in _V. longisporum_-infected wild type, _dde2-2_ and _coi1_ plants

(A) Representative picture of mock-(left panel) and _V .longisporum_-infected (right panel) roots of wild type, _dde2-2_ and _coi1-t_. Pictures were taken at 10 dpi from 4 plants. Plants were grown and infected in the soil system.

(B) Roots of wild type, dde2-2 and coi1-16 were stained with Phloroglucinol-HCl stain and red color of lignin was observed in mock- (left panel) and _V. longisporum_-infected (right panel) at 3 dpi and 7 dpi. Plants were grown and infected in 0.5 MS plates.

3.4 Microarray analysis of Col-0, _dde2-2_ and _coi1-t_ infected petioles at 15 dpi

In order to evaluate whether _V. longisporum_-induced resistance in _coi1_ is due to the up-regulation of defense genes that might confer resistance or whether it is due to the reduced expression of genes that might be important for _V. longisporum_-induced susceptibility,

microarray analysis was performed with wild type, *dde2-2* and *coi1-t* plants. The sampling was done with 16 plants per treatment and genotype from three independent experiments. As shown in section 3.3.1, petioles were severely affected in wild-type and *dde2-2* but not in *coi1-t*. Since microsclerotia also developed primarily around this tissue, petioles were harvested for RNA extraction. 15 dpi was chosen as a time point because the disease phenotype had already become visible, but tissue damage was not yet detected. In infected wild type plants, 1219 genes were more than 2-fold ($p < 0.05$) up-regulated and 475 genes were more than 2-fold ($p < 0.05$) down-regulated. In *dde2-2* plants, 1007 genes were up-regulated and 298 genes were down-regulated. In *coi1-t*, 489 and 59 genes were up- and down- regulated respectively.1385 genes were induced at least 2-fold ($p < 0.05$) in one of the three genotypes. MarVis cluster analysis (Kaever et al., 2009) was performed with this set of genes (Analysis performed by: Dr. Corinna Thurow). The programme arranged the genes in a way that started with those genes that were higher expressed in the wild type as compared to *dde2-2* and *coi1-t* (Figure 19A). This cluster contained 38 JA/COI1-dependent genes that were inducible by *V. longisporum* (Cluster I; Table 1). 112 genes were expressed to similar levels in wild-type and *dde2-2* plants (+/- $2^{0.3}$) and more than 2-fold between *dde2-2* and *coi1-t* (Cluster II, Table 2). 262 genes were induced to a similar extent in all three genotypes (+/- $2^{0.3}$) (Cluster III; Table 3). The above results were confirmed using quantitative real time RT-PCR with RNA from an independent experiment which included another JA biosynthesis mutant *acx1/5* (Figure 19B-19D). Apart from these, other clusters were identified. For example, in cluster IV, many genes were higher expressed in the wild-type with a slight decreased expression in *dde2-2* and further decreased expression in *coi1-t* (e.g. *PR-1*). Cluster V contained genes that showed highest differences between wild type and *coi1-t*, but genes of this cluster were higher expressed in *dde2-2* than in the wild type. A cluster containing genes that were higher expressed in infected-*coi1-t* than in the wild type and *dde2-2* was also identified (Cluster VI). The expression pattern of these genes correlated with the expression pattern of genes those are down-regulated after infection in wild-type and *dde2-2* but to a lesser extent in the *coi1-t* plants. As an example, expression levels of two of such genes were confirmed using quantitative real time RT-PCR with the same RNA as for figure 19B-19D. Figure 19E and 19F represents that genes like, XTH17 and GA2OX1 are down-regulated in the wild-type and *dde2-2* but their expression remains high in the *coi1-t* after infection.
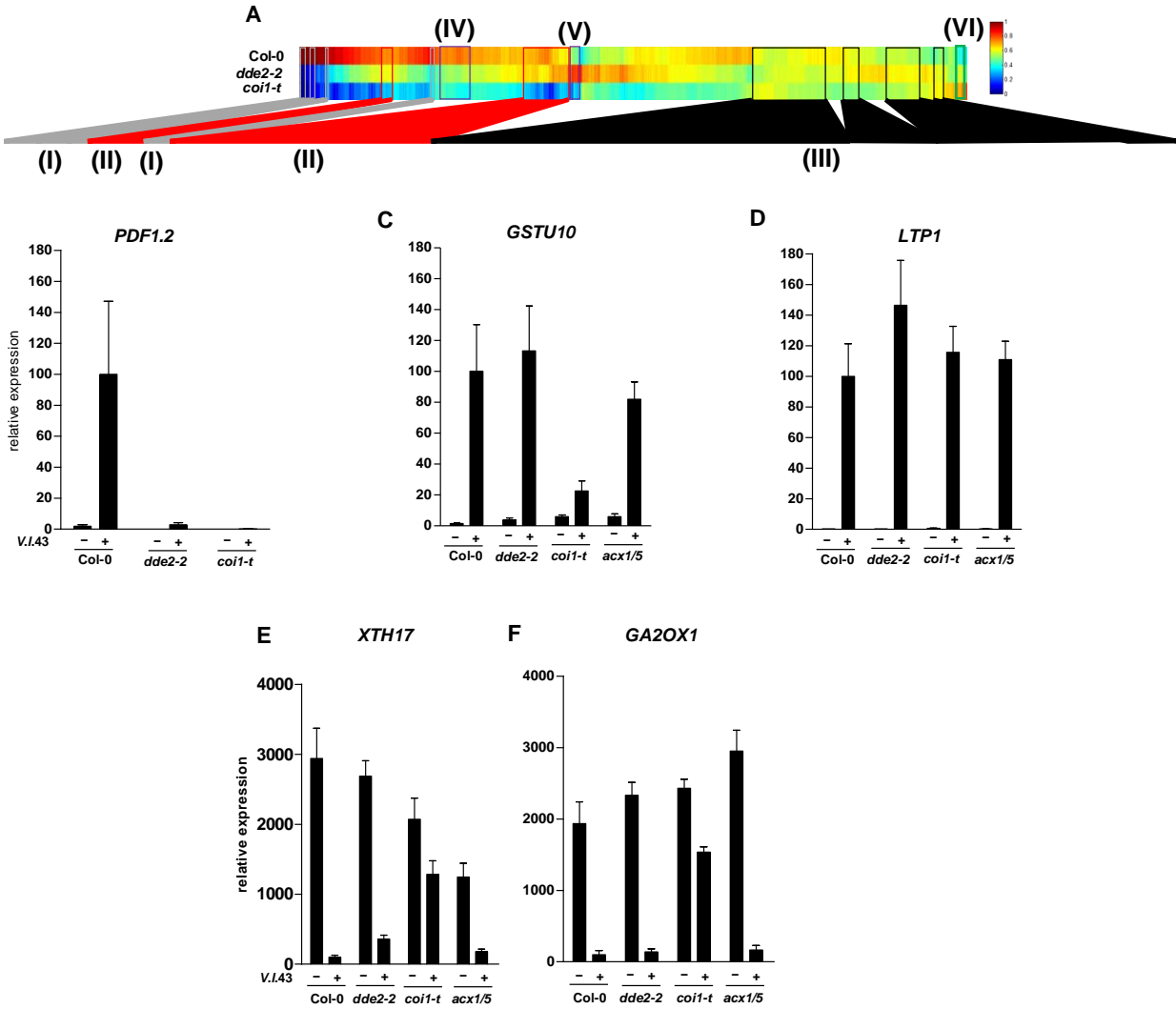
Figure 19 MarVis clustering and verification of microarray expression data from _V. longisporum_-infected _Arabidopsis_ plants

(A) Clustering of 1358 genes that were induced 2-fold (p < 0.05) in one of the genotypes was done by using MarVis clustering tool. The vertical axis represents three genotypes. The horizontal axis corresponds to the cluster numbers. Three important clusters are indicated in brackets. The color was coded according to the indicated scale. Clustering was performed by Corinna Thurow.

(B) Cluster 1, JA/COI1-dependent genes: Quantitative real time RT-PCR analysis of relative _PDF1.2_ transcript levels in petioles from wild type, _dde2-2_, _coi1-t_ and _acx1/5_ plants at 15 days after mock- and _V. longisporum_-infection. Data indicate means (+/- SEM) of 4 replicates from 1 experiment with each replicate containing pool of four plants.

(C) Cluster II, genes expressed to similar levels in wild type and _dde2-2_ plants but to lower levels in _coi1-t_ plants: Quantitative real time RT-PCR analysis of relative _GSTU10_ levels in petioles from wild type, _dde2-2_, _coi1-t_ and _acx1/5_ plants at 15 days after mock- and _V. longisporum_-infection. Data indicate means (+/- SEM) of 4 replicates from 1 experiment with each replicate containing pool of four plants.

(D) Cluster III, genes induced to the same extent in all three genotypes: Quantitative real time RT-PCR analysis of relative _LTP1_ levels in petioles from wild type, _dde2-2_, _coi1-t_ and _acx1/5_ plants at 15 days after mock- and _V. longisporum_-infection. Data indicate means (+/- SEM) of 4 replicates from 1 experiment with each replicate containing pool of four plants.

(E) Quantitative real time RT-PCR analysis of relative *XTH17* transcript levels in petioles from wild type, *dde2-2*, *coi1-t* and *acx1/5* plants at 15 days after mock- and *V. longisporum*-infection. Data indicate means (+/- SEM) of 4 replicates from 1 experiment with each replicate containing pool of four plants.

(F) Quantitative real time RT-PCR analysis of relative *GA2OX1* transcript levels in petioles from wild type, *dde2-2*, *coi1-t* and *acx1/5* plants at 15 days after mock- and *V. longisporum*-infection. Data indicate means (+/- SEM) of 4 replicates from 1 experiment with each replicate containing pool of four plants.

Table 1 List of 38 JA/COI1-dependent genes from cluster I of *Verticillium*-induced genes according to MarVis clustering.

Table represents genes with higher expression levels in the wild-type and similar expression levels in wild-type and *dde2-2*. Values denote the fold-induction between mock and infected plants with p< 0.05.

		Col-0 inf/ Col-0 mock		dde2-2 inf/ dde2-2 mock		coi1-t inf/ coi1-t mock	
		x-fold ind	p-value	x-fold ind	p-value	x-fold ind	p-value
Cell Wall							
AT4G24000	ATCSLG2	2.4	5E-04	1.3	2E-01	1.1	6E-01
Amino Acid metabolism							
AT1G64660	ATMGL	3.2	2E-02	1.9	2E-01	1.5	4E-01
Secondary metabolism							
AT1G61120	TPS04 (TERPENE SYNTHASE 04)	2.4	5E-07	1.0	9E-01	1.0	8E-01
AT1G54020	myrosinase-associated protein, putative	14.7	1E-09	0.9	7E-01	1.1	6E-01
AT1G52030	MBP1 (MYROSINASE-BINDING PROTEIN 1)	5.9	8E-09	0.4	1E-04	0.7	2E-02
AT3G55970	oxidoreductase	44.6	4E-12	1.0	9E-01	1.1	7E-01
AT2G38240	oxidoreductase	5.1	4E-08	0.9	7E-01	0.8	3E-01
AT5G05600	oxidoreductase	3.8	2E-04	1.3	4E-01	1.2	5E-01
AT4G22870	leucoanthocyanidin dioxygenase, putative	2.3	4E-02	0.5	1E-01	0.9	7E-01
Hormone metabolism							
AT1G44350	ILL6	2.0	1E-02	0.7	2E-01	1.2	6E-01
AT1G19640	JMT	6.8	3E-09	1.0	9E-01	1.1	6E-01
AT3G25780	AOC3	2.1	1E-01	4.3	3E-03	3.3	1E-02
Major CHO metabolism							
AT4G15210	BAM5	4.8	6E-05	0.3	1E-03	0.9	9E-01
Stress							
AT1G72260	THI2.1 (THIONIN 2.1)	26.0	5E-07	1.0	1E+00	1.0	1E+00
AT5G09980	PROPEP4	2.9	2E-05	1.1	5E-01	1.0	8E-01
Nucleotide metabolism							
AT1G14230	nucleoside phosphatase family protein	2.1	1E-04	1.5	1E-02	1.2	2E-01
Biodegradation of Xenobiotics							
AT5G16080	AtCXE17	2.6	3E-04	0.9	7E-01	0.9	5E-01
Misc.							
AT5G36220	CYP81D1 (CYTOCHROME P450 81D1)	4.6	1E-08	2.0	2E-04	1.4	3E-02
AT2G39330	JAL23 (JACALIN-RELATED LECTIN 23)	5.1	1E-05	0.4	2E-03	0.9	6E-01
AT1G52000	jacalin lectin family protein	2.6	5E-03	0.7	3E-01	1.2	6E-01
AT4G22610	lipid transfer protein (LTP) family protein	3.9	1E-11	1.1	4E-01	1.1	2E-01
AT2G39030	GCN5-related N-acetyltransferase (GNAT) family protein	40.2	6E-15	1.0	8E-01	1.2	2E-01
AT1G66280	BGLU22	2.9	3E-06	0.9	6E-01	1.0	8E-01
RNA							
AT1G43160	RAP2.6	6.0	1E-06	1.4	1E-01	1.0	9E-01
Protein							
AT4G17470	palmitoyl protein thioesterase family protein	2.5	1E-04	0.9	7E-01	1.0	8E-01

AT4G15100	scpl30	12.0	1E-12	1.4	6E-03	1.1	3E-01
AT4G11320	cysteine proteinase, putative	2.4	8E-03	0.9	6E-01	0.8	5E-01
Signalling							
AT3G24982	protein binding	2.7	8E-06	1.4	4E-02	1.3	9E-02
AT1G52410	TSA1	2.5	1E-03	0.4	1E-03	0.9	6E-01
Cell cycle							
AT3G43250	cell cycle control protein-related	2.1	9E-04	1.1	7E-01	1.2	4E-01
Development							
AT5G24770	VSP2	8.2	6E-08	1.2	4E-01	1.4	1E-01
Not assigned							
AT5G19110	extracellular dermal glycoprotein-related	2.2	5E-03	0.6	4E-02	0.7	3E-01
AT4G30460	glycine-rich protein	23.6	3E-08	27.1	2E-08	28.6	1E-08
AT2G47950	unknown protein	10.0	2E-11	3.7	6E-08	3.2	2E-07
AT5G13220	JAZ10	2.5	3E-03	0.9	8E-01	1.1	6E-01
AT2G06255	ELF4-L3 (ELF4-Like 3)	2.5	5E-07	1.4	4E-03	1.1	5E-01
AT4G02360	unknown protein	2.2	2E-05	0.9	6E-01	1.0	9E-01
OPP							
AT5G24420	glucosamine/galactosamine-6-phosphate isomerase-related	6.4	3E-05	0.5	2E-02	0.9	7E-01

Table 2 List of genes from cluster II of *Verticillium*-induced genes according to MarVis analysis.

Table represents 112 genes expressed to similar levels in the wild type and *dde2-2* (+/- 2 $^{0.3}$) and to a lower level in *coi1-t*. Values denote the fold-induction between mock and infected plants with p< 0.05.

		Col-0 inf/ Col-0 mock		dde2-2 inf/ dde2-2 mock		coi1-t inf/ coi1-t mock	
		x-fold ind	p-value	x-fold ind	p-value	x-fold ind	p-value
Cell wall							
AT1G76930	ATEXT4 (EXTENSIN 4)	3.1	4E-08	2.5	7E-07	1.4	1E-02
AT5G62150	peptidoglycan-binding LysM domain-containing protein	4.0	5E-05	2.9	6E-04	1.7	5E-02
AT5G06860	PGIP1	4.0	2E-06	3.0	3E-05	1.6	2E-02
Lipid metabolism							
AT1G06520	GPAT1	7.3	1E-04	8.4	5E-05	3.5	5E-03
AT5G22500	FAR1	5.2	4E-04	3.3	5E-03	1.5	3E-01
Metal handling							
AT1G07610	MT1C	5.4	3E-04	5.7	2E-04	1.9	1E-01
Secondary metabolism							
AT1G74010	strictosidine synthase family protein	3.5	7E-05	2.6	1E-03	1.2	4E-01
AT5G39050	transferase	4.2	6E-04	5.4	1E-04	1.8	9E-02
Hormone metabolism							
AT3G60690	auxin-responsive family protein	6.7	4E-05	6.6	4E-05	1.3	5E-01
AT2G03760	ST1	4.2	7E-08	3.5	4E-07	1.4	3E-02
AT4G29740	CKX4	2.6	6E-04	1.4	1E-01	0.7	8E-02
AT1G05680	UDP-glucoronosyl/UDP-glucosyl transferase family protein	3.7	9E-08	2.8	1E-06	2.0	1E-04
Major CHO metabolism							
AT3G13790	ATBFRUCT1	3.9	1E-07	3.5	3E-07	1.1	4E-01
Stress							
AT4G23260	ATP binding	9.5	2E-05	6.0	2E-04	1.2	6E-01
AT2G15120	disease-resistance family protein	3.3	1E-03	2.7	4E-03	1.1	6E-01
AT1G19610	PDF1.4	4.8	3E-09	3.6	5E-08	2.2	2E-05
AT2G43580	chitinase, putative	11.0	7E-12	11.1	6E-12	4.0	2E-08
AT2G38870	protease inhibitor, putative	2.5	3E-03	1.8	5E-02	1.0	9E-01
AT1G33960	AIG1 (AVRRPT2-INDUCED GENE 1)	2.8	3E-03	1.9	4E-02	0.8	6E-01
AT1G72890	disease resistance protein (TIR-NBS class), putative	2.4	5E-04	1.7	2E-02	1.0	8E-01
AT1G57630	disease resistance protein (TIR class), putative	5.7	1E-06	6.4	6E-07	3.1	2E-04
AT3G04320	endopeptidase inhibitor	3.7	5E-05	4.1	3E-05	1.7	3E-02
AT3G01420	ALPHA-DOX1	3.6	2E-07	3.8	9E-08	1.9	5E-04

Redox							
AT1G69880	ATH8	6.1	1E-07	7.0	5E-08	3.0	5E-05
AT1G03850	glutaredoxin family protein	3.9	2E-04	2.1	2E-02	0.7	3E-01
Nucleotide metabolism							
AT4G29570	cytidine deaminase, putative	2.1	4E-03	1.9	1E-02	0.9	7E-01
Misc.							
AT5G67310	CYP81G1	4.0	1E-07	4.0	1E-07	1.6	4E-03
AT2G45570	CYP76C2	2.2	5E-04	2.0	1E-03	1.2	4E-01
AT2G34500	CYP710A1	2.6	2E-03	3.7	2E-04	1.4	2E-01
AT3G26230	CYP71B24	5.4	4E-05	4.4	2E-04	2.7	4E-03
AT2G01890	PAP8	5.1	1E-05	5.6	7E-06	2.8	1E-03
AT5G53870	plastocyanin-like domain-containing protein	5.0	2E-06	3.4	5E-05	1.4	1E-01
AT1G62510	protease inhibitor	4.5	1E-03	7.3	7E-05	2.2	5E-02
AT5G50700	AtHSD1	23.9	7E-08	15.7	5E-07	3.6	1E-03
AT1G65610	ATGH9A2	10.4	9E-11	10.8	7E-11	4.4	5E-08
AT3G04010	glycosyl hydrolase family 17 protein	2.9	3E-05	4.0	1E-06	2.1	8E-04
AT4G12290	copper amine oxidase family protein	3.3	2E-04	2.7	1E-03	1.7	6E-02
AT1G30720	FAD-binding domain-containing protein	5.1	6E-05	3.7	4E-04	1.3	4E-01
AT1G30700	FAD-binding domain-containing protein	3.5	8E-08	3.0	4E-07	1.7	1E-03
AT5G02780	In2-1 protein, putative	3.8	4E-05	3.9	3E-05	1.4	2E-01
AT3G09270	ATGSTU8	3.4	9E-05	3.1	2E-04	1.3	2E-01
AT1G74590	GSTU10	3.2	8E-06	4.1	7E-07	1.2	3E-01
AT1G69930	ATGSTU11	7.2	2E-10	6.0	7E-10	1.7	1E-03
RNA							
AT2G02990	RNS1	2.6	2E-04	3.2	2E-05	1.4	1E-01
AT3G11580	DNA-binding protein, putative	9.4	5E-06	8.8	8E-06	2.0	5E-02
AT1G13300	myb family transcription factor	2.4	2E-03	1.5	9E-02	1.1	7E-01
AT5G59780	MYB59	13.7	7E-09	11.9	2E-08	2.3	3E-03
AT4G05100	AtMYB74	5.1	4E-08	4.6	9E-08	2.0	7E-04
AT3G04070	anac047	5.5	2E-05	4.6	8E-05	2.6	4E-03
AT4G39780	AP2 domain-containing transcription factor, putative	13.1	9E-10	9.7	5E-09	4.2	2E-06
AT5G61890	AP2 domain-containing transcription factor family protein	6.8	2E-11	7.3	1E-11	3.0	5E-08
AT2G20880	AP2 domain-containing transcription factor, putative	5.6	2E-08	4.1	3E-07	1.2	3E-01
AT5G46350	ATWRKY8	13.8	3E-09	6.6	2E-07	1.4	1E-01
AT1G76590	zinc-binding family protein	4.8	1E-05	3.6	1E-04	0.9	6E-01
Protein							
AT1G32940	SBT3.5	2.6	3E-03	2.3	7E-03	0.5	1E-02
AT1G22500	zinc finger (C3HC4-type RING finger) family protein	2.5	5E-05	2.0	7E-04	1.0	9E-01
AT1G60190	armadillo/beta-catenin repeat family protein	4.8	2E-07	4.7	2E-07	1.9	2E-03
AT2G42360	zinc finger (C3HC4-type RING finger) family protein	2.9	3E-03	3.7	6E-04	1.9	4E-02
AT3G61390	U-box domain-containing protein	2.9	7E-07	2.1	4E-05	1.0	9E-01
AT5G50260	cysteine proteinase, putative	7.3	4E-09	5.0	7E-08	2.3	2E-04
AT3G12240	SCPL15	7.8	2E-09	5.2	3E-08	1.4	8E-02
AT3G28540	AAA-type ATPase family protein	20.1	3E-11	8.2	5E-09	1.5	4E-02
AT5G40010	AATP1	6.6	8E-05	4.6	6E-04	1.7	2E-01
AT3G28510	AAA-type ATPase family protein	5.5	3E-03	4.8	5E-03	2.9	4E-02
Minor CHO metabolism							
AT2G37760	aldo/keto reductase family protein	7.6	2E-07	6.4	7E-07	1.6	5E-02
Signalling							
AT5G09440	EXL4	6.4	4E-08	5.1	2E-07	0.9	5E-01
AT5G48400	GLR1.2	6.1	1E-03	6.4	1E-03	1.3	6E-01
AT2G02710	PLPB	7.2	2E-05	5.6	7E-05	1.8	9E-02
AT5G24080	protein kinase family protein	9.1	8E-11	6.7	7E-10	1.5	1E-02
AT1G51860	leucine-rich repeat protein kinase, putative	4.4	4E-08	2.8	4E-06	1.1	4E-01
AT3G22060	receptor protein kinase-related	8.7	4E-08	6.5	3E-07	1.7	2E-02
AT1G51890	leucine-rich repeat protein kinase, putative	8.5	2E-07	6.7	1E-06	1.5	1E-01
AT3G46280	protein kinase-related	32.6	2E-12	25.7	5E-12	4.0	5E-07
AT1G51800	leucine-rich repeat protein kinase, putative	4.7	1E-04	3.9	3E-04	1.0	1E+00
AT4G18430	AtRABA1e	6.4	2E-05	3.0	3E-03	0.9	8E-01
Cell							
AT5G55400	fimbrin-like protein, putative	11.6	6E-06	8.0	4E-05	1.3	4E-01
Development							
AT1G52690	LEA protein, putative	10.2	5E-06	8.8	1E-05	1.1	7E-01
AT1G69490	NAP (NAC-like, activated by AP3/PI)	15.5	3E-09	15.0	4E-09	2.4	1E-03
AT2G41380	embryo-abundant protein-related	11.4	9E-09	10.3	2E-08	1.5	7E-02
AT2G39210	nodulin family protein	4.4	1E-07	5.9	1E-08	1.3	2E-01
AT3G49780	ATPSK4	7.4	2E-08	6.6	4E-08	2.7	6E-05
AT5G13170	SAG29	3.6	1E-04	3.2	3E-04	1.1	6E-01
AT4G01430	nodulin MtN21 family protein	3.0	1E-03	1.9	3E-02	0.5	1E-02
Transport							

AT4G23700	ATCHX17	4.6	1E-09	4.8	1E-09	1.6	1E-03
AT5G46050	PTR3	15.1	1E-07	11.9	3E-07	3.8	3E-04
AT3G60970	ATMRP15	3.3	3E-05	3.1	6E-05	1.4	1E-01
AT2G39350	ABC transporter family protein	13.1	8E-09	13.2	8E-09	5.9	1E-06
AT1G71890	SUC5	35.5	2E-08	25.9	8E-08	9.4	8E-06
AT5G17860	CAX7	10.9	5E-09	7.0	8E-08	1.7	2E-02
AT4G21120	AAT1	2.9	3E-05	2.7	5E-05	1.2	4E-01
AT5G50200	WR3	10.2	1E-05	8.6	3E-05	4.1	1E-03
Not assigned							
AT4G15120	VQ motif-containing protein	2.4	3E-04	2.2	9E-04	1.1	7E-01
AT1G55780	metal ion binding	4.2	2E-05	4.9	5E-06	2.5	1E-03
AT1G15040	glutamine amidotransferase-related	9.9	2E-06	7.8	7E-06	2.1	3E-02
AT1G65690	harpin-induced protein-related	3.4	3E-04	2.2	8E-03	1.0	1E+00
AT2G44380	DC1 domain-containing protein	2.5	2E-04	2.5	2E-04	1.4	1E-01
AT2G28400	unknown protein	2.3	3E-04	2.1	8E-04	1.1	7E-01
AT2G29995	unknown protein	7.1	1E-07	9.3	2E-08	4.4	4E-06
AT5G61820	unknown protein	12.1	4E-05	11.9	4E-05	2.6	4E-02
AT5G10210	unknown protein	2.8	2E-04	3.2	5E-05	1.5	9E-02
AT5G02020	unknown protein	11.5	3E-06	12.6	2E-06	1.6	2E-01
AT5G39520	unknown protein	3.2	5E-06	4.0	6E-07	2.3	2E-04
no_match	no match	3.3	2E-04	2.9	6E-04	1.8	3E-02
AT3G18250	unknown protein	6.2	2E-06	5.1	8E-06	1.4	2E-01
AT1G73750	unknown protein	52.4	6E-11	46.5	9E-11	7.7	5E-07
AT4G33666	unknown protein	31.0	5E-11	24.3	1E-10	13.2	3E-09
AT3G13950	unknown protein	1.9	1E-04	2.1	2E-05	1.2	1E-01
AT2G44240	unknown protein	5.1	1E-05	7.2	1E-06	2.2	8E-03
AT1G27990	unknown protein	10.6	2E-08	12.2	1E-08	3.4	6E-05
AT2G32190	unknown protein	2.4	1E-03	2.9	2E-04	1.3	3E-01
AT2G20875	EPF1	4.7	1E-06	5.7	2E-07	1.4	9E-02
AT3G57950	unknown protein	2.7	5E-04	2.7	5E-04	2.0	8E-03

Table 3 List of genes from cluster III of *Verticillium*-induced genes according to MarVis analysis

Table represents genes those are expressed to a similar level in all three genotypes after infection. Values denote the fold-induction between mock and infected plants with p< 0.05.

		Col-0 inf/ Col-0 mock		dde2-2 inf/ dde2-2 mock		coi1-t inf/ coi1-t mock	
		x-fold ind	p-value	x-fold ind	p-value	x-fold ind	p-value
Cell wall							
AT2G28760	UXS6	1.9	2E-05	1.7	9E-05	2.1	3E-06
AT3G46440	UXS5	2.2	2E-03	1.8	2E-02	1.3	2E-01
AT4G18780	IRX1	2.4	4E-04	2.3	7E-04	2.7	1E-04
AT5G44030	CESA4	2.9	1E-04	2.8	1E-04	3.2	5E-05
AT5G17420	IRX3	2.4	5E-04	2.4	5E-04	2.6	2E-04
AT5G15630	IRX6	2.5	2E-04	2.4	4E-04	2.6	2E-04
AT2G37090	IRX9	4.2	6E-07	4.5	4E-07	4.5	4E-07
AT2G22470	AGP2	4.1	5E-06	3.4	3E-05	3.3	3E-05
AT5G56540	AGP14	7.5	1E-08	8.0	9E-09	7.1	2E-08
AT4G16790	hydroxyproline-rich glycoprotein family protein	10.1	5E-12	9.4	7E-12	6.8	7E-11
AT1G21310	ATEXT3 (EXTENSIN 3)	3.1	4E-04	2.7	1E-03	1.5	1E-01
AT5G01930	(1-4)-beta-mannan endohydrolase, putative	3.3	2E-07	3.7	6E-08	4.3	1E-08
AT4G33810	glycosyl hydrolase family 10 protein	2.0	7E-05	2.5	3E-06	2.5	4E-06
AT1G23760	JP630	8.1	5E-09	9.3	2E-09	9.2	2E-09
AT1G23470	polygalacturonase (pectinase)	12.5	5E-12	14.9	2E-12	13.2	4E-12
AT3G61490	glycoside hydrolase family 28 protein	9.2	4E-09	9.2	4E-09	11.1	1E-09
AT2G18660	EXLB3	32.1	6E-09	16.4	1E-07	2.6	6E-03
AT1G05310	pectinesterase family protein	3.2	2E-06	3.2	2E-06	3.7	5E-07
AT5G09760	pectinesterase family protein	3.6	1E-06	5.2	5E-08	4.6	1E-07
AT3G09410	Unknown	2.9	2E-02	2.2	6E-02	1.3	6E-01
AT3G47400	pectinesterase family protein	2.8	3E-05	2.6	5E-05	2.5	9E-05
Lipid metabolism							
AT5G59320	LTP3	37.3	7E-06	15.2	1E-04	10.6	6E-04
AT5G54500	FQR1	2.5	1E-05	2.1	1E-04	1.5	9E-03

AT1G52760	thioesterase family protein	1.8	6E-07	2.1	3E-08	1.8	1E-06
AT3G14360	lipase class 3 family protein	2.5	9E-07	2.1	1E-05	2.2	5E-06
AT4G18550	lipase class 3 family protein	2.3	3E-05	2.5	1E-05	2.2	8E-05
AT5G65110	ACX2 (ACYL-COA OXIDASE 2)	2.2	4E-04	1.9	3E-03	1.4	6E-02
Amino acid metabolism							
AT1G22410	2-dehydro-3-deoxyphosphoheptonate aldolase, putative	2.0	2E-05	2.4	2E-06	2.1	1E-05
AT5G22630	ADT5	2.1	1E-02	4.1	5E-05	2.8	1E-03
AT1G08250	ADT6	1.4	7E-02	1.9	2E-03	2.0	9E-04
Metal handling							
AT5G60950	COBL5 (COBRA-LIKE PROTEIN 5 PRECURSOR)	3.9	2E-06	3.5	6E-06	1.2	4E-01
AT3G56240	CCH (COPPER CHAPERONE)	3.3	1E-08	3.1	3E-08	2.6	3E-07
Secondary metabolism							
AT5G05390	LAC12	1.9	3E-03	1.5	3E-02	2.0	1E-03
AT5G60020	LAC17	2.8	2E-06	2.9	2E-06	3.1	8E-07
AT5G01190	LAC10	3.7	4E-07	3.8	3E-07	4.3	1E-07
AT2G38080	IRX12	3.4	1E-07	3.9	4E-08	4.2	2E-08
AT2G37040	ATPAL1	3.2	5E-04	7.1	2E-06	6.8	2E-06
AT3G21240	4CL2	1.9	2E-02	2.9	3E-04	2.9	3E-04
AT4G34050	caffeoyl-CoA 3-O-methyltransferase, putative	2.7	9E-05	3.5	8E-06	3.0	3E-05
AT4G31500	CYP83B1	1.0	9E-01	2.1	3E-03	1.7	2E-02
AT1G02205	CER1	1.4	3E-01	1.3	4E-01	2.5	2E-02
AT5G49690	UDP-glucosyl transferase family protein	3.2	8E-07	3.1	1E-06	2.7	6E-06
AT1G75280	isoflavone reductase, putative	2.6	3E-04	3.1	6E-05	3.6	2E-05
Hormone metabolism							
AT5G57050	ABI2 (ABA INSENSITIVE 2)	2.1	8E-05	1.6	6E-03	1.7	1E-03
AT5G50720	ATHVA22E	6.3	4E-07	4.9	3E-06	4.2	8E-06
AT2G04850	auxin-responsive protein-related	3.3	1E-05	3.4	9E-06	4.7	5E-07
AT3G12830	auxin-responsive family protein	2.7	1E-03	1.7	5E-02	1.1	8E-01
AT5G53590	auxin-responsive family protein	3.0	9E-06	3.4	3E-06	3.1	6E-06
AT3G23150	ETR2	2.3	3E-04	1.6	2E-02	1.3	1E-01
AT2G40940	ERS1	2.3	2E-03	1.9	8E-03	1.3	3E-01
Tetrapyrrole synthesis							
AT1G58300	ho4	2.6	7E-05	2.3	2E-04	1.5	4E-02
Major CHO metabolism							
AT1G06020	pfkB-type carbohydrate kinase family protein	2.1	8E-06	1.6	2E-03	2.0	3E-05
AT5G20830	SUS1	3.3	3E-05	2.1	2E-03	1.4	9E-02
Stress							
AT4G39030	EDS5	3.0	7E-04	3.8	1E-04	2.3	5E-03
AT3G16920	chitinase	2.7	7E-06	2.7	7E-06	3.1	1E-06
AT3G11660	NHL1	2.0	5E-03	2.4	8E-04	1.6	3E-02
AT5G40020	pathogenesis-related thaumatin family protein	16.5	9E-10	21.6	3E-10	15.4	1E-09
AT3G52430	PAD4	4.6	1E-05	5.1	5E-06	1.7	5E-02
AT4G33300	ADR1-L1	2.4	4E-05	2.2	2E-04	1.5	2E-02
AT2G24160	leucine rich repeat protein family	2.2	3E-04	2.1	5E-04	1.0	9E-01
AT2G02100	LCR69	2.3	2E-02	1.4	3E-01	1.5	2E-01
AT1G64060	ATRBOH F	2.5	1E-05	2.8	3E-06	2.7	4E-06
AT3G25020	AtRLP42	2.6	1E-05	1.9	6E-04	1.0	8E-01
AT1G55210	disease resistance response	2.9	5E-06	3.7	4E-07	3.4	1E-06
AT2G14580	ATPRB1	1.7	8E-03	2.3	2E-04	1.0	8E-01
AT4G23690	disease resistance-responsive family protein	8.3	3E-09	12.5	3E-10	12.7	3E-10
AT3G05650	AtRLP32	2.3	3E-03	1.8	2E-02	1.3	2E-01
AT3G08970	ATERDJ3A	1.7	1E-02	2.0	1E-03	1.7	1E-02
AT4G36988	CPuORF49	3.5	1E-05	3.8	7E-06	2.8	1E-04
AT4G15910	ATDI21	2.5	4E-08	2.4	5E-08	2.1	6E-07
AT5G42050	Unknown	2.2	2E-02	2.4	1E-02	2.0	4E-02
AT3G10080	germin-like protein, putative	1.8	5E-05	1.7	2E-04	2.3	1E-06
AT3G62020	GLP10	4.1	6E-09	4.0	7E-09	4.1	5E-09
AT5G66400	RAB18	4.1	5E-04	2.6	1E-02	2.4	2E-02
Redox							
AT4G39830	L-ascorbate oxidase, putative	3.7	2E-03	2.4	3E-02	1.6	2E-01
AT4G11600	ATGPX6	2.1	3E-03	1.7	3E-02	1.3	2E-01
AT5G63030	glutaredoxin, putative	2.2	7E-07	2.1	2E-06	1.4	2E-03
Nucleotide metabolism							
AT4G20320	CTP synthase	5.3	2E-04	5.1	2E-04	3.5	2E-03
AT5G09290	3'(2'),5'-bisphosphate nucleotidase, putative	3.4	7E-07	2.5	2E-05	1.4	4E-02
AT1G14240	CD39 family protein	4.6	1E-06	5.3	4E-07	4.3	2E-06
AT5G64000	SAL2	3.3	2E-05	2.7	1E-04	1.4	1E-01
AT4G25434	ATNUDT10	3.5	3E-06	3.5	3E-06	3.2	8E-06
AT2G01670	atnudt17	2.2	2E-04	1.9	1E-03	1.3	9E-02
AT3G53620	AtPPa4	1.7	2E-04	1.7	1E-04	2.0	7E-06

Misc.							
AT3G26125	CYP86C2	3.8	1E-08	3.6	2E-08	4.8	1E-09
AT2G37130	peroxidase 21 (PER21)	5.7	4E-09	4.0	9E-08	2.9	2E-06
AT5G15180	peroxidase, putative	8.1	4E-10	7.6	7E-10	6.3	3E-09
AT1G13750	calcineurin-like phosphoesterase family protein	2.5	5E-05	2.0	7E-04	1.1	5E-01
AT3G52820	PAP22	5.1	3E-08	3.9	3E-07	4.0	2E-07
AT2G38600	acid phosphatase class B family protein	11.6	5E-10	16.6	7E-11	17.6	5E-11
AT5G18470	curculin-like (mannose-binding) lectin family protein	5.7	4E-03	4.7	8E-03	3.3	3E-02
AT1G33790	jacalin lectin family protein	3.0	1E-04	2.8	2E-04	1.8	2E-02
AT2G47670	invertase/pectin methylesterase inhibitor family protein	5.3	3E-08	4.9	6E-08	6.0	1E-08
AT5G26330	plastocyanin-like domain-containing protein	2.3	1E-04	2.4	7E-05	3.1	3E-06
AT3G27200	plastocyanin-like domain-containing protein	4.3	6E-07	3.8	2E-06	4.1	9E-07
AT2G16890	UDP-glucosyl transferase family protein	2.8	8E-04	2.7	1E-03	5.1	8E-06
AT4G27480	glycosyltransferase family 14 protein	2.7	7E-05	2.6	7E-05	1.8	5E-03
AT4G33330	PGSIP3	2.2	8E-05	1.8	1E-03	2.0	2E-04
AT1G27440	GUT2	2.5	5E-08	2.6	2E-08	2.4	7E-08
AT3G53980	lipid transfer protein (LTP) family protein	31.7	8E-10	43.1	3E-10	37.5	4E-10
AT5G55450	lipid transfer protein (LTP) family protein	3.6	6E-06	3.0	3E-05	1.1	5E-01
AT1G54790	GDSL-motif lipase/hydrolase family protein	3.8	1E-06	4.6	2E-07	3.7	1E-06
AT5G11320	YUC4 (YUCCA4)	3.4	4E-06	3.2	5E-06	3.2	6E-06
AT2G17720	2OG-Fe(II) oxygenase family protein	1.8	8E-06	2.0	1E-06	1.3	1E-02
AT2G43080	AT-P4H-1	2.1	3E-05	2.0	6E-05	1.6	3E-03
AT2G34790	MEE23	12.0	1E-11	13.2	7E-12	11.3	2E-11
RNA							
AT1G26820	RNS3	6.3	8E-10	7.4	2E-10	6.6	5E-10
AT3G60580	zinc finger (C2H2 type) family protein	2.1	2E-05	1.6	1E-03	1.3	5E-02
AT3G13810	AtIDD11	2.2	4E-03	2.0	8E-03	1.2	4E-01
AT5G03510	zinc finger (C2H2 type) family protein	4.6	8E-08	6.1	8E-09	4.2	2E-07
AT1G68360	zinc finger protein-related	2.2	8E-05	2.3	3E-05	2.6	6E-06
AT4G32880	ATHB-8 (HOMEOBOX GENE 8)	1.9	5E-04	2.0	2E-04	2.0	1E-04
AT1G67970	AT-HSFA8; DNA binding / transcription factor	3.8	8E-04	2.0	5E-02	1.4	3E-01
AT5G12870	MYB46	2.9	9E-08	3.0	6E-08	3.7	8E-09
AT2G16720	MYB7	3.5	4E-07	4.6	3E-08	3.5	3E-07
AT1G79180	MYB63	1.8	6E-06	2.1	2E-07	1.8	5E-06
AT3G25730	AP2 domain-containing transcription factor, putative	2.1	4E-04	1.8	3E-03	1.7	4E-03
AT5G07310	AP2 domain-containing transcription factor, putative	5.3	6E-07	5.7	3E-07	6.0	2E-07
AT2G38250	DNA-binding protein-related	2.7	1E-06	2.3	6E-06	2.3	9E-06
AT2G25000	WRKY60	4.0	4E-05	3.5	1E-04	2.8	6E-04
AT1G31290	PAZ domain-containing protein	2.4	2E-04	2.3	3E-04	2.0	2E-03
AT1G61660	basic helix-loop-helix (bHLH) family protein	2.1	2E-03	2.2	1E-03	2.1	1E-03
AT5G09800	U-box domain-containing protein	1.8	6E-03	1.9	2E-03	2.2	4E-04
AT1G20900	ESC (ESCAROLA)	2.3	1E-03	2.3	1E-03	1.7	2E-02
AT3G57540	remorin family protein	2.1	4E-03	2.0	6E-03	1.7	3E-02
AT5G63880	VPS20.1	2.1	2E-03	1.4	1E-01	1.0	1E+00
DNA							
AT3G52900	unknown protein	2.4	2E-05	2.5	1E-05	2.7	5E-06
AT1G11190	BFN1	14.7	5E-12	15.1	5E-12	10.3	4E-11
AT1G75090	methyladenine glycosylase family protein	2.5	2E-04	1.9	5E-03	2.0	2E-03
Protein							
AT1G13950	ELF5A-1	1.8	4E-03	2.7	4E-05	1.4	7E-02
AT3G27070	TOM20-1	2.2	8E-05	1.9	6E-04	2.6	1E-05
AT1G20350	ATTIM17-1	4.7	5E-07	5.6	1E-07	2.6	1E-04
AT1G30640	protein kinase, putative	2.3	1E-03	2.2	1E-03	1.5	5E-02
AT5G01700	PP2C, putative	2.0	4E-05	2.0	3E-05	1.9	8E-05
AT1G07430	PP2C, putative	3.6	1E-06	2.7	2E-05	2.7	2E-05
AT3G17420	GPK1	2.4	3E-04	2.5	2E-04	2.2	7E-04
AT5G56460	protein kinase, putative	2.0	4E-04	2.5	3E-05	2.1	3E-04
AT3G45010	scpl48	3.6	4E-09	4.4	6E-10	3.9	2E-09
AT4G00230	XSP1	2.1	5E-06	2.4	8E-07	2.3	2E-06
AT1G01900	SBTI1.1	3.2	4E-06	3.0	9E-06	3.5	2E-06
AT5G55170	SUMO3	3.9	1E-06	3.2	7E-06	1.4	1E-01
AT5G42300	UBL5	2.1	6E-07	2.0	1E-06	1.4	8E-04
AT5G10650	zinc finger (C3HC4-type RING finger) family protein	3.0	6E-05	2.2	2E-03	1.7	2E-02
AT5G10380	RING1	6.7	1E-07	6.1	2E-07	2.1	3E-03
AT2G20650	zinc finger (C3HC4-type RING finger) family protein	2.1	4E-04	2.0	7E-04	2.0	7E-04
AT1G67800	copine-related	2.0	1E-05	1.8	5E-05	1.4	1E-02
AT5G18780	F-box family protein	2.3	4E-04	1.6	2E-02	1.1	7E-01
AT3G07870	F-box family protein	2.8	3E-07	2.2	1E-05	1.2	1E-01
AT1G01640	speckle-type POZ protein-related	5.6	2E-05	4.8	4E-05	2.5	5E-03
AT3G45620	WD-40 repeat family protein	2.1	9E-08	1.8	2E-06	1.1	2E-01
AT4G35350	XCP1	7.3	7E-10	6.3	2E-09	6.8	1E-09

AT1G20850	XCP2	3.2	3E-07	3.1	5E-07	3.4	2E-07
AT4G39090	RD19	2.5	2E-04	1.7	2E-02	1.2	3E-01
AT3G22260	OTU-like cysteine protease family protein	1.8	4E-04	2.2	2E-05	1.7	9E-04
AT1G49050	aspartyl protease family protein	2.6	6E-07	2.2	5E-06	1.3	3E-02
AT1G63120	ATRBL2	3.9	1E-07	3.3	7E-07	3.6	2E-07
AT4G12910	scpl20	6.5	2E-09	6.3	2E-09	6.4	2E-09
AT2G45040	matrix metalloproteinase	2.1	1E-06	1.5	4E-04	2.0	5E-06
AT3G28580	AAA-type ATPase family protein	5.3	3E-05	5.2	4E-05	3.5	5E-04
Minor CHO metabolism							
AT4G12430	trehalose-6-phosphate phosphatase, putative	2.3	3E-04	2.8	4E-05	3.6	4E-06
AT4G22590	trehalose-6-phosphate phosphatase, putative	2.9	9E-03	3.3	4E-03	4.0	1E-03
AT5G08380	AtAGAL1	3.1	3E-05	2.4	4E-04	1.7	1E-02
Signalling							
AT3G26740	CCL (CCR-LIKE)	2.2	6E-03	1.3	3E-01	0.9	7E-01
AT2G31880	LRR transmembrane protein kinase, putative	2.5	5E-04	2.1	3E-03	1.3	3E-01
AT3G45860	receptor-like protein kinase, putative	3.2	1E-05	2.8	5E-05	0.8	3E-01
AT1G79620	LRR transmembrane protein kinase, putative	2.7	1E-05	2.7	1E-05	3.1	3E-06
AT3G15050	IQD10	2.0	1E-04	2.5	6E-06	2.3	1E-05
AT1G73805	calmodulin binding	4.2	2E-03	3.4	5E-03	1.7	2E-01
AT1G76040	CPK29	2.7	9E-03	2.9	6E-03	2.2	3E-02
AT2G41410	calmodulin, putative	3.0	1E-03	2.9	2E-03	1.9	4E-02
AT3G47480	calcium-binding EF hand family protein	16.4	2E-10	14.5	4E-10	4.1	2E-06
AT4G29900	ACA10	3.1	9E-07	3.1	8E-07	1.9	3E-04
AT1G73805	calmodulin binding	4.1	6E-04	3.7	1E-03	1.4	3E-01
AT5G26920	CBP60G	3.2	1E-02	2.6	4E-02	1.4	5E-01
AT1G08450	CRT3	3.4	9E-08	3.4	1E-07	1.4	3E-02
AT5G61900	BON1	2.4	2E-02	2.6	1E-02	2.2	3E-02
AT2G17290	CPK6	2.4	2E-02	2.5	2E-02	2.0	7E-02
AT2G46600	calcium-binding protein, putative	1.9	3E-02	2.1	1E-02	1.6	9E-02
AT5G45970	ARAC2	4.5	5E-08	3.2	1E-06	3.7	3E-07
AT1G08340	rac GTPase activating protein, putative	2.4	9E-06	2.6	4E-06	2.3	2E-05
AT1G49740	phospholipase C/ phosphoric diester hydrolase	3.0	3E-05	3.5	7E-06	3.8	3E-06
Cell							
AT3G53350	myosin heavy chain-related	2.6	2E-06	2.7	2E-06	2.7	1E-06
AT1G10340	ankyrin repeat family protein	5.6	2E-05	4.7	5E-05	1.6	1E-01
AT2G31200	ADF6	2.0	8E-05	2.4	5E-06	1.6	2E-03
AT2G16700	ADF5	3.0	2E-04	2.3	3E-03	1.3	2E-01
AT4G26120	ankyrin repeat family protein	2.9	6E-04	2.7	9E-04	2.1	8E-03
AT5G16490	RIC4	2.0	2E-03	2.2	5E-04	2.7	8E-05
AT5G02100	UNE18	2.0	1E-03	2.1	6E-04	1.3	1E-01
AT1G76970	VHS domain-containing protein	2.4	2E-05	2.1	8E-05	1.1	3E-01
Development							
AT1G01470	LEA14	2.3	7E-03	1.9	4E-02	1.5	1E-01
AT4G02380	SAG21	2.6	4E-02	1.7	2E-01	0.9	7E-01
AT5G65870	ATPSK5	2.7	5E-03	4.5	2E-04	3.6	9E-04
AT3G50650	SCL7	2.1	6E-04	1.3	2E-01	1.4	9E-02
AT5G62380	VND6	1.6	2E-02	2.0	2E-03	2.5	1E-04
AT1G71930	VND7	15.7	1E-11	14.7	2E-11	15.6	1E-11
AT2G25690	senescence-associated protein-related	3.9	1E-06	4.4	5E-07	3.6	3E-06
AT1G68795	CLE12	2.0	4E-04	1.8	1E-03	2.0	4E-04
AT2G40900	nodulin MtN21 family protein	2.2	1E-04	2.5	3E-05	2.1	3E-04
AT4G17670	senescence-associated protein-related	6.4	8E-08	5.8	2E-07	3.1	3E-05
AT1G12260	ANAC007	2.6	4E-05	2.5	6E-05	2.1	4E-04
AT1G34180	anac016	4.5	2E-08	5.7	2E-09	1.9	3E-04
AT1G28470	ANAC010	3.1	7E-06	3.2	6E-06	3.0	1E-05
AT5G47060	senescence-associated protein-related	2.1	4E-05	1.7	1E-03	1.2	2E-01
AT3G48740	nodulin MtN3 family protein	1.5	4E-02	2.1	9E-04	1.8	5E-03
Transport							
AT1G14360	UTR3	1.8	1E-02	2.2	2E-03	1.7	2E-02
AT2G02810	UTR1	1.9	1E-02	2.5	7E-04	1.7	2E-02
AT5G45380	DUR3	4.9	1E-06	4.5	2E-06	1.5	5E-02
AT1G30420	ATMRP12	2.1	5E-05	1.7	6E-04	1.4	2E-02
AT3G16340	PDR1	1.9	2E-05	2.2	3E-06	2.3	2E-06
AT3G47780	ATATH6	4.0	4E-08	3.7	1E-07	2.9	1E-06
AT3G54820	PIP2;5	14.5	4E-11	14.0	5E-11	16.9	2E-11
AT2G37180	PIP2B	5.3	2E-06	9.4	6E-08	8.9	8E-08
AT2G36830	GAMMA-TIP	2.1	1E-04	2.3	5E-05	2.2	8E-05
AT1G22710	SUC2	2.8	7E-08	2.3	1E-06	2.0	1E-05
AT4G01010	ATCNGC13	2.2	2E-03	2.0	4E-03	1.3	2E-01
Not assigned							
AT5G62180	AtCXE20	2.4	5E-05	1.9	1E-03	1.4	4E-02

AT5G45500	unknown protein	2.0	6E-04	1.6	9E-03	0.9	7E-01
AT5G05460	mannosyl-glycoprotein endo-beta-N-acetylglucosaminidase	2.0	4E-03	1.8	2E-02	1.1	8E-01
AT3G11230	yippee family protein	2.0	1E-04	1.6	2E-03	1.0	8E-01
AT1G74440	unknown protein	2.3	1E-04	1.8	3E-03	1.0	8E-01
AT2G46760	FAD-binding domain-containing protein	4.3	1E-07	3.8	3E-07	4.5	6E-08
AT5G07080	transferase family protein	4.9	2E-07	5.1	1E-07	5.5	7E-08
AT3G62160	transferase family protein	2.4	7E-05	2.7	2E-05	2.7	2E-05
AT4G18280	glycine-rich cell wall protein-related	1.9	2E-02	1.6	6E-02	2.1	7E-03
AT1G48280	hydroxyproline-rich glycoprotein family protein	2.1	2E-05	1.8	1E-04	1.7	4E-04
AT5G09530	hydroxyproline-rich glycoprotein family protein	2.0	1E-02	2.2	6E-03	1.8	4E-02
AT3G60470	unknown protein	3.9	2E-05	2.9	3E-04	1.4	1E-01
AT3G50220	unknown protein	2.0	3E-05	2.1	2E-05	2.5	2E-06
AT3G47510	unknown protein	2.9	1E-04	2.2	1E-03	2.0	4E-03
no_match	no match	2.2	1E-05	1.8	2E-04	1.2	9E-02
AT2G20500	unknown protein	1.9	7E-05	2.0	2E-05	1.8	1E-04
AT4G23885	unknown protein	2.1	1E-05	2.4	1E-06	2.0	3E-05
AT1G64370	unknown protein	2.0	4E-03	2.3	1E-03	1.8	1E-02
AT2G44000	unknown protein	1.9	6E-06	1.9	1E-05	2.2	6E-07
AT5G60720	unknown protein	4.4	5E-08	5.2	1E-08	5.2	1E-08
AT5G14550	unknown protein	2.8	2E-02	1.5	3E-01	1.2	6E-01
AT5G01360	unknown protein	3.3	2E-06	3.0	6E-06	3.8	5E-07
AT1G33700	catalytic/ glucosylceramidase	4.7	5E-07	5.9	8E-08	5.9	8E-08
AT1G10800	unknown protein	5.8	5E-07	5.3	1E-06	5.0	1E-06
AT5G22540	unknown protein	3.6	2E-04	3.2	5E-04	1.4	2E-01
no_match	no match	2.1	2E-04	2.1	2E-04	1.8	1E-03
AT4G16240	unknown protein	2.2	7E-04	1.7	1E-02	1.9	4E-03
AT2G05910	unknown protein	2.1	1E-05	1.9	3E-05	1.6	5E-04
AT2G02370	unknown protein	2.2	3E-05	1.8	6E-04	1.5	6E-03
AT4G18425	unknown protein	16.1	3E-09	17.4	2E-09	12.7	1E-08
AT2G38820	unknown protein	2.3	8E-07	2.1	2E-06	1.9	1E-05
AT2G18690	unknown protein	2.5	2E-02	2.2	4E-02	1.0	1E+00
AT5G19870	unknown protein	3.1	1E-06	3.3	6E-07	3.1	1E-06
AT5G66440	unknown protein	6.8	1E-11	6.9	1E-11	6.3	3E-11
AT5G46230	unknown protein	4.6	3E-08	4.0	1E-07	1.7	2E-03
AT3G21550	unknown protein	3.0	1E-06	3.3	5E-07	3.2	8E-07
AT1G43790	TED6	2.9	3E-06	3.4	5E-07	2.8	4E-06
AT1G22885	unknown protein	3.3	1E-08	3.6	5E-09	2.9	5E-08
AT2G44080	ARL	2.3	9E-03	1.6	1E-01	1.1	6E-01
AT5G25470	DNA binding	1.6	1E-03	2.0	5E-05	1.3	4E-02
AT5G64510	unknown protein	1.9	9E-02	3.6	3E-03	1.9	9E-02
AT5G45320	unknown protein	2.4	5E-04	3.0	4E-05	3.0	5E-05
AT2G32160	unknown protein	2.6	6E-05	2.6	6E-05	1.0	9E-01
AT2G41800	unknown protein	2.7	8E-07	3.1	2E-07	3.4	6E-08
Glycolysis							
AT4G26270	PFK3	2.5	7E-05	1.7	8E-03	1.1	4E-01
Fermentation							
AT1G23800	ALDH2B7	2.2	3E-05	2.0	1E-04	2.1	4E-05
Gluconeogenese							
AT2G42790	CSY3	2.4	1E-05	1.7	2E-03	1.5	1E-02

3.5 Functional analysis of selected genes

3.5.1 Infection of *drp-tir-class* mutant

The cluster analysis has revealed 112 genes whose expression levels correlated with the disease phenotype. The expression levels were found to be low in the *coi1-t* mutant as compared to the other two susceptible genotypes. Expression of selected genes was re-analyzed in the *nahG* plants, which were as susceptible as the wild-type. If the expression would be lower in the *nahG* plants, these genes can be excluded from the further analysis. For

this purpose, genes from cluster II (Figure 19, Table 2), like disease resistance protein (DRP-*TIR-class; AT1G57630*), *MYB DOMAIN PROTEIN 59* (*MYB59*; *AT5G59780*) and *AP2/B3 like TF* (*AT3G11580*) were selected. Quantitative real-time RT-PCR revealed that these genes were expressed in the susceptible genotypes as shown by the analysis of the wild type and the *nahG* plants but remained low in the resistant *coi1-1* and *coi1-1/nahG* double mutant plants (Figure 20A-20B), in contrast to the lower expression levels of *ALPHA-DOX1* that were lower in *nahG* plants (Figure 20D).
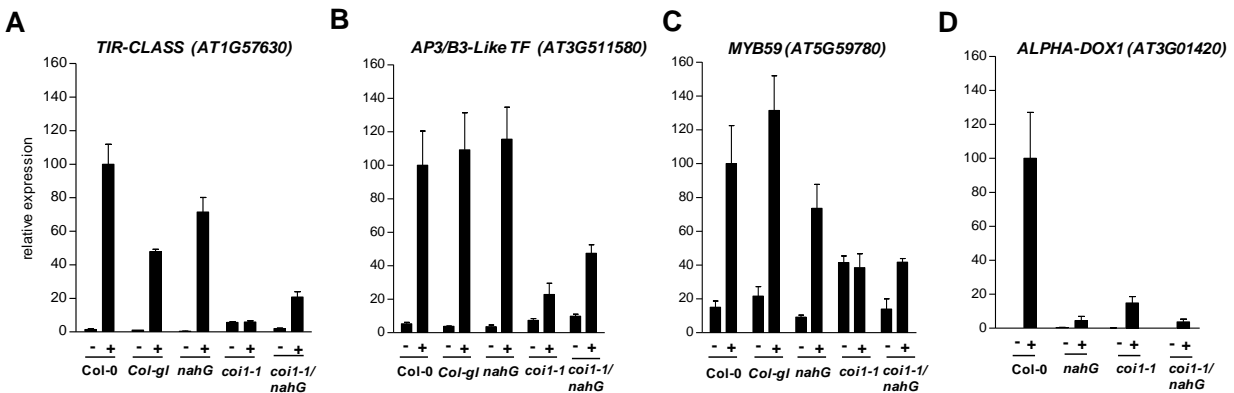
Figure 20 Gene expression analyses of mock and *V. longisporum*-infected wild type, *nahG*, *coi1-1* and *coi1-1/nahG* plants.

(A)   Quantitative RT-PCR analysis of relative transcript levels of DRP-*TIR-Class (AT1G57630)* in petioles from wild-type*, nahG*, coi1-1 *and coi1-t1/nahG* plants at 15 days after mock and *V. longisporum* infection.

(B)   Quantitative RT-PCR analysis of relative transcript levels of *AP3/B3-Like TF (AT3G511580)* in petioles from wild-type*, nahG*, coi1-1 *and coi1-t1/nahG* plants at 15 days after mock and *V. longisporum* infection.

(C)   Quantitative RT-PCR analysis of relative transcript levels of *MYB59 (AT5G59780)*in petioles from wild-type*, nahG*, coi1-1 *and coi1-t1/nahG* plants at 15 days after mock and *V. longisporum* infection

Data indicate means (+/- SEM) of 3-4 pools per treatment and genotype (same material as in Figure 15B) with each pool containing petioles from 4 plants. Relative transcript levels of the *V.longisporum.*-infected wild-type were set to 100%.

(D)   Quantitative RT-PCR analysis of relative transcript levels of *ALPHA-DOX1 (AT3G01420)* in petioles from wild-type*, nahG*, coi1-1 *and coi1-t1/nahG* plants at 15 days after mock and *V. longisporum* infection.

Data indicate means (+/- SEM) of 4 pools per treatment and genotype with each pool containing petioles from 4 plants. Relative transcripts levels of the *V. longisporum*-infected wild-type were set to 100%.

The overview pictures in Figure 21A shows a direct comparison of wild type and mutant plants after mock and *V. longisporum* infection. Pictures taken after 19dpi revealed that the mutant plants were as susceptible as the respective wild type. Measurement of projected leaf area at 19 dpi (Figure 21B) also confirmed the fact that the mutant was not compromised in disease symptoms.
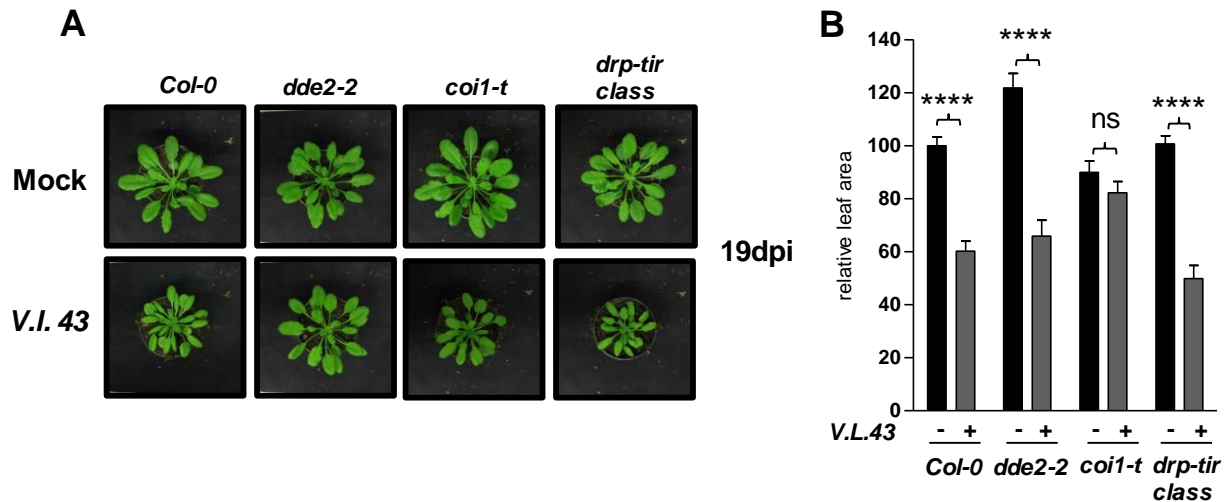
Figure 21 Disease phenotype of *V. longisporum* infected wild type, *dde2-2*, *coi1-t* and *drp-tir class* plants

(A) Typical *V. longisporum* disease symptoms of Col-0, *dde2-2*, *coi1-t* and *drp-tir class* plants at 19 dpi. One representative mock treated plant of each genotype (upper row) and one representative infected plant of each genotype (lower row) is shown.

(B) Projected leaf area of mock-infected and *V. longisporum*-infected wild type, *dde2-2*, *coi1-t* and *drp-tir class* plants. Data indicates means (+/- SEM) from one experiment with 14-16 plants mock infected and 14-16 *V. longisporum* infected plants. Stars indicate significant differences at $P < 0.0001$ (two-way ANOVA followed by Bonferroni multiple comparison test) between *V. longisporum* and mock-infected samples.

3.5.2 Infection of *ckx4 and ckx2,4,5,6* quadruple mutant

The role of cytokinin (CK) in *V. longisporum/Arabidopsis* interaction has been previously shown by Michael Reusche (Reusche 2011). He could demonstrate that exogenous application of CK resulted in the reduction of *V. logisporum*-induced disease symptoms, especially the premature senescence. However, decrease in the fungal biomass was only observed at the later stages of the infection. Arabidopsis cytokinin oxidase/dehydrogenase (CKX) enzymes are responsible for the inactivation of the CK. In the present study, expression of *CKX4* is induced in infected wild type and *dde2-2* plants but not in *coi1-t* plants (Figure 22A) indicating that *V. longisporum* might promote senescence through inducing CK degradation. A *ckx4* knock out mutant and *ckx2,4,5,6* quadruple mutant were subjected to *V. longisporum* infection. 16-18 plants per treatment (Mock/Infected) and genotype were infected. In Figure 22B the representative pictures show typical disease symptoms caused by *V. longisporum* in the wild type, *ckx4* and *ckx2,4,5,6* mutant plants. Figure 22B shows that the reduction in projected leaf area of *ckx4* and *ckx2,4,5,6* mutants were comparable to the infected-wild type plants at 15 dpi.
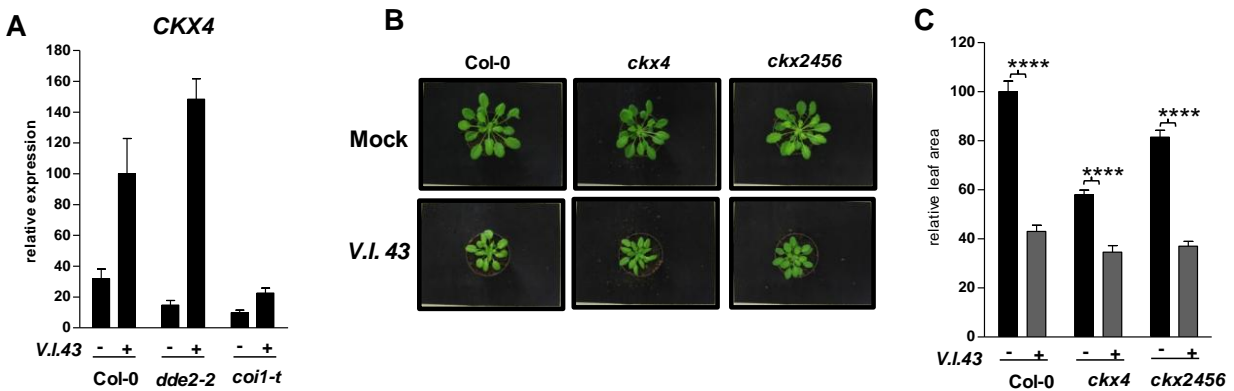
Figure 22 Gene expression analysis of *CKX4* in *V. longisporum*-infected wild type, *dde2-2* and *coi1-t* plants and disease phenotype of *V. longisporum*-infected wild type, *ckx4* and *ckx2456* plants.

(A) Quantitative RT-PCR analysis of relative transcript levels of *CKX4* in petioles of wild-type*, dde2-2 and coi1-t* plants at 15 days after mock and *V. longisporum* infection. Data indicate means (+/- SEM) of 3-4 pools per treatment and genotype with each pool containing petioles from 4 plants. Relative transcript levels of the *V.longisporum.*-infected wild-type were set to 100%.

(B) Typical V. longisporum disease symptoms of wild type, *ckx4* and *ckx2456* plants at 15 dpi. One representative mock treated plant of each genotype and one representative infected plant of each genotype is shown.

(C) Projected leaf area of mock-infected and *V. longisporum*-infected wild type, *ckx4* and *ckx2456* plants. Data indicates means (+/- SEM) from 14-16 plants mock infected and 14-16 *V. longisporum* infected plants from one experiment. Stars indicate significant differences at P < 0.0001 (two-way ANOVA followed by Bonferroni multiple comparison test) between *V. longisporum* and mock-infected samples.

3.5.3 Infection of *erf53/erf54* double mutant

This AP2 domain-containing transcription factor family protein (*ATERF54*) was found to be up-regulated in petioles five days post *Verticillium* infection (H. Tappe 2008). Expression of *AtERF54* was studied in *V. longisporum*-infected petioles of wild type, *dde2-2* and *coi1-t* at 15 dpi and in the roots of wild type, *dde2-2* and *coi1-t* at 5 dpi. It was induced in the petioles of wild type with a decrease in its expression level in the petioles of *dde2-2* plants and a further decrease in the *coi1-t* plants at 15 dpi (Figure 23A). Expression analysis of the roots indicated that the regulation of transcription of *AtERF54* started already at 5 dpi in the roots independently from the genotype (Figure 23B). Since the *AtERF54* single mutant showed a susceptible phenotype like the wild type and due to the existence of strong co-expression of *AtERF53* and *AtERF54* (ATTED; http://atted.jp/data/locus/At4g28140.shtml), an *erf53/erf54* double mutant was generated in this study. *AtERF53* is also an AP2 domain containing transcription factor belonging to AP2/ERF subfamily and is induced with a lower expression in the petioles of *V. longisporum* infected *coi1-1* plants at 15 dpi when compared to the wild type plants (Supplement figure S3). To elucidate the role of these transcription factors in the disease against *V.*

longisporum, double mutant was subjected to infection as described in section 2.2.3.1. Figure 23C shows typical *V. longisporum* induced disease symptoms in wild type as well as in the double mutant plants. The projected leaf area from 18 plants per genotype and treatment were measured at 15 dpi. The relative leaf area was calculated from three independent experiments.
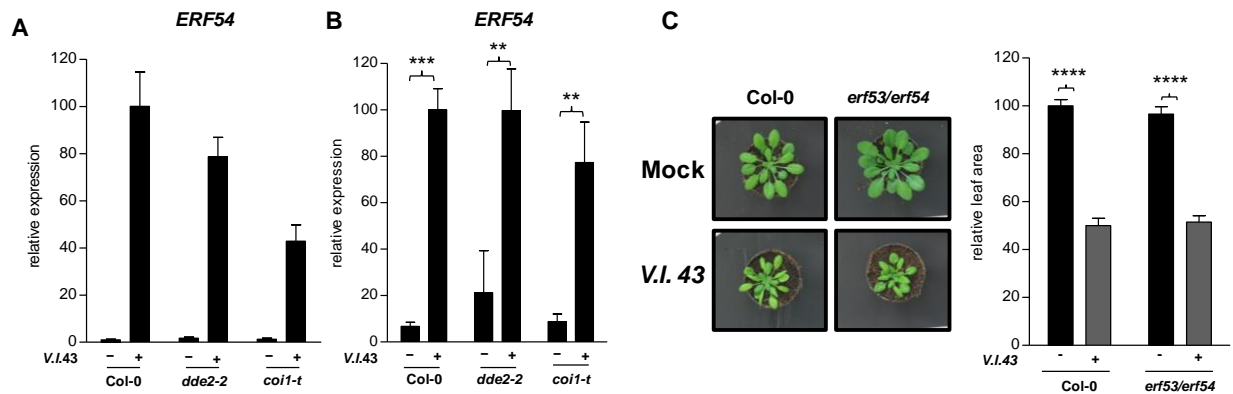

Figure 23 Gene expression analysis of *ERF54* in *V. longisporum*-infected wild type, *dde2-2* and *coi1-t* plants and disease phenotype of *V. longisporum*-infected wild type and *erf53/erf54* plants.

(A)   Quantitative RT-PCR analysis of relative transcript levels of *ERF54* in petioles of wild-type*, dde2-2 and coi1-t* plants at 15 days after mock and *V. longisporum* infection. Data indicate means (+/- SEM) of 3-4 pools per treatment and genotype with each pool containing petioles from 4 plants. Relative transcript levels of the *V.longisporum.-* infected wild-type were set to 100%.

(B)   Quantitative RT-PCR analysis of relative transcript levels of *ERF54* in roots of wild-type*, dde2-2 and coi1-t* plants at 5 days after mock and *V. longisporum* infection. Data indicate means (+/- SEM) of 3-4 pools per treatment and genotype with each pool containing petioles from 4 plants. Relative transcript levels of the *V.longisporum.-* infected wild-type were set to 100%.

(C)   Typical *V. longisporum* disease symptoms of wild type (left panel and *erf53/erf54* (right panel) plants at 15 dpi. One representative mock treated plant of each genotype (upper row) and one representative infected plant of each genotype (lower row) is shown.

(D)   Projected leaf area of mock-infected and *V. longisporum*-infected wild type and *erf53/erf54* plants. Data indicates means (+/- SEM) from three independent experiments with 14-16 plants mock infected and 14-16 *V. longisporum* infected plants/experiment.

Stars indicate significant differences at P < 0.0001 (two-way ANOVA followed by Bonferroni multiple comparison test) between *V. longisporum* and mock-infected samples.

3.6   Role of the ethylene pathway in defense against *Verticillium longisporum*

ET is a gaseous hormone that influences germination, plant growth and development (Abeles et al. 1992). It is also known to be involved in plant responses to biotic stresses (Broekaert *et al*., 2006). Previously, the role of ET as a root-borne susceptibility factor has been demonstrated. The expression of an ACC-deaminase in roots of tomato plants renders tolerance towards *V. dahliae* (Robinson et al., 2001). Moreover, the Arabidopsis ET receptor mutant *etr1-1* showed

reduced symptoms and reduced *V. dahliae* biomass from 5 dpi on. To assess the role of ET in *Arabidopsis* in response to *V. longisporum,* mutants impaired in ET signaling, *ein2-1* (ethylene insensitive mutant; Guzman and Ecker, 1990), *etr1-1* (carries a dominant negative mutation in one of the ethylene receptor genes) and *ein3-1/eil1-1* (two closely related *Arabidopsis* transcription factors known to regulate downstream ethylene signaling) were infected.

Under the infection conditions used here (Section 2.2.3.1) the *ein2-1* mutant showed a variable disease phenotype. Figure 24 represents a direct comparison of wild type and the *ein2-1* mutant plants infected with *V. longisporum*. Disease scoring was done at 13 dpi, 24dpi, and 28 dpi. Leaf area of 16-18 plants from wild-type and *ein2-1* per treatment was measured at 13 dpi. Infected *ein2-1* plants showed similar reduction (~40%) in the leaf area as in the wild-type (Figure 24A). At 24 dpi and 28 dpi *ein2-1* showed consistent reduction in the leaf area which was comparable to the wild-type (Figure 24B and 24C). Stunted growth and premature senescence were as pronounced in the *etr1-1* mutant as in the infected wild type plants at 28 dpi (Figure 24C). Apart from reduced leaf area, the *ein2-1* mutants showed reduced senescence which is in contrast to the wild type. To support this idea, compilations of all single photos from two independent experiments are presented in supplement figure S4. These results suggest that *EIN2* might control partially the premature senescence-like phenotype in response to *V. longisporum*.
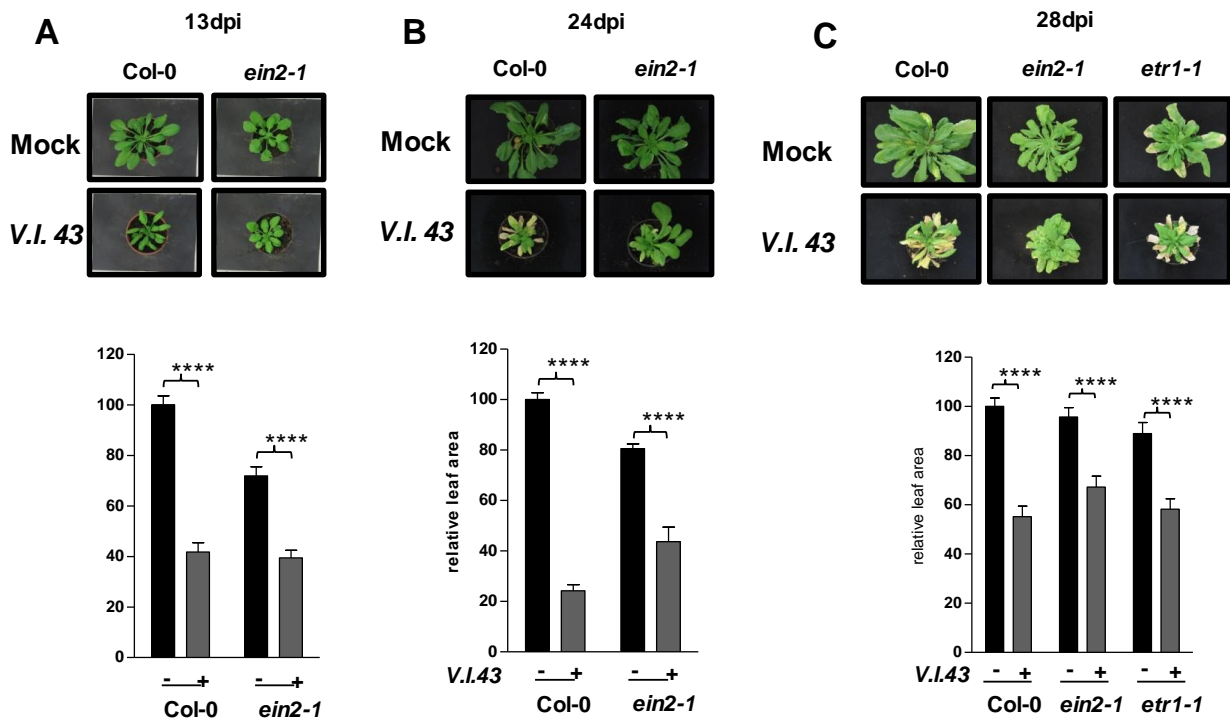
Figure 24 Disease phenotype of *V. longisporum* infected Col-0, *ein2-1* and *etr1-1* plants

One representative picture of mock-treated plant per genotype and one for infected plant/ genotype are shown. Projected leaf area of mock- and *V. longisporum*-infected wild type, *ein2-1* and *etr1-1* plants was measured at 13 dpi, 24 dpi and 28 dpi. Data indicates means (+/- SEM) from 14-16 plants mock infected and 14-16 *V. longisporum* infected plants.

Stars indicate significant differences at P < 0.0001 (two-way ANOVA followed by Bonferroni multiple comparison test) between *V. longisporum* and mock-infected samples.

The *ein3/eil1* double mutant was consistently more resistant than the wild type in two independent experiments. Leaf area from 16-18 plants per genotype and treatment and experiment was measured at 19dpi (Figure 25A). To quantify the fungal biomass in infected plants, 4 pools of petioles from 4 plants per genotype and treatment were made in descending order of the severity of the disease symptoms. The overall tendency of low amounts of fungal DNA in the resistant *ein3/eil1* double mutant plants was consistent when compared with the wild type pools (Figure 25B).
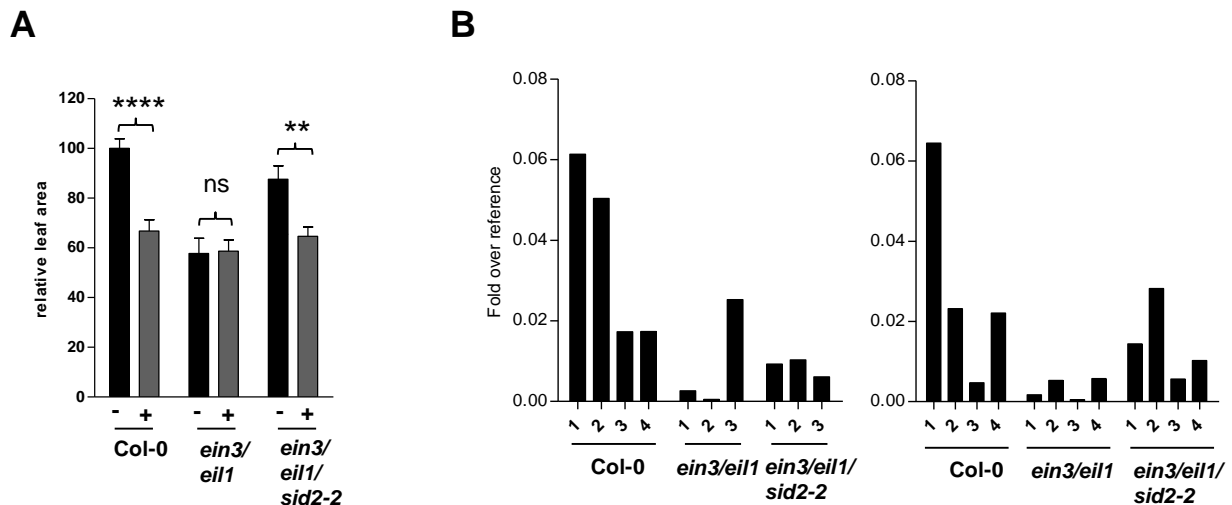

Figure 25 Leaf area measurement and fungal DNA quantification of *V. longisporum*-infected wild type, *ein3/eil1* and *ein3/eil1/sid2-2* plants

(A) Projected leaf area of mock- and *V. longisporum*-infected wild-type, *ein3/eil1-2* and *ein3/eil1* plants from two independent experiments. Data indicate means (+/- SEM) of 16-18 replicates/experiment. Stars indicate significant differences at P < 0.0001 (two-way ANOVA followed by Bonferroni multiple comparison test; ns, not significant) between *V. longisporum* (*V.l.*)- and mock-infected samples.

(B) Quantification of fungal biomass by real time RT-PCR with DNA isolated from petioles of *V. longisporum* infected wild type, *ein3/eil1* and *ein3/eil1/sid2-2* plants at 19 dpi from two independent experiments. Amplification values for fungal internal ribosomal spacer regions were normalized to the abundance of Arabidopsis *Actin8* sequences. Bars indicate means (+/- SEM) of 8 biological replicates from two independent experiments. The infected wild-type, *ein3/eil1* and *ein3/eil1/sid2-2* plants were sorted according to their disease phenotype; therefore the numbers represents different pools. The severity of the symptoms decreases from pool 1 to pool 4.

Furthermore, EIN3 and EIL1 have been previously shown to act as negative regulators of PAMP-triggered immunity with SALICYLIC ACID INDUCTION DEFICIENT2 (SID2) being a key target. The *ein3/eil1* double mutant plants displayed enhanced PAMP defenses and heightened resistance to *Pseudomonas syringae* bacteria and a mutation in *SID2* can restore normal susceptibility in this double mutant (Chen *et al.* 2009). To evaluate if the mutation in *SID2* could also restore *V. longisporum*-induced susceptibility in the *ein3/eil1* double mutant, the *ein3/eil1/sid2-2* triple mutant was inoculated. From Figure 25A it is evident that there was a partial restoration of disease symptoms in the triple mutant which was consistent in two independent experiments. Measurement of fungal biomass showed that *ein3/eil1/sid2-2* plants exhibit more fugnal DNA as compared to the *ein3/eil1* double mutant plants (Figure 25B). Together these results demonstrated that EIN3 and EIL1 negatively regulate resistance to *V.longisporum* which is partially SID2-dependent.

3.7 Role of absisic acid in defense against *V. longisporum*

Since ABA plays a major role in resistance against pathogens (Adie *et al.*, 2007, de Torres-Zabala *et al.*, 2007, Cao et al., 2011), an *A. thaliana* mutant deficient in ABA biosynthesis was examined for *V. longisporum*-induced disease development. The *aba2-1* mutant is impaired in ABA biosynthesis, being blocked in the conversion of xanthonin to ABA-aldehyde (Schwartz *et al.*, 1997), and exhibits substantial ABA deficiency and impairment of shoot growth in well watered plants (Leon-Kloosterziel *et al.*, 1996). In three independent experiments, 12-16 plants per genotype and treatment were subjected to *V. longisporum* infection. Leaf area was measured at 15 dpi in one experiment and at 19 dpi in two experiments. Infected *aba2-1* mutant plants showed consistently reduced disease symptoms like stunting and senescence at both time points (Figure 26A). From the fungal biomass measurement at 15 dpi it was learnt that there was no significant difference between the wild type and the mutant. At 19dpi, sampling of infected wild-type plants was done according to the severity of the disease symptoms. Pool 1 contained plants with a severe disease phenotype and pool 4 contain plants with almost no symptoms. In both the experiments, the *aba2-1* mutant showed a tendency of having less fungal DNA which correlates with the disease phenotype (Figure 26B). To test whether enhanced disease resistance of *aba2-1* plants against *V. longisporum* is attributed to the ABA-suppression of the JA/ET signaling pathway (Anderson *et al.*, 2004), *PDF1.2* expression was studied in *V. longisporum*-infected wild type and *aba2-1* mutant plants. It was observed that infection with *V. longisporum* induces *PDF1.2* in the infected petioles of wild type plants relative to the mock-treated plants, whereas higher basal transcript levels of *PDF1.2* were found already in the

mock-treated *aba2-1* plants (Figure 26C). However, no hyper induction of *PDF1.2* transcript level was observed in infected *aba2-1* plants. These high levels of *PDF1.2* defense gene observed in the mock-treated *aba2-1* plants might lead to reduction in the fungal proliferation. Next, the transcript levels of *DRP-TIR Class* (At1G57630) were studied in *V. longisporum*-infected wild type and *aba2-1* mutant plants. The expression levels were strongly induced in the *V. longisporum*-infected wild type plants whereas higher basal transcript levels were observed in mock-treated *aba2-1* plants which did not change after infection (Figure 26D). Even though the knock out mutant of *DRP-TIR* gene was as susceptible as the wild type plants, still higher basal levels of this putative disease resistance protein might activate some antimicrobial processes that lead to reduced fungal proliferation in these plants.
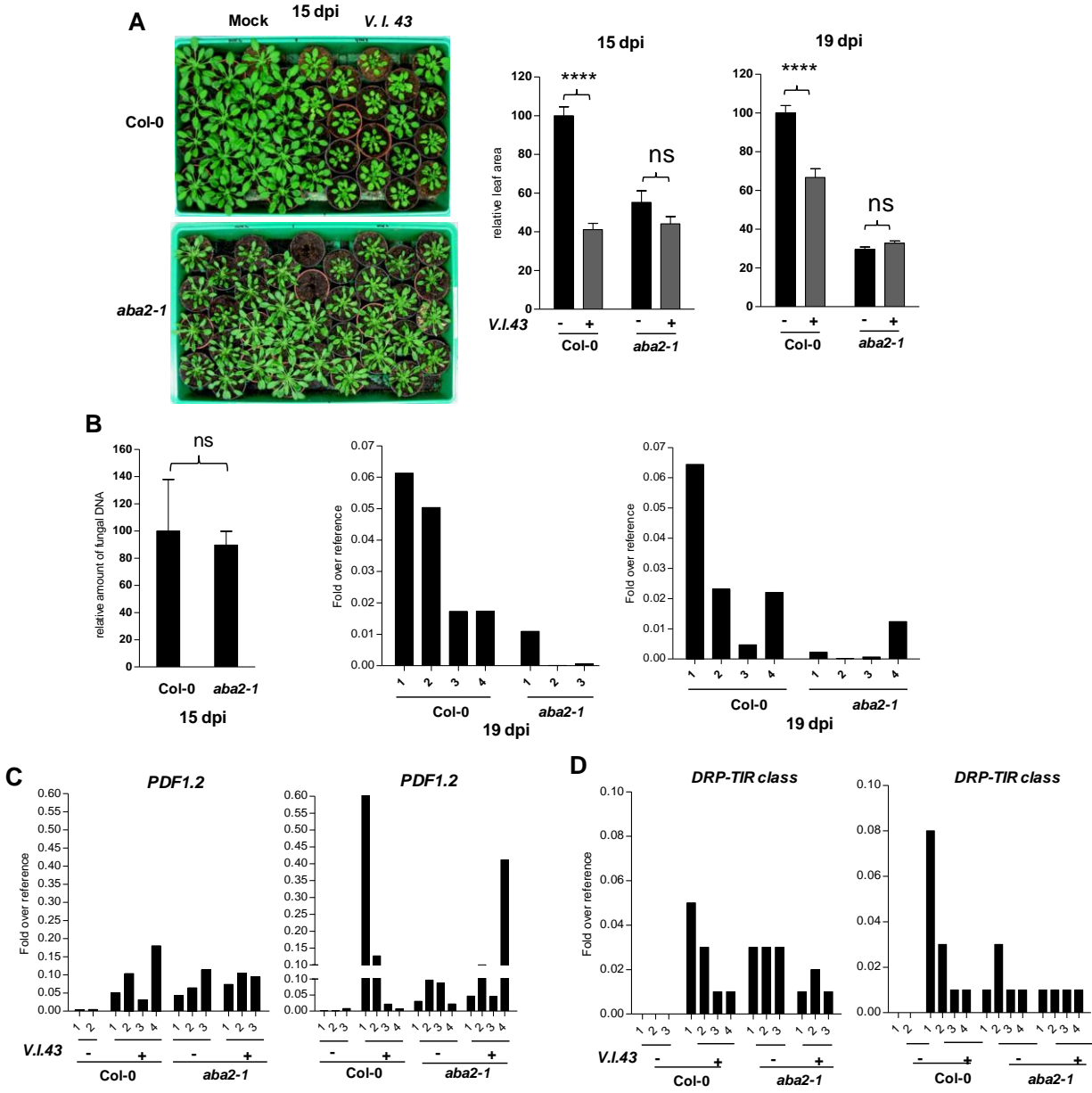
Figure 26 Disease phenotype, fungal DNA quantification and gene expression analysis of *V. longisporum*-infected wild type and *aba2-1* plants

(A) Projected leaf area of mock- and *V. longisporum*-infected wild-type and *aba2-1* plants from 3 independent experiments. One experiment was at 15 dpi and two-independent experiments at 19 dpi. Data indicate means (+/- SEM) of 16-18 replicates/experiment. Stars indicate significant differences at P < 0.0001 (two-way ANOVA followed by Bonferroni multiple comparison test; ns, not significant) between *V. longisporum*- and mock-infected samples.

(B) Quantification of fungal biomass by real time RT-PCR with DNA isolated from petioles of *V. longisporum* infected wild type and *aba2-1* plants at 15 and 19 dpi from two independent experiments. Amplification values for fungal internal ribosomal spacer regions were normalized to the abundance of Arabidopsis *Actin8* sequences. Bars indicate mean (+/- SEM) of 4 replicates from single experiment at 15 dpi. Bars indicate 7-8 biological replicates from two independent experiments for 19 dpi. The infected wild-type plants were sorted according to their disease phenotype; therefore the numbers represents different pools. The severity of the symptoms decreases from pool 1 to pool 4.

69

(C) Quantitative RT-PCR analysis of relative transcript levels of *PDF1.2* in petioles from wild-type *and aba2-1* plants at 19 days after mock and *V. longisporum* infection. Bars indicate 3-4 pools per treatment and genotype (with each pool containing petioles from 4 plants) in two independent experiments. The infected wild-type plants were sorted according to their disease phenotype; therefore the numbers represents different pools. The severity of the symptoms decreases from pool 1 to pool 4.

(D) Quantitative RT-PCR analysis of relative transcript levels of *DRP-TIR class* in petioles from wild-type *and aba2-1* plants at 19 days after mock and *V. longisporum* infection. Bars indicate 3-4 pools per treatment and genotype (with each pool containing petioles from 4 plants) in two independent experiments. The infected wild-type plants were sorted according to their disease phenotype; therefore the numbers represents different pools. The severity of the symptoms decreases from pool 1 to pool 4.

4 DISCUSSION

Verticillium longisporum is a soil-borne fungal pathogen that enters the host plant via roots and the hyphae invade the xylem vessels where conidia are formed. Vascular colonization occurs as conidia are transported along with transpiration stream. Later, tissue damage and plant senescence takes place after which the fungus forms resting structures like microsclerotia. Following dispersal of dead plant tissue into the soil, the microsclerotia are released where they can remain viable for longer than 10 years (Heale, 1999). The long persistence of these resting structures is one of the main causes of the control problems related to this disease. The main hosts of *V. longisporum* have been reported to be *Brassicaceae*. Compared to *V. dahliae* (Fradin & Thomma, 2006), very limited knowledge is available when it comes to issues like defense responses (Floerl et al., 2008, Johansson et al., 2006, Veronese et al., 2003). In the present study, investigations were focused on the interactions between *V. longisporum* and *A. thaliana* to unravel the role of known defense signaling pathways by utilizing *A. thaliana* mutants and gene expression studies.

4.1 Salicylic acid does not play a major role in resistance/susceptibility towards *Verticillium longisporum*

In *A. thaliana*, the role of the SA pathway in response to *Verticillium* infection has been studied previously (Fradin et al., 2011, Johansson et al., 2006, Veronese et al., 2003). Veronese et al., 2003 investigated the inducibility of the SA marker gene, *PR-1*, in *Arabidopsis* after *V. longisporum* inoculation and found no detectable pathogen-induced activation up to 9 dpi. Johannson et al., 2006 reported the induction of *PR-1* and *PR-2* as early as 7 dpi, but found that the plants with a defective SA pathway (*eds1-1*, *NahG*, *npr1-3*, *pad1-4* and *sid2-1*) did not exhibit enhanced susceptibility. As *Arabidopsis* seedlings grown on sucrose-containing medium were analyzed in both studies, the reason for the discrepancy regarding the activation of *PR-1* transcript is unclear. Fradin et al., 2011, described no difference in susceptibility for *eds1-2*, *eds5-1* and *eds9-1* and enhanced susceptibility for *npr1-3* when challenged with *V. dahliae*. A protective role of the SA pathway in Arabidopsis resistance to *Fusarium oxysporum*, another vascular pathogen, has been implicated before: (Edgar et al., 2006) showed that exogenously applied SA before *Fusarium* inoculation provided increased resistance to the plant. Plants defective in SA accumulation/biosynthesis (e.g. *NahG* and *eds5*) but not in SA signaling (e.g. *npr1-1*) showed increased susceptibility towards *F. oxysporum* (Berrocal-Lobo & Molina, 2004,

Diener & Ausubel, 2005, Dombrecht et al., 2007) but no change in susceptibility has been reported by Thatcher et al., 2009.

Since a data set obtained from the microarray analysis showed strong correlation with the data sets from plants with an elevated SA defense response (Supplement table 1), levels of free SA and its metabolites were measured in mock-treated and infected wild-type samples (Figure 10A). Metabolites of the SA pathway were increased after *V. longisporum* infection, leading to the induction of the SA marker gene *PR-1* (Figure 10B). Interestingly, the levels of free SA did not change after infection. This leads to a suggestion that SA derivatives are responsible for the increased expression of *PR-1*. SAG and DHBA, deriving from the activated isochorismate synthase pathway after infection, can be speculated as potential candidates. SAG is generally assumed to serve as a storage form of SA. Therefore, it is unclear whether increased SAG levels contribute to the activation. In contrast DHBA, which has weak *PR-1* inducing activity (Bartsch et al., 2010), might act as an active metabolite. Ratzinger *et al.*, 2009 have already found SAG in the xylem sap of *V. longisporum*-infected *Brassica napus* plants. However, it is not known whether it contributes to the defense. In Arabidopsis, *PR-1* induction was abolished in *sid2-2* and *NahG* plants after infection (Figure 10B). Mutants defective in the SA pathway (*sid2-2*, *NahG* and *npr1-1*) were as susceptible as the wild-type (Figure 10C and 10D). Single photos taken at 21 dpi showed comparable alterations in the senescence or stunting phenotype in infected *npr1-1*, *sid2-2* and *nahG* plants as in the wild type (Supplement figure S1). Measurement of fungal biomass in infected petioles also revealed similar amounts of fungal DNA in all genotypes at 15 dpi (Figure 10E). Overall, these results suggest a very minor role of SA in *Arabidopsis/V. longisporum* interaction under our conditions.

However, exogenous application of SA provided increased resistance against *F. oxysporum* (Edgar et al., 2006). Therefore it can be assumed that an already activated SA defense pathway might provide resistance against *V. longisporum*. Previous studies have demonstrated that the *ein3/eil1* double mutant constitutively express *SID2* and other PAMP responsive genes. Consistently it over accumulates SA, and shows increased resistance to *Pseudomonas syringae* bacteria. The enhanced resistance to *P. syringae* and defense gene expression was abolished in the *ein3/eil1/sid2* mutant (Chen et al., 2009). Similarly, in the present study resistant phenotype of *ein3/eil1* double mutant was compromised in *ein3/eil1/sid2* triple mutant when infected with *V. longisporum* (Figure 25A). Therefore, it can be assumed that the activation of the SA defense pathway after *V. longisporum* infection does not influence the

disease phenotype or fungal propagation but an already activated SA defense pathway (e.g. in mock-treated *ein3/eil1* plants) might confer resistance to such plants.

4.2 Jasmonic acid does not play a major role in resistance/susceptibility towards *Verticillium longisporum*

Previously, it has been shown that the Arabidopsis mutant impaired in JA-Ile conjugate formation (*jar1-1*), did not possess enhanced susceptibility in response to *V. longisporum* and *V. dahliae* when grown on MS media (Johansson et al., 2006, Veronese et al., 2003). In another study, it has been described that *jar1-1* plants, grown on soil, show similar level of disease severity as compared to the wild-type plants after *V. dahlia*e inoculations (Tjamos et al., 2005, Pantelides et al., 2010). However, (Fradin et al., 2011) observed enhanced susceptibility in *jar1-1* plants inoculated with *V. dahliae*. In the present study, *V. longisporum* infection leads to enhanced accumulation of JA and JA-Ile in Arabidopsis petioles (Figure 11A and B). JA-Ile accumulation reached similar levels after *V. longisporum* infection as well as after wounding. In contrast, JA levels showed a stronger increase after wounding as compared to *V. longisporum* infection. Similar amounts of JA-Ile were in accordance with the *VSP2* transcript levels that were induced to comparable amounts under both conditions. In contrast, the JA/ET marker gene *PDF1.2,* which is highly expressed after infection with *B. cinerea*, is not efficiently induced in *V. longisporum*-infected plant tissue (Figure 15B). Efficient induction of JA pathway and inefficient induction of JA/ET pathway after *V. longisporum* infection might indicate low levels of ET (Ellis & Turner, 2001, Lorenzo et al., 2004). However, enhanced levels of ABA after *V. longisporum* infection (Figure 15A) could also explain the suppression of the JA/ET pathway (Anderson et al., 2004). Constitutive expression of *PDF1.2* defense gene was observed in mock-treated *aba2-1* plants but hyper induction was not observed after *V. longisporum* infection (Figure 26C). Enhanced JA responses in the mock-treated *aba2-1* plants might posses' antifungal properties leading to reduced fungal growth and therefore reduced disease phenotype in *aba2-1* mutant plants (Figure 26). The weak activation of the JA/ET signal transduction pathway after *V. longisporum* infection explains that it does not contribute to the defense in a substantial way as revealed by the fact that the *dde2-2* mutant and other JA-Ile biosynthesis mutants showed similar disease phenotype as the wild type.

4.3 COI1 influences the disease phenotype in the absence of JA-Ile or fungal derived jasmonate mimics

It has been shown in previous studies that the Arabidopsis mutant impaired in JA signaling (*coi1-16)* did not possess enhanced susceptibility in response to *V. longisporum* and *V. dahliae* when grown on MS media (Johansson et al., 2006, Veronese et al., 2003) and no difference in susceptibility in *coi1-16* plants when challenged with *V. dahlia*e. In the present study, *coi1-t* showed less severe disease progression (stunted shoot growth, premature senescence, alterations of the anatomy of the vascular bundle and reduced microsclerotia formation) as compared to the wild-type and JA biosynthesis mutants (*dde2-2*, *fad3,7,8 acx1/5* and *jar1-1)* (Figure 12B and 12H). Reduced symptom development of *coi1-1* in comparison to JA biosynthesis mutants (*aos*, *opr3* and *jar1-1*) has also been described for the *F. oxysporum*/Arabidopsis interaction. In this system, wild-type-like initial colonization of *coi1-1* by *F. oxysporum* was followed by compromised fungal propagation at later stages of the infection (Thatcher et al., 2009). Results in this thesis put forward a similar scenario. *V. longisporum* can colonize the xylem of *coi1-t* roots (Figure 14B) and almost similar levels of the fungal biomass were detected in *coi1-t* petioles at 10 dpi (Figure 14A). At later time points (15 and 19 dpi) differences in fungal biomass between *coi1-t* and wild-type increased leading finally to a higher percentage of wild-type plants with microsclerotia development as compared to *coi1-t* (Figure 14A and 12E). Therefore it can be demonstrated that it is COI1 and not JA-Ile, which is required for disease symptom development following infection by *V. longisporum.*

Even though the initial *V. longisporum* colonization is similar in *dde2-2* and *coi1-t* roots, more fungal biomass was measured in *dde2-2* as compared to *coi1-t* at later stages of the infection (Figure 14A). This phenomenon can be explained by assuming that the fungus might synthesize JA-Ile or a JA-Ile mimic that can activate COI1 in *dde2-2* plants leading to disease phenotype. For the *V. longisporum* infections, this explanation is considered as unlikely because any JA-mimic should induce the known COI1-dependent defense genes. However, this does not seem to be the case since *V. longisporum*-infected *dde2-2* mutant plants do not activate known COI1-dependent responses that are induced by JA-Ile like, activation of the marker genes *VSP2* or *PDF1.2* (Figure 15B). Rather the idea that COI1 functions in a JA-Ile-independent manner is favored. Thus, *V. longisporum* requires COI1 through a mechanism that is different from that evolved by virulent *Pseudomonas* strains (Laurie-Berry et al., 2006). Their group provide experimental data in support of the hypothesis that *P. syringae* pv. *tomato* produces the JA-Ile

mimic COR to suppress SA-dependent defense responses in a COI1-dependent manner. A higher susceptibility of the JA biosynthesis mutant *dde2-2* as compared to the JA perception mutant *coi1-1* has also been described for the *F. oxysporum*/*Arabidopsis* interaction (Thatcher et al., 2009). It was speculated that the *F. oxysporum*-derived oxylipins might induce a senescence-promoting COI1 function that would facilitate disease. *V. longisporum* induces a novel COI1 function that enhances susceptibility through yet unknown compounds that do not elicit *VSP2* and *PDF1.2* expression. Since the expression of JA or JA/ET-responsive genes was not analyzed in the *F. oxysporum*-infected *dde2-2* mutant, the above explanation might be considered for this pathosystem as well. Another example for a non-canonical COI1 function was described in the root knot nematode (*Meloidogyne* spp.)/Tomato interaction. Root knot nematodes produce less number of eggs per g root on the tomato JA-receptor mutant *jai1* than on the tomato JA biosynthesis mutant *def1* (Bhattarai et al., 2008). This might be due to a nematode-derived effector triggering COI1 to promote egg production. Analysis of JA-Ile-dependent responses in the infected *def1* mutant would reveal whether this effector is a JA-Ile mimic or a different signal. A JA-Ile-independent COI1 function in roots was recently described for ET-mediated root-growth inhibition in *Arabidopsis* (Adams & Turner, 2010). The two JA biosynthesis mutants *dde2-2* and *opr3* show a wild-type root growth inhibition response on 4 µM of the ET precursor ACC, whereas root growth of the *coi1-16* mutant was less sensitive.

4.4 Possible mechanisms involved in *coi1*-mediated resistance in *Arabidopsis*

Previous studies have shown that *PR-1* expression is hyper-induced in *coi1* mutant plants after infections with *P. syringae* (Kloek et al., 2001) and *P. cucumeria* (Hernández-Blanco et al., 2007) where *coi1* shows a resistant phenotype, suggesting that increased SA-responsive defense gene expression might be responsible for the increased resistance observed in the *coi1* mutant. In the *P. syringae/ A. thaliana* interaction, suppression of SA pathway by the JA-Ile mimic COR induced resistance in *coi1* plants which was reverted to susceptibility after transformation with *NahG* gene (Berrocal-Lobo & Molina, 2004, Laurie-Berry et al., 2006). When the transcript levels of *PR-1* were measured in *V. longisporum*-infected wild type, *dde2-2* and *coi1-t* plants, it was observed that the expression was partially reduced in *dde2-2* plants and even further compromised in *coi1-t* (Figure 16B). The reduction of *PR-1* gene expression in infected *dde2-2* and *coi1-t* plants corresponds well with the relative amounts of SAG and DHBA (Figure 16A). Consistent with our hypothesis that COI1 is not induced by a JA or JA-Ile mimic, *PR1* is not hyper induced. However, microarray analysis of the mock-treated wild-type, *dde2-2* and *coi1-t* petioles revealed 354 genes that were differentially expressed (> 2 fold, p < 0.05) in

at least one of the three genotypes, out of which of 47 genes were expressed to a higher level in *coi1-t* mock petioles as compared to wild type and *dde2-2* (Supplement table 2). Higher expression levels of genes related to SA signaling (e.g. ATNUDT6 and PAD4) were detected in this dataset. Moreover, enhanced levels of SA metabolites were also observed in *coi1-t* mock-infected plants (Figure 16), which could lead to enhanced resistance in *coi1-t* plants. However, the resistant phenotype of *coi1* in the *sid2-2* or *nahG* background Figure 17B) rules out the possibility that the enhanced SA defense in *coi1* mock plants can provide resistance against *V. longisporum*. Given the observation that the SA pathway is not up-regulated in *V. longisporum*-infected *coi1-t* plants and that *coi1/nahG* or *coi1/sid2* plants show resistance against *V. longisporum*, it can be concluded that the *coi1*-mediated tolerance is independent of SA.

Moreover, by comparing the expression levels of all the genes between the three genotypes after infection, further insights whether *V. longisporum* elicits any known developmental or defense programs in *coi1* leading to the resistant phenotype can be deduced. Out of 697 genes those were expressed to a different level (> 2 fold, $p < 0.05$) in at least one of the three genotypes, 22 genes were expressed to a higher level (> 2 fold, $p < 0.05$) in *coi1-t* as compared to the expression levels in wild type and *dde2-2* plants (between $2^{-0.3}$ and $2^{+0.3}$, Supplement Table 3). Comparing the induction levels of these genes it was observed that they were down regulated in the wild type and *dde2-2* plants after infection but were down regulated to a lesser extent in the *coi1-t* plants. Considering the result that *coi1-t* possess less fungal biomass at 15 dpi, this might be a possible reason of less down-regulation of these set of genes in infected *coi1-t* plants. Therefore, it can be concluded that the resistance in *coi1* is not due to the induction of any resistance genes. However, the suppression of these genes in wild-type and *dde2-2* suggests that *V. longisporum* can inhibit the expression of certain defense genes in these susceptible genotypes but not as efficiently in the resistant *coi1-t* plants.

V. longisporum might induce susceptibility genes which require COI1 leading to effective disease progression. These susceptibility genes must be highly induced in the susceptible genotypes (wild-type and *dde2-2*) whereas to a lower extent in the *coi1* resistant genotype. From the 1358 genes that were significantly up-regulated in at least one of the three genotypes, 112 genes were expressed to similar levels in wild-type and *dde2-2* plants but to a lower extent in *coi1-t* after *V. longisporum* infection (Table 2). However, reduced amounts of *V. longisporum* biomass at 15 dpi in *coi1-t* petioles might be a possible reason for the reduced expression of these genes. Expression analysis of the Arabidopsis disease resistance protein- Toll-Interleukin-Resistance Class (*DRP-TIR-Class*) correlated with the reduced disease phenotype of *coi1-1*

and a susceptible phenotype of wild-type and *nahG* plants (Figure 20A) suggesting that it might act as a susceptibility gene after *V. longisporum* infection. But, infection studies with the *drp-tir* class mutant revealed that mutant plants were as susceptible as the wild type plants (Figure 19A and B). On the other hand, the transcript levels of *DRP-TIR* gene were elevated in the mock-treated *aba2-1* mutant plants (Figure 26D) showing resistance to *V. longisporum*. Therefore, *DRP-TIR* gene, when present in abundance, might act as a resistance protein that can inhibit fungal growth in *aba2-1* plants. To further elucidate whether *DRP-TIR* behaves as a disease resistance protein against *V. longisporum*, *DRP-TIR* overexpressor lines and a double cross between *drp-tir class* and *aba2-1* must be tested for fungal susceptibility.

Analysis of alterations in vascular bundle of wild type, *dde2-2* and *coi1-t* revealed differences in wild-type and *coi1-t* plants (Figure 13). At 15 dpi, the newly formed cells appeared at the abaxial side in the wild-type, whereas the *coi1-t* mutant contained several layers of cells with denser cytosol in this region. The difference between wild-type and *coi1-t* vascular alterations at 15 dpi might be the transition state of these cells which seems to be delayed in *coi1-t*. To investigate this further, *V. longisporum*-induced alteration in vascular bundles were studied in wild-type and *coi1-t* plants at 10 dpi and was found that these characteristically stained cells were also observed in the wild-type at this early stage of the disease. The appearance of cells with dense cytosol in the vascular bundle has been described before when petioles were treated with 1 mg/L 2,4-dichlorophenoxyacetic (Li et al., 2012). As previously observed for *V. albo-atrum*-infected hop (Talboys, 1958), *Arabidopsis* forms additional xylem-like cells. This hyper induction of the xylem-like vessels might be important for the fungus to cause senescence-like phenotype in *Arabodpsis*. Reusche (2011) could demonstrate that by genetically inhibiting the process of hyperplastic xylem formation and trans-differentiation in *Arabidopsis*, there was reduced senescence-like phenotype at least at the upper part of the rosette. Therefore it can be speculated that *V. longisporum* causes alterations in the vascular tissue (like; formation of xylem-like cells) which might require COI1 at the early stages of the infection to promote disease symptoms. In *coi1-t* plants, the de-differentiation process is already visible at 10 dpi, but less intense than in the wild-type. At 15 dpi, these cells have not yet re-differentiated into xylem-like cells. Whether the delayed restructuring of the vascular system in *coi1-t* limits proliferation of the fungus, or slight reductions in fungal biomass already at 10 dpi are responsible for the observed slower restructuring is still unclear.

Moreover, up regulation of cytokinin oxidase (*CKX4*) in wild type and *dde2-2* but not in *coi1-t* implicates that the fungus might promote senescence through inducing cytokinin degradation.

Role of cytokinin in delaying senescence and nutrient mobilization has been previously demonstrated (Walters, 2006). Single knock out mutant of cytokinin oxidase 4 (*ckx4*) and *ckx quadruple* mutant did not show any delay in senescence when infected with *V. longisporum* (Figure 22B and C). This implicates that cytokinin oxidation might not be the only susceptibility factor in *V. longisporum* infections. However, the *Arabidopsis* plants lacking EIN2 showed reduced senescence-like phenotype when compared to wild-type (Supplement figure 4) although the stunting phenotype was clearly visible (Figure 24). This result suggests that the COI1-dependent senescence program induced by *V. longisporum* might be mediated through components of ET pathway.

4.5 COI1 in the roots influences the disease phenotype of the shoots

V. longisporum colonizes the vascular system of the roots and subsequently invades the aerial parts of the plants. Therefore resistance to this pathogen might be determined by the roots, shoots or both the tissues. In the present study it is observed that at 10 dpi, petioles of all three genotypes showed similar amounts of fungal biomass which became less vigorous at later stages of the infection (15 dpi and 19 dpi; Figure 14A). Microscopic studies of the roots, at early stages of the infection, revealed that the *coi1* roots were as prone to fungal colonization as the wild type or the *dde2-2* roots (Figure 14B). Also, similar amounts of fungal biomass were observed in roots of *V. longisporum* infected wild type, *dde2-2* and *coi1-t* plants at 10 dp. At 16 dpi, reduced amounts of fungal biomass were observed in the roots of *coi1-t* plants as compared to the roots of *dde2-2* plants (Figure 14C). Wild type like initial colonization of *coi1* roots followed by compromised fungal propagation in the shoots at later stages of the infection was also observed in the *F. oxysporum*/Arabidopsis interaction (Thatcher et al., 2009). In this system, the similar amount of fungal DNA was detected in wild-type and *coi1* shoots before the onset of necrosis indicating that fungal entry and initial fungal growth was not restricted. Only later, when senescence processes were initiated in a COI1-dependent manner, fungal growth was restricted in *coi1*. Moreover, when wild-type scions were grafted onto *coi1* roots, foliar chlorosis and wilting symptoms were inhibited as observed in intact *coi1* plants. A similar grafting study with *coi1* roots was performed by Sonja Schoettle (Ralhan et al., 2012). For this purpose, chimeric plants with either a wild-type shoot grafted on a *coi1-16* root or a *coi1-16* shoot grafted on a wild type root were generated. It was shown that impaired shoot growth and early senescence was dependent on a functional COI1 allele in the roots, whereas COI1 in shoots was not necessary for a visible disease. In accordance to what has been described for the *F. oxysporum*/Arabidopsis system, a wild-type shoot developed lesser disease symptoms

when the root stock was from the *coi1-16* genotype whereas a *coi1-16* shoot showed disease symptoms when the root stock was from wild-type plants. Since *V. longisporum* does not change the water status (Floerl, 2010, Floerl et al., 2008), clogging of the vessels in the root might not be responsible for the induction of disease symptoms of the shoot. Rather the idea that susceptibility of the shoot is caused by a mobile signal generated in the roots can be postulated. One option is that a mobile signal released from *coi1* roots induces a yet unknown antifungal resistance program in the shoot. This possibility seems unlikely because the microarray from the *coi1* shoots did not reveal any over representation of such processes. An alternative explanation is that the mobile signal is synthesized in a COI1-dependent manner and favors premature senescence. This developmental program initiates the mobilization of nutrients from the mesophyll (Quirino et al., 2000). The mobile signal might either be sufficient to induce premature senescence, or alternatively, it might alter the responsiveness of the above-ground-tissue to the infection. In the latter case, a feed-forward loop would be generated, with initial small manipulations of the senescence program facilitating fungal growth which in turn leads to an acceleration of these disease-promoting processes.

In the present study disease symptoms were similar in wild-type, *dde2-2* and *sid2-2* hence, plant-derived jasmonates or salicylates as potential candidates for the postulated mobile signal are questioned. ET has been shown to influence senescence and growth of the plant therefore the disease phenotype might be related to this hormone or its precursor 1-aminocyclopropane-1-carboxylic acid (ACC). Experimental evidence for the role of ET as a root-borne susceptibility factor has been reported before: expression of an ACC-deaminase in roots of tomato plants generated tolerance (e.g. reduced symptoms albeit wild-type-like colonization) towards *V. dahliae* (Robinson et al., 2001). Moreover, in the current work it has been shown that the *Arabidopsis* ET receptor mutant *ein3-1/eil1-2* is resistant against *V. longisporum* and possess reduced fungal biomass at 19 dpi suggesting a negative regulation between component of ET signaling and *V. longisporum* responses (Figure 25). Whether this *EIN3*/*EIL1*-mediated response is occurring in the roots as in the case of COI1 or if this is regulated in the shoots after a signal is generated in the roots in a COI1-dependent manner, is still inconclusive. Also, *ein2-1* showed similar reduction in the leaf area as compared to the wild type but partial dependence of the senescence phenotype was observed as *V. longisporum* infected *ein2-1* plants showed reduced senescence-like phenotype as compared to the wild type plants (Figure 24 and Supplement figure 4). No significant alterations in disease resistance/susceptibility towards *F. oxysporum* were found in ET-signaling mutants *ein2* and *etr1-1* (Thatcher et al., 2009). Still, as these alleles might not affect all ET responses, further studies with transgenic or mutant

79

Arabidopsis plants with reduced production of ACC in the roots are required. Additionally, measurement of ET in the roots and petioles at early time points of the infection can provide important evidence in support of the above hypothesis. In future, analyzing the *V. longisporum*-infected roots via whole genome microarray and metabolomic studies can elucidate the mechanism of JA-independent COI1 function in roots which leads to enhanced susceptibility in shoots. However, other hormones which may be discussed with respect to root-to-shoot signaling like e.g. cytokinins have to be taken into account (Dodd, 2005).

5 SUMMARY

Verticillium longisporum is a soil-borne fungal pathogen causing vascular disease predominantly in oilseed rape. The pathogen enters its host through the roots and maintains a parasitic life stage in the xylem before invading other tissues late in the infection cycle. *Arabidopsis thaliana* was used as a model plant to characterize the response of the aerial parts of the plants towards this pathogen. It was shown that *V. longisporum* infections lead to increased amounts of salicylic acid metabolites, jasmonic acid-isoleucine and abscisic acid in the petioles of infected *Arabidopsis* plants at 15 dpi. Infection of salicylic acid biosynthesis and signaling mutants resulted in similar disease phenotype as in the wild type depicting a weak role of salicylic acid in *V. longisporum/*Arabidopsis interaction. It was found that the jasmonic acid/ethylene pathway was not as highly activated as by the necrotrophic pathogen Botrytis cinereae, whereas the jasmonic acid pathway was as efficiently induced as after wounding. Infection of the jasmonic acid receptor mutant, *coi1,* led to reduced disease symptoms towards *V. longisporum* as compared to the corresponding wild type and the jasmonic acid biosynthesis mutant *dde2-2*. Initial colonization of the roots was comparable in wild type and *coi1* plants and similar amounts of fungal biomass were accumulated in petioles of both genotypes at 10 dpi. It was shown that COI1 acts independently of any JA-Ile or JA-Ile mimics. Whole genome microarray experiments using petioles of wild type, *dde2-2* and *coi1-t* plants at 15 dpi did not reveal over/under-representation of any known defense pathways in *coi1-t* plants that might lead to the resistance phenotype. However, genes related to cell wall processes were over-represented in the cluster of genes that were induced to a similar extent in all three genotypes. Assessment of *V. longisporum*-induced alterations of the vascular bundles revealed that the de-differentiation process is visible in the wild type petioles at 10 dpi and appeared to be less pronounced in the resistant *coi1-t* plants. Grafting studies revealed that impaired shoot growth and early senescence was dependent on a functional *COI1* allele in the roots, whereas COI1 in the shoots was not necessary for a visible phenotype (Ralhan *et al.*, 2012). Since *V. longisporum* infection does not lead to the clogging of the vessel (Floerl *et al.*, 2008, 2010), a mobile signal generated in the roots has been postulated that might be responsible for the induction of the disease symptoms in the shoots.

6 REFERENCES

Abeles, F. B., P. W. Morgan, et al. (1992). Ethylene in Plant Biology, Academic Press, San Diego.

Adams, E. and J. Turner (2010). "COI1, a jasmonate receptor, is involved in ethylene-induced inhibition of Arabidopsis root growth in the light." J Exp Bot 61: 4373-4386.

Adie, B. A. T., J. Pérez-Pérez, et al. (2007). "ABA Is an Essential Signal for Plant Resistance to Pathogens Affecting JA Biosynthesis and the Activation of Defenses in Arabidopsis." The Plant Cell Online 19(5): 1665-1681.

Ahuja, I., R. Kissen, et al. (2012). "Phytoalexins in defense against pathogens." Trends in Plant Science 17(2): 73-90.

An, F., Q. Zhao, et al. (2010). "Ethylene-Induced Stabilization of ETHYLENE INSENSITIVE3 and EIN3-LIKE1 Is Mediated by Proteasomal Degradation of EIN3 Binding F-Box 1 and 2 That Requires EIN2 in Arabidopsis." The Plant Cell Online 22(7): 2384-2401.

Anderson, J. P., E. Badruzsaufari, et al. (2004). "Antagonistic interaction between abscisic acid and jasmonate-ethylene signaling pathways modulates defense gene expression and disease resistance in Arabidopsis." Plant Cell 16(12): 3460-3479.

Asselbergh, B., K. Curvers, et al. (2007). "Resistance to *Botrytis cinerea* in *sitiens*, an Abscisic Acid-Deficient Tomato Mutant, Involves Timely Production of Hydrogen Peroxide and Cell Wall Modifications in the Epidermis." Plant Physiology 144(4): 1863-1877.

Buettner, D. and U. Bonas (2006). "Who comes first? How plant pathogenic bacteria orchestrate type III secretion." Current Opinion in Microbiology 9(2): 193-200.

Barbara, D. J. and E. Clewes (2003). "Plant pathogenic *Verticillium* species: how many of them are there?" Molecular Plant Pathology 4(4): 297-305.

Bartsch, M., P. Bednarek, et al. (2010). "Accumulation of Isochorismate-derived 2,3-Dihydroxybenzoic 3-O-β-d-Xyloside in Arabidopsis Resistance to Pathogens and Ageing of Leaves." Journal of Biological Chemistry 285(33): 25654-25665.

Beckman, C. H. (1987). "The nature of wilt diseases of plants." St Paul, Minn: APS Press.

Bent, A. F., R. W. Innes, et al. (1992). Disease development in ethylene-insensitive *Arabidopsis thaliana* infected with virulent and avirulent *Pseudomonas* and *Xanthomonas* pathogens." Molecular Plant-Microbe Interactions 5(5): 372-378.

Berlanger, I. and M. L. Powelson (2000). "*Verticillium* wilt. ." The Plant Health Instructor. APSnet Plant Disease Lesson.

Berrocal-Lobo, M. and A. Molina (2004). "Ethylene response factor 1 mediates Arabidopsis resistance to the soilborne fungus *Fusarium oxysporum*." Molecular Plant-Microbe Interactions 17(7): 763-770.

Berrocal-Lobo, M., A. Molina, et al. (2002). "Constitutive expression of ETHYLENE-RESPONSE-FACTOR1 in Arabidopsis confers resistance to several necrotrophic fungi." The Plant Journal 29(1): 23-32.

Bhattarai, K. K., Q.-G. Xie, et al. (2008). "Tomato Susceptibility to Root-Knot Nematodes Requires an Intact Jasmonic Acid Signaling Pathway." Molecular Plant-Microbe Interactions 21(9): 1205-1214.

Binder, B. M., J. M. Walker, et al. (2007). "The Arabidopsis EIN3 Binding F-Box Proteins EBF1 and EBF2 Have Distinct but Overlapping Roles in Ethylene Signaling." The Plant Cell Online 19(2): 509-523.

Bishop, C. D. and R. M. Cooper (1983). "An ultrastructural study of vascular colonization in three vascular wilt diseases I. Colonization of susceptible cultivars." Physiological Plant Pathology 23(3): 323-343.

Blanco, F., V. Garreton, et al. (2005). "Identification of NPR1-Dependent and Independent Genes Early Induced by Salicylic Acid Treatment in Arabidopsis." Plant Molecular Biology 59(6): 927-944.

Bolstad, B. M., R. A. Irizarry, et al. (2003). "A comparison of normalization methods for high density oligonucleotide array data based on variance and bias." Bioinformatics 19(2): 185-193.

Boutrot, F., C. Segonzac, et al. (2010). "Direct transcriptional control of the Arabidopsis immune receptor FLS2 by the ethylene-dependent transcription factors EIN3 and EIL1." Proceedings of the National Academy of Sciences 107(32): 14502-14507.

Brooks, D. M., G. Hernández-Guzmán, et al. (2004). "Identification and Characterization of a Well-Defined Series of Coronatine Biosynthetic Mutants of *Pseudomonas syringae* pv. *tomato* DC3000." Molecular Plant-Microbe Interactions 17(2): 162-174.

Cao, H., S. A. Bowling, et al. (1994). "Characterization of an Arabidopsis Mutant That Is Nonresponsive to Inducers of Systemic Acquired Resistance." The Plant Cell Online 6(11): 1583-1592.

Cao, H., J. Glazebrook, et al. (1997). "The Arabidopsis NPR1 gene that controls systemic acquired resistance encodes a novel protein containing ankyrin repeats." Cell 88(1): 57-63.

Chae, H. S. and J. J. Kieber (2005). "Eto Brute? Role of ACS turnover in regulating ethylene biosynthesis." Trends in Plant Science 10(6): 291-296.

Chao, Q., M. Rothenberg, et al. (1997). "Activation of the ethylene gas response pathway in *Arabidopsis* by the nuclear protein ethylene-insensitive3 and related proteins." Cell 89(7): 1133-1144.

Chen, H., L. Xue, et al. (2009). "Ethylene-insensitive3 and ethylene-insensitive3-like1 repress salicylic acid induction deficient2 expression to negatively regulate plant innate immunity in *Arabidopsis.*" The Plant Cell Online 21(8): 2527-2540.

Chen, Z., Z. Zheng, et al. (2009). "Biosynthesis of salicylic acid in plants." Plant Signaling & Behavior 4(6): 493-496.

Chinchilla, D., Z. Bauer, et al. (2006). "The Arabidopsis Receptor Kinase FLS2 Binds flg22 and Determines the Specificity of Flagellin Perception." The Plant Cell Online 18(2): 465-476.

Chini, A., S. Fonseca, et al. (2007). "The JAZ family of repressors is the missing link in jasmonate signalling." Nature 448(7154): 666-671.

Choi, J., S. U. Huh, et al. (2010). "The Cytokinin-Activated Transcription Factor ARR2 Promotes Plant Immunity via TGA3/NPR1-Dependent Salicylic Acid Signaling in Arabidopsis." Developmental Cell 19(2): 284-295.

Colmenares, A. J., J. Aleu, et al. (2002). "The Putative Role of Botrydial and Related Metabolites in the Infection Mechanism of *Botrytis cinerea*." Journal of Chemical Ecology 28(5): 997-1005.

Coquoz, J.-L., A. Buchala, et al. (1998). "The Biosynthesis of Salicylic Acid in Potato Plants." Plant Physiology 117(3): 1095-1101.

Costacurta, A. and J. Vanderleyden (1995). "Synthesis of Phytohormones by Plant-Associated Bacteria." Critical Reviews in Microbiology 21(1): 1-18.

Cutler, S. R., P. L. Rodriguez, et al. (2010). "Abscisic Acid: Emergence of a Core Signaling Network." Annual Review of Plant Biology 61(1): 651-679.

de Torres-Zabala, M., W. Truman, et al. (2007). "*Pseudomonas syringae* pv. *tomato* hijacks the Arabidopsis abscisic acid signalling pathway to cause disease." EMBO J 26(5): 1434-1443.

De Vos, M., V. R. Van Oosten, et al. (2005). "Signal Signature and Transcriptome Changes of Arabidopsis During Pathogen and Insect Attack." Molecular Plant-Microbe Interactions 18(9): 923-937.

Deak, M., G. B. Kiss, et al. (1986). "Transformation of *Medicago* by *Agrobacterium* mediated gene transfer." Plant Cell Reports 5(2): 97-100.

Dewdney, J., T. L. Reuber, et al. (2000). "Three unique mutants of Arabidopsis identify eds loci required for limiting growth of a biotrophic fungal pathogen." Plant J 24(2): 205-218.

Diener, A. C. and F. M. Ausubel (2005). "*Resistance to Fusarium oxysporum 1*, a dominant *Arabidopsis* disease-resistance gene, is not race specific." Genetics 171(1): 305-321.

Dixon, R. A., M. J. Harrison, et al. (1994). "Early Events in the Activation of Plant Defense Responses." Annual Review of Phytopathology 32(1): 479-501.

Dodd, I. C. (2005). "Root-to-shoot signalling: assessing the roles of 'up' in the up and down world of long-distance signalling in planta. " Plant Soil 74: 257–275.

Dombrecht, B., G. P. Xue, et al. (2007). "MYC2 differentially modulates diverse jasmonate-dependent functions in Arabidopsis." Plant Cell 19(7): 2225-2245.

Dunker, S., H. Keunecke, et al. (2008). "Impact of *Verticillium longisporum* on Yield and Morphology of Winter Oilseed Rape (*Brassica napus*) in Relation to Systemic Spread in the Plant." Journal of Phytopathology 156(11-12): 698-707.

Durrant, W. E. and X. Dong (2004). "Systemic acquired resistance." Annual Review of Phytopathology 42(1): 185-209.

Edgar, C. I., K. C. McGrath, et al. (2006). "Salicylic acid mediates resistance to the vascular wilt pathogen *Fusarium oxysporum* in the model host *Arabidopsis thaliana*." Australasian Plant Pathology 35(6): 581-591.

El-Basyouni SZ, C. d., Ibrahim RK, Neish AC, Towers GHN (1964). " The biosynthesis of hydroxybenzoic acids in higher plants." Phytochemistry 3: 485–492.

Ellis, C. and J. G. Turner (2001). "The Arabidopsis Mutant *cev1* Has Constitutively Active Jasmonate and Ethylene Signal Pathways and Enhanced Resistance to Pathogens." The Plant Cell Online 13(5): 1025-1033.

Eynck, C., B. Koopmann, et al. (2007). "Differential interactions of *Verticillium longisporum* and *V. dahliae* with *Brassica napus* detected with molecular and histological techniques " Eur J Plant Pathol 118: 259-274.

Fan, J., L. Hill, et al. (2009). "Abscisic Acid Has a Key Role in Modulating Diverse Plant-Pathogen Interactions." Plant Physiology 150(4): 1750-1761.

Felix, G., J. D. Duran, et al. (1999). "Plants have a sensitive perception system for the most conserved domain of bacterial flagellin." The Plant Journal 18(3): 265-276.

Fernández-Calvo, P., A. Chini, et al. (2011). "The Arabidopsis bHLH Transcription Factors MYC3 and MYC4 Are Targets of JAZ Repressors and Act Additively with MYC2 in the Activation of Jasmonate Responses." The Plant Cell Online 23(2): 701-715.

Feys, B., C. E. Benedetti, et al. (1994). "Arabidopsis Mutants Selected for Resistance to the Phytotoxin Coronatine Are Male Sterile, Insensitive to Methyl Jasmonate, and Resistant to a Bacterial Pathogen." The Plant Cell Online 6(5): 751-759.

Feys, B. J. and J. E. Parker (2000). "Interplay of signaling pathways in plant disease resistance." Trends in Genetics 16(10): 449-455.

Floerl, S. (2010). "Disease symptoms and mineral nutrition in *Arabidopsis thaliana* in response to *Verticillium longisporum Vl43* infection." Journal of Plant Pathology 92 ((3),): 695-702.

Floerl, S., C. Druebert, et al. (2008). "Defence reactions in the apoplastic proteome of oilseed rape (Brassica napus var. napus) attenuate *Verticillium longisporum* growth but not disease symptoms." BMC Plant Biology 8(1): 129.

Fonseca, S., A. Chini, et al. (2009). "(+)-7-iso-Jasmonoyl-L-isoleucine is the endogenous bioactive jasmonate." Nat Chem Biol 5(5): 344-350.

Fradin, E. F., A. Abd-El-Haliem, et al. (2011). "Interfamily Transfer of Tomato Ve1 Mediates Verticillium Resistance in Arabidopsis." Plant Physiology 156(4): 2255-2265.

Fradin, E. F. and B. P. H. J. Thomma (2006). "Physiology and molecular aspects of Verticillium wilt diseases caused by V. dahliae and V. albo-atrum." Molecular Plant Pathology 7(2): 71-86.

Frugier, F., S. Kosuta, et al. (2008). "Cytokinin: secret agent of symbiosis." Trends in Plant Science 13(3): 115-120.

Gómez- Gómez, L. and T. Boller (2002). "Flagellin perception: a paradigm for innate immunity." Trends in Plant Science 7(6): 251-256.

Gagne, J. M., J. Smalle, et al. (2004). "Arabidopsis EIN3-binding F-box 1 and 2 form ubiquitin-protein ligases that repress ethylene action and promote growth by directing EIN3 degradation." Proceedings of the National Academy of Sciences of the United States of America 101(17): 6803-6808.

Gahan and B., P. (1984.). "Plant histochemistry and cytochemistry - an introduction. ." London : Academic Press, .

Geng, X., J. Cheng, et al. (2012). "The Coronatine Toxin of Pseudomonas syringae Is a Multifunctional Suppressor of Arabidopsis Defense." The Plant Cell Online 24(11): 4763-4774.

Glawischnig, E. (2007). "Camalexin." Phytochemistry 68(4): 401-406.

Glazebrook, J. (2005). "Contrasting Mechanisms of Defense Against Biotrophic and Necrotrophic Pathogens." Annual Review of Phytopathology 43(1): 205-227.

Greenberg, J. T., F. P. Silverman, et al. (2000). "Uncoupling Salicylic Acid-Dependent Cell Death and Defense-Related Responses From Disease Resistance in the Arabidopsis Mutant acd5." Genetics 156(1): 341-350.

Greenberg, J. T. and N. Yao (2004). "The role and regulation of programmed cell death in plant–pathogen interactions." Cellular Microbiology 6(3): 201-211.

Guo, H. and J. R. Ecker (2003). "Plant Responses to Ethylene Gas Are Mediated by SCFEBF1/EBF2-Dependent Proteolysis of EIN3 Transcription Factor." Cell 115(6): 667-677.

Guo, H. and J. R. Ecker (2004). "The ethylene signaling pathway: new insights." Current Opinion in Plant Biology 7(1): 40-49.

Guzmán, P. and J. R. Ecker (1990). "Exploiting the triple response of Arabidopsis to identify ethylene-related mutants." The Plant Cell Online 2(6): 513-523.

Haffner, E., P. Karlovsky, et al. (2010). "Genetic and environmental control of the Verticillium syndrome in Arabidopsis thaliana." BMC Plant Biology 10(1): 235.

Hammerschmidt, R. (1999). "Phytoalexins: What Have We Learned After 60 Years?" Annual Review of Phytopathology 37(1): 285-306.

Hanahan, D. (1983). "Studies on transformation of *Escherichia coli* with plasmids." Journal of Molecular Biology 166(4): 557-580.

He, P., L. Shan, et al. (2006). "Specific Bacterial Suppressors of MAMP Signaling Upstream of MAPKKK in Arabidopsis Innate Immunity." Cell 125(3): 563-575.

Heale, J. (1999). "The *Verticillium* threat to Canada's major oilseed crop: canola. ." Canadian Journal of Plant Pathology 21, : 1-7.

Henfling, J., R. Bostock, et al. (1980). "Effect of abscisic acid on rishitin and lubimin accumulation and resistance to *Phytophthora infestans* and *Cladosporium cucumerinum* in potato tuber tissue slices." Phytopathology 70(11): 1074-1078.

Hernández-Blanco, C., D. X. Feng, et al. (2007). "Impairment of Cellulose Synthases Required for Arabidopsis Secondary Cell Wall Formation Enhances Disease Resistance." The Plant Cell Online 19(3): 890-903.

Hubbard, K. E., N. Nishimura, et al. (2010). "Early abscisic acid signal transduction mechanisms: newly discovered components and newly emerging questions." Genes & Development 24(16): 1695-1708.

Inderbitzin, P., R. M. Davis, et al. (2011). "The Ascomycete *Verticillium longisporum* Is a Hybrid and a Plant Pathogen with an Expanded Host Range." PLoS ONE 6(3): e18260.

Iven, T., S. König, et al. (2012). "Transcriptional Activation and Production of Tryptophan-Derived Secondary Metabolites in Arabidopsis Roots Contributes to the Defense against the Fungal Vascular Pathogen *Verticillium longisporum*." Molecular Plant.

Jach, G., B. Görnhardt, et al. (1995). "Enhanced quantitative resistance against fungal disease by combinatorial expression of different barley antifungal proteins in transgenic tobacco." The Plant Journal 8(1): 97-109.

Jensen, M. K., P. H. Hagedorn, et al. (2008). "Transcriptional regulation by an NAC (NAM–ATAF1,2–CUC2) transcription factor attenuates ABA signalling for efficient basal defence towards Blumeria graminis f. sp. hordei in Arabidopsis." The Plant Journal 56(6): 867-880.

Johansson, A., J.-K. Goud, et al. (2006). "Plant Host Range of *Verticillium longisporum* and Microsclerotia Density in Swedish Soils." European Journal of Plant Pathology 114(2): 139-149.

Johnson, P. R. and J. R. Ecker (1998). "The ethylene gas signal transduction pathway: A molecular perspective." Annual Review of Genetics 32(1): 227-254.

Jones, J. D. G. and J. L. Dangl (2006). "The plant immune system." Nature 444(7117): 323-329.

Joosten, M. and P. de Wit (1999). "THE TOMATO–CLADOSPORIUM FULVUM INTERACTION: A Versatile Experimental System to Study Plant-Pathogen Interactions." Annual Review of Phytopathology 37(1): 335-367.

Kaever, A., T. Lingner, et al. (2009). "MarVis: a tool for clustering and visualization of metabolic biomarkers." BMC Bioinformatics 10(1): 92.

Karapapa, V. K., B. W. Bainbridge, et al. (1997). "Morphological and molecular characterization of *Verticillium longisporum* comb. nov., pathogenic to oilseed rape." Mycological Research 101((11)): 1281-1294.

Karimi, M., D. Inzé, et al. (2002). "GATEWAY™ vectors for Agrobacterium-mediated plant transformation." Trends in Plant Science 7(5): 193-195.

Kende, H. (1993). "Ethylene Biosynthesis." Annual Review of Plant Physiology and Plant Molecular Biology 44(1): 283-307.

Kesarwani, M., J. Yoo, et al. (2007). "Genetic interactions of TGA transcription factors in the regulation of pathogenesis-related genes and disease resistance in Arabidopsis." Plant Physiol 144(1): 336-346.

Kloek, A. P., M. L. Verbsky, et al. (2001). "Resistance to *Pseudomonas syringae* conferred by an *Arabidopsis thaliana* coronatine-insensitive (*coi1*) mutation occurs through two distinct mechanisms." Plant J 26(5): 509-522.

Klosterman, S. J., K. V. Subbarao, et al. "Comparative Genomics Yields Insights into Niche Adaptation of Plant Vascular Wilt Pathogens." PLoS Pathog 7(7): e1002137.

Konishi, M. and S. Yanagisawa (2008). "Ethylene signaling in Arabidopsis involves feedback regulation via the elaborate control of EBF2 expression by EIN3." The Plant Journal 55(5): 821-831.

Kruijt, M., M. J. D. De Kock, et al. (2005). "Receptor-like proteins involved in plant disease resistance." Molecular Plant Pathology 6(1): 85-97.

Kurakawa, T., N. Ueda, et al. (2007). "Direct control of shoot meristem activity by a cytokinin-activating enzyme." Nature 445(7128): 652-655.

Lamb, C. and R. A. Dixon (1997). "The oxidative burst in plant disease resistance." Annual Review of Plant Physiology and Plant Molecular Biology 48(1): 251-275.

Lammers, P., G. A. Tuskan, et al. (2004). "Mycorrhizal symbionts of Populus to be sequenced by the United States Department of Energy's Joint Genome Institute." Mycorrhiza 14(1): 63-64.

Laurie-Berry, N., V. Joardar, et al. (2006). "The Arabidopsis thaliana JASMONATE INSENSITIVE 1 gene is required for suppression of salicylic acid-dependent defenses during infection by Pseudomonas syringae." Mol Plant Microbe Interact 19(7): 789-800.

Lawton, K., K. Weymann, et al. (1995). "Systemic acquired resistance in Arabidopsis requires salicylic acid but not ethylene." Mol Plant Microbe Interact 8(6): 863-870.

Lee, H. I., J. León, et al. (1995). "Biosynthesis and metabolism of salicylic acid." Proceedings of the National Academy of Sciences 92(10): 4076-4079.

Leon-Reyes, A., S. H. Spoel, et al. (2009). "Ethylene modulates the role of NONEXPRESSOR OF PATHOGENESIS-RELATED GENES1 in cross talk between salicylate and jasmonate signaling." Plant Physiol 149(4): 1797-1809.

Li, X., Z. Cui, et al. (2012). "The effect of 2,4-D and kinetin on dedifferentiation of petiole cells in Arabidopsis thaliana." Biologia Plantarum 56: 121-125.

Liu, H. and S. L. Stone (2010). "Abscisic Acid Increases Arabidopsis ABI5 Transcription Factor Levels by Promoting KEG E3 Ligase Self-Ubiquitination and Proteasomal Degradation." The Plant Cell Online 22(8): 2630-2641.

Liu, Y. and S. Zhang (2004). "Phosphorylation of 1-Aminocyclopropane-1-Carboxylic Acid Synthase by MPK6, a Stress-Responsive Mitogen-Activated Protein Kinase, Induces Ethylene Biosynthesis in Arabidopsis." The Plant Cell Online 16(12): 3386-3399.

Livak, K. J. and T. D. Schmittgen (2001). "Analysis of relative gene expression data using real-time quantitative PCR and the 2(-Delta Delta C(T)) Method." Methods 25(4): 402-408.

Lohse, M., A. Nunes-Nesi, et al. (2010). "Robin: An intuitive wizard application for R-based expression microarray quality assessment and analysis." Plant Physiology.

Lopez-Molina, L., S. Mongrand, et al. (2003). "AFP is a novel negative regulator of ABA signaling that promotes ABI5 protein degradation." Genes & Development 17(3): 410-418.

Lorenzo, O., J. M. Chico, et al. (2004). "JASMONATE-INSENSITIVE1 Encodes a MYC Transcription Factor Essential to Discriminate between Different Jasmonate-Regulated Defense Responses in Arabidopsis." The Plant Cell Online 16(7): 1938-1950.

Lund, S. T., R. E. Stall, et al. (1998). "Ethylene Regulates the Susceptible Response to Pathogen Infection in Tomato." The Plant Cell Online 10(3): 371-382.

Ma, N., H. Tan, et al. (2006). "Transcriptional regulation of ethylene receptor and CTR genes involved in ethylene-induced flower opening in cut rose (Rosa hybrida) cv. Samantha." Journal of Experimental Botany 57(11): 2763-2773.

Marumo, S., M. Katayama, et al. (1982). "Microbial production of abscisic acid by *Botrytis cinerea*." Agricultural and biological chemistry 46(7): 1967-1968.

Mauch-Mani, B. and A. J. Slusarenko (1996). "Production of Salicylic Acid Precursors Is a Major Function of Phenylalanine Ammonia-Lyase in the Resistance of Arabidopsis to *Peronospora parasitica*." The Plant Cell Online 8(2): 203-212.

McConn, M. and J. Browse (1996). "The Critical Requirement for Linolenic Acid Is Pollen Development, Not Photosynthesis, in an Arabidopsis Mutant." The Plant Cell Online 8(3): 403-416.

Meuwly, P., W. Molders, et al. (1995). "Local and Systemic Biosynthesis of Salicylic Acid in Infected Cucumber Plants." Plant Physiology 109(3): 1107-1114.

Mittal, S. and K. R. Davis (1995). "Role of the phytotoxin coronatine in the infection of *Arabidopsis thaliana* by *Pseudomonas syringae* pv. *tomato*." Molecular Plant Microbe interaction.

Mohr, P. and D. Cahill (2007). "Suppression by ABA of salicylic acid and lignin accumulation and the expression of multiple genes, in Arabidopsis infected with *Pseudomonas syringae* pv. *tomato*." Functional & Integrative Genomics 7(3): 181-191.

Mohr, P. G. and D. M. Cahill (2003). "Abscisic acid influences the susceptibility of *Arabidopsis thaliana* to *Pseudomonas syringae* pv. *tomato* and *Peronospora parasitica*." Functional Plant Biology 30(4): 461-469.

Mol, L., K. Scholte, et al. (1995). "Effects of crop rotation and removal of crop debris on the soil population of two isolates of *Verticillium dahliae*." Plant Pathology 44((6):): 1070-1074.

Mosblech, A., C. Thurow, et al. (2011). "Jasmonic acid perception by COI1 involves inositol polyphosphates in *Arabidopsis thaliana*." The Plant Journal 65(6): 949-957.

Mou, Z., W. Fan, et al. (2003). "Inducers of Plant Systemic Acquired Resistance Regulate NPR1 Function through Redox Changes." Cell 113(7): 935-944.

Muller, B. and J. Sheen (2007). "Arabidopsis Cytokinin Signaling Pathway." Sci. STKE 2007(407)

Murphy, A. M., E. Pryce-Jones, et al. (1997). "Comparison of cytokinin production *in vitro* by *Pyrenopeziza brassicae* with other plant pathogens." Physiological and Molecular Plant Pathology 50(1): 53-65.

Murray, J. D., B. J. Karas, et al. (2007). "A Cytokinin Perception Mutant Colonized by Rhizobium in the Absence of Nodule Organogenesis." Science 315(5808): 101-104.

Nambara, E. and A. Marion-Poll (2005). "Abscisic acid biosynthesis and catabolism." Annual Review of Plant Biology 56(1): 165-185.

Nawrath, C. and J.-P. Métraux (1999). "Salicylic Acid Induction–Deficient Mutants of Arabidopsis Express *PR-2* and *PR-5* and Accumulate High Levels of Camalexin after Pathogen Inoculation." The Plant Cell Online 11(8): 1393-1404.

Nishimura, N., A. Sarkeshik, et al. (2010). "PYR/PYL/RCAR family members are major in-vivo ABI1 protein phosphatase 2C-interacting proteins in Arabidopsis." The Plant Journal 61(2): 290-299.

NÜRnberger, T. and V. Lipka (2005). "Non-host resistance in plants: new insights into an old phenomenon." Molecular Plant Pathology 6(3): 335-345.

O'Donnell, P. J., C. Calvert, et al. (1996). "Ethylene as a Signal Mediating the Wound Response of Tomato Plants." Science 274(5294): 1914-1917.

O'Donnell, P. J., E. A. Schmelz, et al. (2003). "Susceptible to intolerance – a range of hormonal actions in a susceptible Arabidopsis pathogen response." The Plant Journal 33(2): 245-257.

Pantelides, I. S., S. E. Tjamos, et al. (2010). "Ethylene perception via ETR1 is required in Arabidopsis infection by *Verticillium dahliae*." Molecular Plant Pathology 11(2): 191-202.

Park, J.-H., R. Halitschke, et al. (2002). "A knock-out mutation in *allene oxide synthase* results in male sterility and defective wound signal transduction in Arabidopsis due to a block in jasmonic acid biosynthesis." The Plant Journal 31(1): 1-12.

Parkin, I. A. P., S. M. Gulden, et al. (2005). "Segmental Structure of the *Brassica napus* Genome Based on Comparative Analysis With *Arabidopsis thaliana*." Genetics 171(2): 765-781.

Pauwels, L., G. F. Barbero, et al. (2010). "NINJA connects the co-repressor TOPLESS to jasmonate signalling." Nature 464(7289): 788-791.

Pegg, G. F. and B. L. Brady (2002). "*Verticillium* Wilts." Wallingford: CABI.

Penninckx, I. A. M. A., B. P. H. J. Thomma, et al. (1998). "Concomitant Activation of Jasmonate and Ethylene Response Pathways Is Required for Induction of a Plant Defensin Gene in Arabidopsis." The Plant Cell Online 10(12): 2103-2113.

Perilli, S., L. Moubayidin, et al. (2010). "The molecular basis of cytokinin function." Current Opinion in Plant Biology 13(1): 21-26.

Pieterse, C. M. J., A. Leon-Reyes, et al. (2009). "Networking by small-molecule hormones in plant immunity." Nat Chem Biol 5(5): 308-316.

Pieterse, C. M. J. and L. C. van Loon (1999). "Salicylic acid-independent plant defence pathways." Trends in Plant Science 4(2): 52-58.

Pilloff, R. K., S. K. Devadas, et al. (2002). "The Arabidopsis gain-of-function mutant *dll1* spontaneously develops lesions mimicking cell death associated with disease." The Plant Journal 30(1): 61-70.

Qiao, H., K. N. Chang, et al. (2009). "Interplay between ethylene, ETP1/ETP2 F-box proteins, and degradation of EIN2 triggers ethylene responses in Arabidopsis." Genes & Development 23(4): 512-521.

Quirino, B. F., Y.-S. Noh, et al. (2000). "Molecular aspects of leaf senescence." Trends in Plant Science 5(7): 278-282.

Ralhan, A., S. Schoettle, et al. (2012). "The vascular pathogen *Verticillium longisporum* requires a jasmonic acid-independent COI1 function in roots to elicit disease symptoms in *Arabidopsis thaliana* shoots." Plant Physiology.

Ratzinger, A., N. Riediger, et al. (2009). "Salicylic acid and salicylic acid glucoside in xylem sap of *Brassica napus* infected with *Verticillium longisporum*." Journal of Plant Research 122(5): 571-579.

Robert-Seilaniantz, A., M. Grant, et al. (2011). "Hormone Crosstalk in Plant Disease and Defense: More Than Just JASMONATE-SALICYLATE Antagonism." Annual Review of Phytopathology 49(1): 317-343.
Robinson, M. M., J. Shah, et al. (2001). "Reduced symptoms of *Verticillium* wilt in transgenic tomato expressing a bacterial ACC deaminase. ." Mol. Plant. Pathol. 2: 135-145.

Rogers, E. E. e. a. ((1996)). "Mode of action of the *Arabidopsis thaliana* phytoalexin camalexin and its role in Arabidopsis–pathogen interactions." Mol. Plant Microbe Interact. 9, : 748–757.

Rushton, P. J. and I. E. Somssich (1998). "Transcriptional control of plant genes responsive to pathogens." Current Opinion in Plant Biology 1(4): 311-315.

Rygulla, W., W. Friedt, et al. (2007). "Combination of resistance to *Verticillium longisporum* from zero erucic acid *Brassica oleracea* and oilseed *Brassica rapa* genotypes in resynthesized rapeseed (*Brassica napus)* lines." Plant Breeding 126(6): 596-602.

Sanger, F. (1977). ""Nucleotide sequence of bacteriophage φX174 DNA." Nature, 265, : 687–695.

Santner, A., L. I. A. Calderon-Villalobos, et al. (2009). "Plant hormones are versatile chemical regulators of plant growth." Nat Chem Biol 5(5): 301-307.

Schaible, L., O. S. Cannon, et al. (1951). "Inheritance of resistance of to *Verticillium* wilt in a tomato cross." Phytopathology 41(11): 986-990.

Schilmiller, A. L., A. J. Koo, et al. (2007). "Functional diversification of acyl-coenzyme a oxidases in jasmonic Acid biosynthesis and action." Plant Physiol 143(2): 812-824.

Schmelz, E. A., J. Engelberth, et al. (2003). "Simultaneous analysis of phytohormones, phytotoxins, and volatile organic compounds in plants." Proceedings of the National Academy of Sciences 100(18): 10552-10557.

Siewers, V., L. Kokkelink, et al. (2006). "Identification of an Abscisic Acid Gene Cluster in the Grey Mold *Botrytis cinerea*." Applied and Environmental Microbiology 72(7): 4619-4626.

Song, S., T. Qi, et al. (2011). "The Jasmonate-ZIM Domain Proteins Interact with the R2R3-MYB Transcription Factors MYB21 and MYB24 to Affect Jasmonate-Regulated Stamen Development in Arabidopsis." The Plant Cell Online 23(3): 1000-1013.

Spaepen, S., J. Vanderleyden, et al. (2007). "Indole-3-acetic acid in microbial and microorganism-plant signaling." FEMS Microbiology Reviews 31(4): 425-448.

Spoel, S. H., Z. Mou, et al. (2009). "Proteasome-mediated turnover of the transcription coactivator NPR1 plays dual roles in regulating plant immunity." Cell 137(5): 860-872.

Spoel, S. H., Y. Tada, et al. (2010). "Post-translational protein modification as a tool for transcription reprogramming." New Phytol 186(2): 333-339.

Stark, C. (1961). "Das Auftreten der *Verticillium*-Tracheomykosen in Hamburger Gartenbau-Kulturen." Gartenbauwissenschaft 26: 493–528.

Staswick, P. E., W. Su, et al. (1992). "Methyl jasmonate inhibition of root growth and induction of a leaf protein are decreased in *an Arabidopsis thaliana* mutant." Proceedings of the National Academy of Sciences 89(15): 6837-6840.

Stepanova, A. N. and J. M. Alonso (2009). "Ethylene signaling and response: where different regulatory modules meet." Current Opinion in Plant Biology 12(5): 548-555.

Steventon, L. A., J. Fahleson, et al. (2002). "Identification of the causal agent of *Verticillium* wilt of winter oilseed rape in Sweden, *V. longisporum*." Mycological Research 106(5): 570-578.

Stone, S. L., L. A. Williams, et al. (2006). "KEEP ON GOING, a RING E3 Ligase Essential for Arabidopsis Growth and Development, Is Involved in Abscisic Acid Signaling." The Plant Cell Online 18(12): 3415-3428.

Talboys, P. W. (1958). "Association of tylosis and hyperplasia of the xylem with vascular invasion of the hop by *Verticillium albo-atrum*." Transactions of the British Mycological Society 41(2): 249-IN248.

Thatcher, L. F., J. M. Manners, et al. (2009). "*Fusarium oxysporum* hijacks COI1-mediated jasmonate signaling to promote disease development in Arabidopsis." The Plant Journal 58(6): 927-939.

Thomma, B. P. H. J., K. Eggermont, et al. (1998). "Separate jasmonate-dependent and salicylate-dependent defense-response pathways in Arabidopsis are essential for resistance to distinct microbial pathogens." Proceedings of the National Academy of Sciences 95(25): 15107-15111.

Tjamos, S. E., E. Flemetakis, et al. (2005). "Induction of Resistance to *Verticillium dahliae* in *Arabidopsis thaliana* by the Biocontrol Agent K-165 and Pathogenesis-Related Proteins Gene Expression." Molecular Plant-Microbe Interactions 18(6): 555-561.

To, J. P. C., J. Deruère, et al. (2007). "Cytokinin Regulates Type-A Arabidopsis Response Regulator Activity and Protein Stability via Two-Component Phosphorelay." The Plant Cell Online 19(12): 3901-3914.

Turner, J. G., C. Ellis, et al. (2002). "The Jasmonate Signal Pathway." The Plant Cell Online 14(suppl 1): S153-S164.

Valls, M., S. p. Genin, et al. (2006). "Integrated Regulation of the Type III Secretion System and Other Virulence Determinants in *Ralstonia solanacearum*." PLoS Pathog 2(8): e82.

van Aalten, D. M. F., B. Synstad, et al. (2000). "Structure of a two-domain chitotriosidase from Serratia marcescens at 1.9-Å resolution." Proceedings of the National Academy of Sciences 97(11): 5842-5847.

van Loon, L. C., M. Rep, et al. (2006). "Significance of Inducible Defense-related Proteins in Infected Plants." Annual Review of Phytopathology 44(1): 135-162.

VanEtten, H. D., J. W. Mansfield, et al. (1994). "Two Classes of Plant Antibiotics: Phytoalexins versus "Phytoanticipins"." The Plant Cell Online 6(9): 1191-1192.

Veronese, P., M. L. Narasimhan, et al. (2003). "Identification of a locus controlling *Verticillium* disease symptom response in *Arabidopsis thaliana.*" Plant Journal 35(5): 574-587.

Wang, K. L. C., H. Yoshida, et al. (2004). "Regulation of ethylene gas biosynthesis by the Arabidopsis ETO1 protein." Nature 428(6986): 945-950.

Wang, X., H. Kong, et al. (2009). "F-box proteins regulate ethylene signaling and more." Genes & Development 23(4): 391-396.

Wasternack, C. (2007). "Jasmonates: An Update on Biosynthesis, Signal Transduction and Action in Plant Stress Response, Growth and Development." Annals of Botany 100(4): 681-697.

Weingart, H., H. Ullrich, et al. (2001). "The Role of Ethylene Production in Virulence of *Pseudomonas syringae* pvs. *glycinea* and *phaseolicola*." Phytopathology 91(5): 511-518.

Whalen, M. C., R. W. Innes, et al. (1991). "Identification of *Pseudomonas syringae* pathogens of Arabidopsis and a bacterial locus determining avirulence on both Arabidopsis and soybean." The Plant Cell Online 3(1): 49-59.

Wildermuth, M. C., J. Dewdney, et al. (2001). "Isochorismate synthase is required to synthesize salicylic acid for plant defence." Nature 414(6863): 562-565.

Wilhelm, S. (1955). "Longevity of the *Verticillium* wilt fungus in the laboratory and field." Phytopathology 45((3)): 180-181.

Xie, D.-X., B. F. Feys, et al. (1998). "COI1: An Arabidopsis Gene Required for Jasmonate-Regulated Defense and Fertility." Science 280(5366): 1091-1094.

Zeise, K. and A. v. Tiedemann* (2001). "Morphological and Physiological Differentiation among Vegetative Compatibility Groups of *Verticillium dahliae* in Relation to *V. longisporum*." Journal of Phytopathology 149(7-8): 469-475.

Zeise, K. and A. Von Tiedemann (2002). "Host Specialization among Vegetative Compatibility Groups of *Verticillium dahliae* in Relation to *Verticillium longisporum*." Journal of Phytopathology 150(3): 112-119.

Zhou, L., Q. Hu, et al. (2006). "*Verticillium longisporum* and *V. dahliae*: infection and disease in *Brassica napus*." Plant Pathology 55(1): 137-144.

Zipfel, C. and G. Felix (2005). "Plants and animals: a different taste for microbes?" Current Opinion in Plant Biology 8(4): 353-360.

7 ACKNOWLEGEMENTS

8 SUPPLEMENTAL MATERIAL

Supplement Table 1 Correlation analysis using Spearman rank correlation coefficient.

Spearman rank coefficient (r_s) was calculated ($p < 0.0001$) for 1693 genes that were up or down regulated in one of the three genotypes. The chosen parameters from the microarray database (GENEVSTIGATOR) are indicated. AT-numbers represents the name of the microarray experiments.

Parameter	AT-Number Genevestigator	Spearman r_s
P. syringae study 15 (Col-0)	**AT-00406**	**0.6061**
cpr5	**AT-00175**	**0.5971**
salicylic acid study 3	**AT-00320**	**0.5856**
osmotic (late)	**AT-00120**	**0.5843**
K+ starvation (shoot)	**AT-00234**	**0.5783**
mkk1/mkk2	**AT-00291**	**0.573**
B. tabaci type B	**AT-00203**	**0.5348**
wounding (late)	**AT-00120**	**0.5257**
CaLCuV	**AT-00318**	**0.5235**
B. cinerea	**AT-00147**	**0.509**
night extension (late)	**AT-00281**	**0.5073**
penta	**AT-00391**	**0.5039**
HrpZ (4h)	**AT-00107**	**0.4727**
P. infestans	**AT-00108**	**0.472**
N depletion (Col-0)	**AT-00405**	**0.4634**
ahk2/ahk3/ahk4	**AT-00341**	**0.4623**
senescence	**AT-00088**	**0.4602**
benzothiadiazole (Col-0)	**AT-00278**	**0.4455**
csn5 (csn5a-2 csn5b)	**AT-00276**	**0.4399**
salt (late)	**AT-00120**	**0.4278**
drought (Lawton et al.)	**AT-00290**	**0.4222**
sni1	**AT-00236**	**0.4158**
FLG22 study 2 (3h)	**AT-00253**	**0.4103**
nudt7-1	**AT-00421**	**0.3932**
mannitol (4h)	**AT-00199**	**0.3898**
35S::CKX1	**AT-00156**	**0.3773**
circadian clock (Ca2+)cyt / ni	**AT-00398**	**0.3499**
B. graminis (Col-0)	**AT-00309**	**0.3486**
low nitrogen	**AT-00154**	**0.3415**
E. orontii	**AT-00146**	**0.3394**
E. cichoracearum	**AT-00085**	**0.3248**

syringolin study 3 (late)	**AT-00325**	**0.3237**
phytoprostane A1 (Col-0)	**AT-00293**	**0.3139**
P deficiency study 4 (leaf)	**At-00122**	**0.3055**
ABA study 4 (Col-0)	**AT-00241**	**0.3037**
OPDA study 2 (Col-0)	**AT-00293**	**0.2913**
nitrate starvation	**AT-00155**	**0.2809**
M. persicae	**AT-00082**	**0.2683**
IAA	**AT-00110**	**0.2585**
wounding (early)	**AT-00120**	**0.2565**
GA3	**AT-00110**	**0.2196**
camta3-1	**AT-00289**	**0.1988**
shift SD to LD (9d)	**AT-00326**	**0.1902**
BL	**AT-00110**	**0.1864**
high light study 7 (exposed)	**AT-00345**	**0.1761**
MeJa study 4 (Col-0)	**AT-00251**	**0.173**
light/drought (Col-0)	**AT-00319**	**0.1649**
anoxia	**AT-00158**	**0.1162**
ga1-3	**AT-00210**	**0.1062**
BL/H3BO3	**AT-00174**	**0.1007**
BA (Col-0)	**AT-00351**	**0.04926**
abi1-1#1	**AT-00196**	**0.03643**
aba1-1#1	**AT-00196**	**0.01663**
sid2	**AT-00278, AT-00393, AT-00406**	**-0.0606**
heat study 6 (Col-0)	**AT-00402**	**-0.135**
ctr1	**AT-00180**	**-0.1567**
coi1	**AT-00406**	**-0.1928**
cold study 9 (Col-0)	**AT-00389**	**-0.2082**
atgsnor1-3	**AT-00393**	**-0.2249**
etr1	**AT-00099**	**-0.2433**
A. brassicicola (Ler)	**AT-00391**	**-0.2453**
ein2	**AT-00406**	**-0.2986**
npr1-1	**AT-00406**	**-0.3036**
pad4	**AT-00406**	**-0.462**

Supplement Table 2 List of 47 genes having higher expression levels in *coi1-t* mock plants

354 genes that were differentially expressed (> 2- fold, p< 0.05) in at least one of the three genotype were sorted such as their expression levels remains similar between wild-type and *dde2-2* (+/- $2^{0.3}$) and > 2-fold between wild-type and *coi1-t* mock plants.

AGI	Description	*coi1-t* mock/Col-0 mock	Col-inf/Col-mock	aos-inf/aos-mock	ecoi-inf/ecoi-mock
		x-fold	x-fold	x-fold	x-fold
AT3G30720	QQS	6.60	0.82	1.06	0.83
AT4G10500	oxidoreductase, 2OG-Fe(II) oxygenase family protein	4.63	19.94	14.22	1.55
AT3G28510	AAA-type ATPase family protein	4.52	11.52	12.59	1.56
AT2G04450	ATNUDT6	4.31	13.51	12.66	2.54
AT5G52760	heavy-metal-associated domain-containing protein	3.82	4.82	4.68	1.56
AT4G13920	AtRLP49	3.67	13.25	15.42	2.22
AT3G23120	AtRLP38	3.41	7.78	9.97	2.77
AT3G47480	calcium-binding EF hand family protein	3.30	16.43	14.54	4.07
AT1G33960	AIG1	3.29	52.39	46.54	7.66
AT5G60950	COBL5	3.27	3.93	3.48	1.18
AT5G45380	ATDUR3	3.15	4.90	4.49	1.52
AT5G11920	AtcwINV6	3.13	7.97	8.50	2.20
AT3G26470	ADR1-L1 (ADR1-like 1)	3.09	8.47	9.19	2.27
AT5G25260	unknown protein	3.09	3.63	2.87	1.00
AT3G51330	aspartyl protease family protein	3.06	3.47	4.29	1.04
AT5G40230	nodulin-related	2.98	3.45	2.52	0.79
AT1G35710	leucine-rich repeat transmembrane protein kinase, putative	2.94	3.95	4.65	1.26
AT5G10380	RING1	2.91	6.74	6.14	2.07
AT5G24530	DMR6	2.86	8.57	6.90	1.49
AT1G08450	CRT3	2.70	3.45	3.36	1.38
AT1G73805	calmodulin binding	2.69	4.13	3.65	1.39
AT2G32160	unknown protein	2.68	2.60	2.60	0.98
AT5G59670	leucine-rich repeat protein kinase, putative	2.62	0.98	0.98	0.44
AT3G52430	PAD4	2.54	4.64	5.12	1.66
AT5G55170	SUM3	2.49	3.89	3.18	1.36
AT1G43910	AAA-type ATPase family protein	2.42	11.79	17.45	5.80
AT5G52750	heavy-metal-associated domain-containing protein	2.41	1.54	1.75	0.87
AT4G23610	unknown protein	2.39	3.66	3.26	1.23
AT3G26220	CYP71B3	2.38	6.66	4.31	0.92
AT1G13300	myb family transcription factor	2.37	2.60	2.30	0.47
AT4G30640	FBL19	2.37	2.85	2.52	0.91
AT2G26400	ATARD3	2.35	6.61	4.95	1.16
AT3G28540	AAA-type ATPase family protein	2.30	6.67	6.60	1.27
AT2G24160	leucine rich repeat protein family	2.29	2.19	2.13	0.99
AT2G34940	vacuolar sorting receptor, putative	2.28	2.72	2.86	0.96
AT4G01700	chitinase, putative	2.28	17.95	12.58	5.48
AT5G60900	RLK1	2.26	2.67	1.84	0.83
AT5G59680	leucine-rich repeat protein kinase, putative	2.22	1.06	0.72	0.41
AT1G69720	ho3	2.12	2.73	2.26	0.95
AT3G13950	unknown protein	2.06	6.35	5.11	0.89
AT1G30900	vacuolar sorting receptor, putative	2.06	7.17	6.73	2.34
AT5G53550	YSL3	2.05	1.76	1.21	0.57
AT3G24900	AtRLP39	2.04	2.33	3.05	1.12
AT3G48640	unknown protein	2.03	2.94	4.84	1.90
AT1G15790	unknown protein	2.02	3.48	3.14	1.26
AT1G10970	ZIP4	2.02	0.40	0.40	0.40
AT5G61250	AtGUS1	1.82	2.31	1.48	0.72

Supplement table 3 List of 22 genes having higher expression levels in infected-*coi1-t* plants

697 genes, that were differentially expressed (> 2- fold, p< 0.05) in at least one of the three genotype after infection, were sorted such as their expression levels remains similar between wild-type and *dde2-2* (+/- $2^{0.3}$) and > 2-fold between wild-type and *coi1-t* mock plants.

AGI	Description	col-inf/ *coi1-t*-inf	aos-inf/ *coi1-t*-inf	Col-inf/ Col-mock	aos-inf/ aos-mock	*coi1-t*-inf/ *coi1-t*-mock
		x-fold	x-fold	x-fold	x-fold	x-fold
AT1G52190	proton-dependent oligopeptide transport (POT) family protein	3.1	2.5	0.3	0.4	0.8
AT5G12940	leucine-rich repeat family protein	2.6	2.2	0.6	0.5	0.7
AT5G53250	AGP22	2.5	2.2	0.4	0.5	1.1
AT1G74670	gibberellin-responsive protein, putative	2.5	2.2	0.4	0.4	0.6
AT1G78450	SOUL heme-binding family protein	2.4	2.2	0.2	0.2	0.5
AT1G56430	NAS4	2.3	2.0	0.2	0.3	0.5
AT1G10550	XTH33	2.2	1.9	0.6	0.5	0.8
AT3G48970	copper-binding family protein	2.2	1.8	0.4	0.3	0.5
AT1G78020	senescence-associated protein-related	2.2	1.9	0.3	0.4	0.6
AT5G03120	unknown protein	2.2	1.9	0.5	0.6	0.8
AT5G25810	TINY	2.2	1.9	0.4	0.3	0.6
AT5G56040	leucine-rich repeat protein kinase, putative	2.1	1.8	0.6	0.7	1.0
AT3G12610	DRT100 (DNA-DAMAGE REPAIR/TOLERATION 100)	2.1	1.9	0.5	0.5	0.8
AT4G01680	MYB55	2.1	1.9	0.5	0.6	1.0
AT5G64770	unknown protein	2.1	1.9	0.4	0.4	0.7
AT4G28250	ATEXPB3 (ARABIDOPSIS THALIANA EXPANSIN B3)	2.1	1.7	0.3	0.4	0.9
AT3G07010	pectate lyase family protein	2.0	1.7	0.5	0.4	0.7
AT1G10970	ZIP4	2.0	1.7	0.4	0.4	0.4
AT1G20190	ATEXPA11	2.0	1.6	0.7	0.6	0.8
AT1G67750	pectate lyase family protein	2.0	2.1	0.3	0.3	0.6
AT1G04240	SHY2 (SHORT HYPOCOTYL 2)	1.7	2.0	0.5	0.3	0.6

Supplement figure 1

Col-0
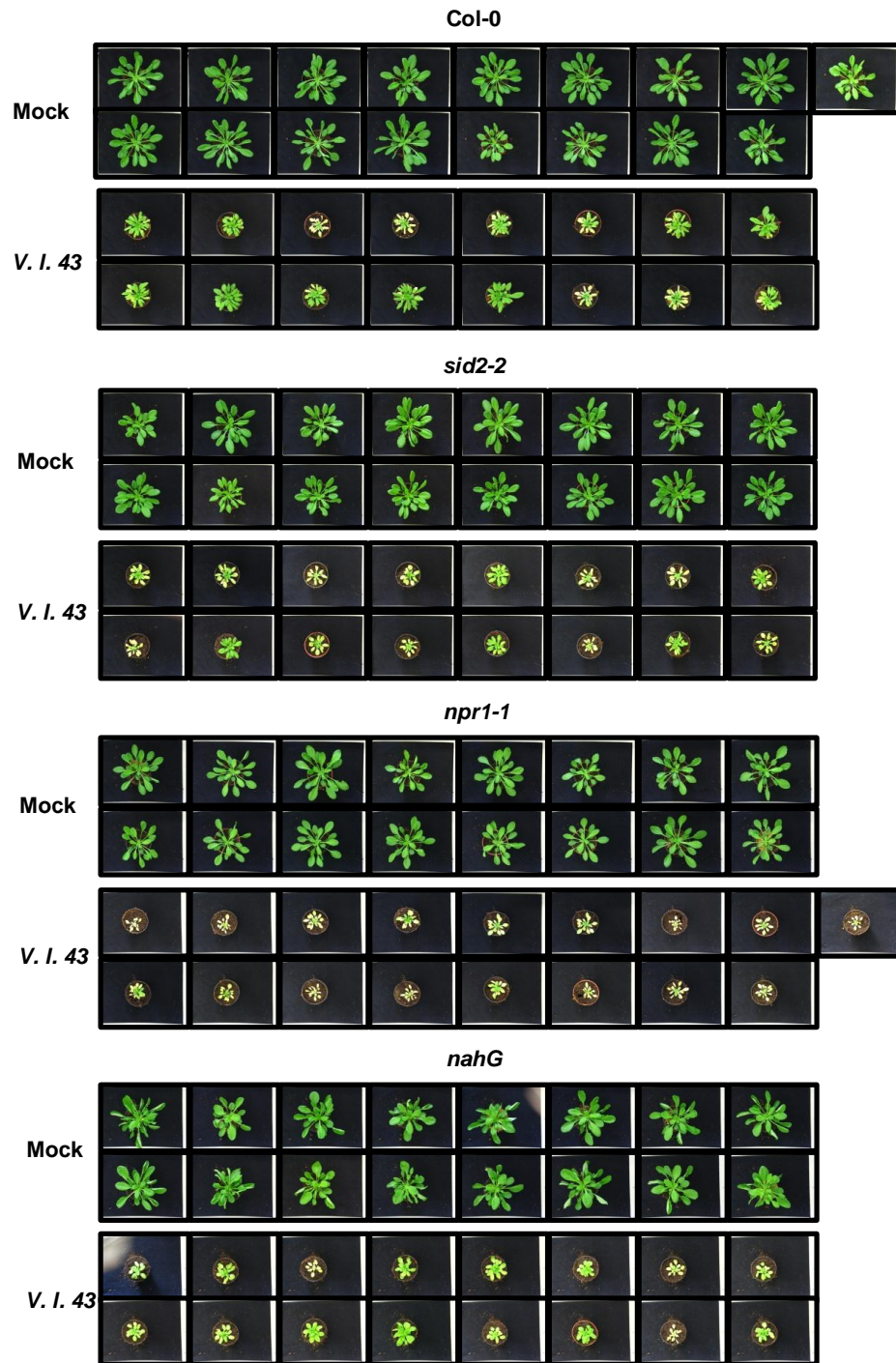
sid2-2

npr1-1

nahG

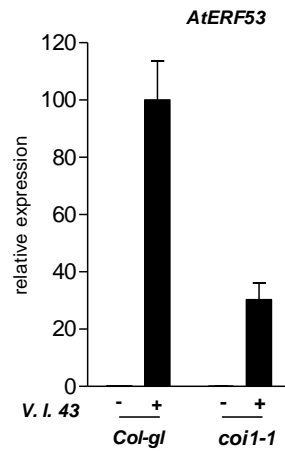**Supp. Fig 1 Disease phenotype of *V. longisporum* infected wild type, *sid2-2*, *npr1-1*, *nahG* plants**

Single photos from mock-treated and *V. longisporum*-infected at 21 dpi.

Supplement figure 3

Supp. Fig. 3 Expression analysis of *AtERF53* in *V. longisporum*-infected wild type and *coi1-1* plants

Quantitative RT-PCR analysis of relative transcript levels in petioles from wild-type and coi1-1 plants at 15 days after mock- and *V. longisporum* infection. Data indicate means (+/- SEM) of 3-4 pools per treatment and genotype with each pool containing petioles from 4 plants. Relative transcript levels of the *V.l.*-infected wild-type were set to 100%.

Supplement figure 4

28 dpi
Col-0

ein2-1

etr1-1

ein3-1/eil1-2

24 dpi
Col-0
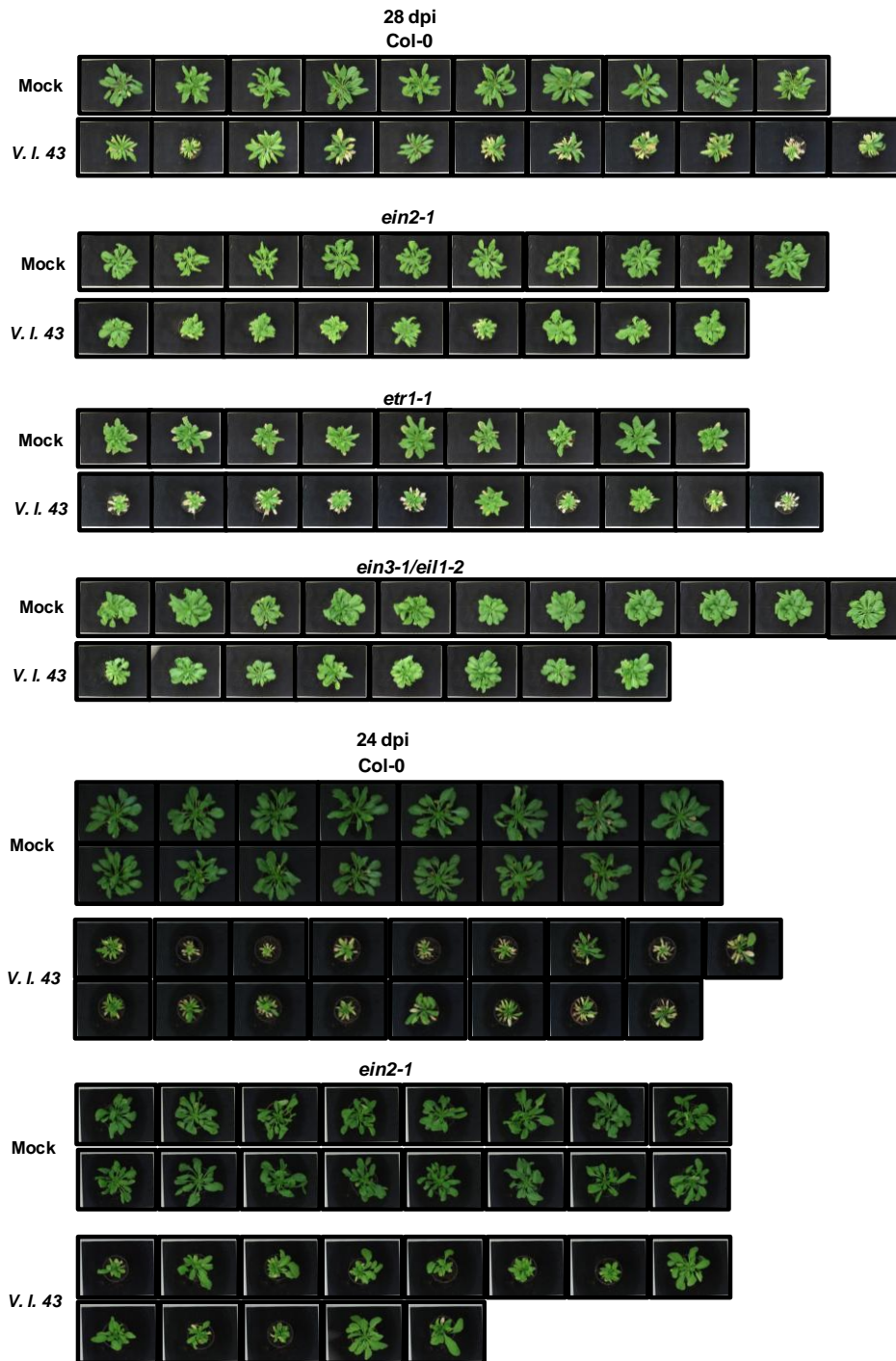
ein2-1

Supp. Fig. 4 Disease phenotype of *V. longisporum*-infected wild type, *ein2-2*, *etr1-1* and *ein3-1/eil1-2* plants

(A) Single photos from mock-treated (upper panel) and *V. longisporum*-infected (lower panel) wild type, *ein2-1*, *etr1-1* and *ein3-1/eil1-2* plants at 28 dpi.

(B) Single photos from mock-treated (upper panel) and *V. longisporum*-infected (lower panel) wild type and *ein2-1* plants at 24 dpi.

9 ABBREVIATIONS

2,4-D	2,4-dichlorophenoxyacetic acid
°C	Degree Celsius
µl	Micro litre
µM	Micromolar
A	Adenine
A	Ampere
A. thaliana	*Arabidopsis thaliana*
A. tumefaciens	*Agrobacterium tumefaciens*
ABA	Abscisic acid
AHK	*Arabidopsis*-Histidin-Kinase
AHP	*Arabidopsis*-Phosphattransmitter-Proteine
AOS	ALLENE OXIDE SYNTHASE
APS	Ammonium persulphate
aq	aqueous solution
ARR	*Arabidopsis* Response Regulator
ATCWINV1	ARABIDOSIS THALIANA CELL WALL INVERTASE 1
A_λ	absorbance or optical density
B. cinerea	*Botrytis cinerea*
bp	base pair
bZIP	basic leucine zipper
C	Cytosine
c	concentration
CDB	Czapek dox broth
cDNA	complementary DNA
cm	centimetre
COI1	CORONATINE INSENSITIVE 1
C_t	Cycle threshold
CWD	Cell wall damage
dde2-2	delayed-dehiscence 2-2
DNA	Deoxyribonucleic acid
DNase	Desoxyribonuclease
dNTP	deoxynucleoside triphosphate
dpi	day(s) post infection
DRP-TIR Class	Disease resistance protein-Toll-Interleukin-Resistance Class
dsDNA	double strand DNA
E. coli	*Escherichia coli*
e.g.	exempli gratia; for example
EB	Elution buffer
EDTA	Ethylenediaminetetraacetic acid
EIL1	ETHYLENE INSENSITIVE3-LIKE1
EIN3	ETHYLENE INSENSITIVE3
ERF B-4	ETHYLENE RESPONSE FACTOR subfamily B-4
ET	Ethylene
et al.	Et alii; and others
EtBr	Ethidium bromide
EtOH	ethanol
fwd	forward
G	Guanine

GL1	GLABROUS1
h	Hour
HCl	Hydrochloric acid
IPT	Isopentenyltransferase
JA	Jasmonic acid
l	Litre
LB	Left border primer
LD	Long day
LP	Left primer
M	Molarity
mA	Milliampere
MeJA	Methyl jasmonate
MES	2-[N-Morpholino]-ethanesoulfonic acid
mg	Milligram
$MgCl_2$	Magnesium chloride
min	Minute
ml	Millilitre
mM	Millimolar
mRNA	messenger RNA
MS	Murashige & Skoog medium
MYB59	MYB DOMAIN PROTEIN 59
NaCl	Sodium chloride
NaClO	Sodium hypochlorite
nm	Nanometer
NPR1	Non expresser of PR Genes 1
OPDA	12-oxophytodienoic acid
PCR	Polymerase chain reaction
PDB	Potato dextrose broth
PDF1.2	*Plant defensin 1.2*
pH	negative log^{10} of proton concentration
PR-1	*Pathogenesis related-1*
qRT-PCR	Quantitative real time PCR
rev	Reverse
RNA	Ribonucleic acid
Rnase	Ribonuclease
RP	Right primer
rpm	Rotations per minute
RT	Reverse transcriptase
RT	Room temperature
s	Second
SA	Salicylic acid
SAG	Salicylic acid glucoside
SD	Short day
SDS	Sodium dodecylsulfate
SEM	Standard error of the mean
SID2	SALICYLIC ACID INDUCTION DEFICIENT2
T	Thymine
TAE	tris-acetate-EDTA
taq	*Thermus aquaticus*
T-DNA	Transfer DNA

TEMED	N,N,N',N'-tetramethylethane-1,2-diamine
TF	Transcription factor
Tris	tris-(hydroxymethyl)-aminomethane
UBQ5	Ubiquitin 5
UV	Ultra violet
V	Volt
V. albo-atrum	*Verticillium albo-atrum*
V. dahliae	*Verticillium dahliae*
V. l. 43	*Verticillium longisporum* isolate 43
V. longisporum	*Verticillium longisporum*
W	Watt
w/v	weight per volume
WT	Wild-type

10 CURRICULUM VITAE

Name: Anjali Ralhan

Address: C-7 Anand Vihar
                 Main Vikas Marg
                 Delhi 110092
                 India

Email: aralhan@gwdg.de

Date of Birth: 21.01.1984

RESEARCH EXPERIENCE / ACADEMIC QUALIFICATIONS

Jan2008-   PhD degree in biology
June2012
                Preparation of thesis: "Role of defense signaling pathways in *Arabidopsis thaliana* and *Verticillium longisporum* interaction."

Jan-Aug2007   Research project in GSF- Neuherberg Munich, Germany

                Title: Detection of the endosymbiotic bacteria in *Piriformospora indica* using fluorescence *in situ* hybridisation.

2005-2007   Master of Science (Microbiology and Herbal Medicine), Amity University, Noida, Uttar Pradesh, India.

2002-2005   Bachelors of Science (Chemistry), University of Delhi, Delhi, India

1991-2002   Delhi Public School, Noida, Uttar Pradesh, India (Class I -XII)

LIST OF PUBLICATIONS

Ralhan A, Schöttle S, Thurow C, Iven T, Feussner I, Polle A and Gatz C 2012. The vascular pathogen *Verticillium longisporum* requires a jasmonic acid-independent COI1 function in roots to elicit disease symptoms in *Arabidopsis* shoots. *Plant Physiology* **159**, 1192-203.